Can Biochar Ameliorate Phosphorus Deficiency and Aluminium Phytotoxicity in Acid Soils?

A thesis presented in partial fulfilment of the requirements for the degree of

Doctor of Philosophy of Applied Science

in

Soil Science

at Massey University, Palmerston North, New Zealand.

QINHUA SHEN

2015

ABSTRACT

The use of biochar as soil amendment to enhance soil functionality is being increasingly investigated, with particular attention given to its effects on the sustainable increase of crop production and carbon (C) sequestration. To date, however, limited research has attempted to unravel the effect of biochar on either the chemical and/or biological mobilization of the residual fraction of phosphorus (P) in soil. This fraction tends to accumulate as a result of long–term P fertilization in soils rich in aluminium (Al) and iron (Fe) oxy–hydroxides and short–range ordered aluminosilicates (i.e. allophane). There is also scant information on (i) how the speciation of soluble Al changes when biochar is applied to acid soils, and (ii) whether this application alleviates Al toxicity on plant roots. My objective in this study is therefore to determine the effect of different biochars with contrasting fertilizer and liming values on the chemistry, biology and nutrient fertility of acid mineral soils.

Before studying the effect of different biochars on soil properties, several methodologies for measuring the liming properties and available nitrogen (N) in biochar were evaluated and modified where needed. For this, 19 biochars produced by pyrolysing a wide range of feedstocks under various production temperatures were used. Different pH–buffering capacity (pH–BC) methodologies – originally developed for soils (single vs multiple acid additions, short vs long equilibration times) – were tested, along with the methodology used to measure the liming equivalence. The methodologies were then validated by incubating over 10 d two acid soils (an Haplic Cambisol and an Andic Umbrisol) to which separated amendments of the 19 biochars were made at the rates estimated using both methodologies to target a final pH of 6.5.

The results indicated that the relationship established between the pH–BC of the 19 biochars under study after 30–min equilibration ($pH–BC_{30min}$) with a single addition of acid and that obtained after a 5–d equilibration ($pH–BC_{5d}$) (predicted $pH–BC_{5d} = 2.2 \times pH–BC_{30min} + 20.4$) allowed an adequate estimate of the liming potential of biochars. Similar results were found with the liming equivalent, and both methods were considered suitable to make the recommendation of the application rate. Acid hydrolysis using 6 M HCl has been proved adequate to determine available N in biochar. For this, hydrolysates of biochar are oxidized using potassium peroxodisulfate with a dilution factor of 600 so that chloride interferences are overcome and nitrate–N is then measured. This methodology, originally developed using biochars rich in N, proved not suitable for biochars with low N concentrations. Results obtained in this study have shown that a smaller dilution factor (242) is sufficiently adequate to overcome the chloride interferences while avoiding over–diluting the sample.

In this study, we hypothesized that biochar can increase P availability to plant by stimulating the growth of arbuscular mycorrhizal fungi (AMF) hyphae. Therefore, methodologies to (i) estimate the length of fungal hyphae in soil and (ii) evaluate the transfer of P by AMF hyphae needed to be tested and modified where necessary. In this part of the study, three different biochars and two soil types were used. Two biochars were produced from chipped pine (*Pinus radiata* D. Don) branches at 450^{o}C and 550°C (referred to as BP450 and BP550, respectively); and a third one from chipped weeping willow (*Salix matsudana* L.) branches at 550°C (referred to as BW550). The soils were two sil–andic Andosols of contrasting P status (Olsen P of 4.3 vs 33.3 mg kg^{-1}, referred to as LP and HP soil, respectively).

The traditional visual gridline intersection (VGI) method commonly used to measure the length of AMF hyphae distribution in soil was modified by (i) using a

digital photomicrography technique (referred to as "digital gridline intersection" (DGI) method), and (ii) processing the images using ImageJ software (referred to as the "photomicrography–ImageJ processing" (PIP) method). These methods were first tested with known lengths of possum fur and then applied to measuring the hyphal length in the LP and HP soils after a 32 wk experiment growing *Lotus pedunculatus cv* barsille. The study confirmed that the use of digital photomicrography in conjunction with either the grid–line intersection principle or image processing (with ImageJ software) is a suitable method for the measurement of AMF hyphal lengths in soils.

In addition, the traditional root study container that divides the plant growth medium into two sections – (i) a *root zone* to which both root and AMF hyphae have access and (ii) an *hyphal zone* to which only AMF hyphae have access – by a layer of nylon mesh was further modified by including a 3–mm thickness of tephra under the nylon mesh between two sections. This layer of tephra was found to be adequate to halt P diffusion from the HP soil to the LP soil for a plant growth period of 32 wk. Under such circumstances, the increase in P uptake by plant growth in a combination of a *root zone* of LP soil and a *hyphal zone* of HP soil compared with that in which both *root* and *hyphal zones* were filled with LP soil was only ascribed to the transfer of P from HP soil to LP soil by AMF hyphae. This novel root study container allows the biochar to be added to either the *root zone* or the *hyphal zone* and separates the effect of biochar on AMF hyphae development and P uptake from that on P content and availability (i.e., biochar rich in P; changes in soil pH). This device can contribute to discern whether biochar can influence AMF development and enhance P bioavailability.

In order to investigate the feasibility of adding biochar to soils with high residual P so that this can become bioavailable, *Lotus pedunculatus cv* barsille was grown in LP and HP soils separately amended with BP450, BP550 and BW550 biochars

at an application rate of 10 t ha^{-1} using the novel root study container for 32 wk without any further P and N fertilization. We found that (i) none of the tested biochars conferred any specific advantage to the HP soil; (ii) the addition of BW550 biochar to the LP soil increased plant growth by 59% and P uptake by 73%, while the pine–based biochar (e.g., BP450 and BP550) provided no extra nutrient uptake and no plant growth increase. This was ascribed to supplemental nutrients (especially P) from the BW550 biochar along with its liming effect and associated increase in P availability; (iii) biochar produced from BP450 biochar caused a 70% P uptake increase (and 40% plant growth increase) by stimulating AMF growth and accessing a high–P area (HP soil) to which the plant root had no access. More research is needed to discern the underlying mechanism.

The liming effects of BW550 and BP550 biochars were further compared with those of lime chemicals (e.g., $Ca(OH)_2$ and NaOH) in a short–term (10–d) incubation using two soils with contrasting pH–BC (an Haplic Cambisol and an Andic Umbrisol) to which these amendments were added. The two soils were first amended with BW550, BP550, $Ca(OH)_2$ or NaOH at specific rates so that pH values of 5.4, 5.6, 5.8 and 6.4 were targeted and incubated at room temperature (25 ^{o}C) for 10 d. At the end of the incubation, a radical elongation bioassay using alfalfa (*Medicago sativa* L.) was carried out. Thereafter, soils were characterized with special attention to the Al chemistry, i.e. aqueous reactive Al fractionation and inorganic monomeric Al speciation. The final objective was to reveal the mechanisms through which these biochars alleviate Al toxicity on roots. Results showed that, for a specific soil, a smaller amount of BW550 biochar was required to increase the same unit of pH and reduce a similar amount of exchangeable Al compared with the amount required of BP550 biochar. The addition of BW550 biochar (at application rates < 9.1 %) and $Ca(OH)_2$ stimulated alfalfa (*Medicago sativa* L.) seedling growth, whereas that of BP550 (at application rates >

2.4 %) and NaOH caused inhibition. The distinct responses of the root growth to the presence of $Ca(OH)_2$ and BW550 biochar and to that of NaOH and BP550 biochar were explained by (i) a decrease in both inorganic monomeric Al (mainly in AlF^{2+} and Al^{3+}) and colloidal Al, and (ii) an increase in aqueous Ca^{2+}, in the former, as expected. In the latter there was (i) an increase in aqueous colloidal Al and Na^{+}, and (ii) a decrease in soluble Ca^{2+}. Thus, BW550 biochar was shown to be a more effective liming agent than was BP550 biochar.

The information obtained in this thesis supports the use of biochar to manage high P affinity Andosols and acid soils, which are abundant in New Zealand. The technology of producing biochar from willow woodchips or feedstock alike with resultant solid products of high nutrient status and liming potential may contribute to the recycle of nutrients while increasing soil pH. Pine woodchips produced at relatively low temperature (e.g., 450^{o}C) have been shown to enhance AMF abundance and functionality. Thus, biochar with specific environmental and agricultural purposes should be tailored accordingly. The root study container with a layer of "P diffusion break" and the measurement of AMF hyphal length using the photomicrography in conjunction with image software analysis (e.g., ImageJ) will advance studies of the responses of AMF to soil additives (e.g., biochar or green waste) and their associated enhancement of soil functions.

ACKNOWLEDGEMENTS

I had never thought of writing a Ph.D thesis in a second language, in English, but now I did it!!! I am feeling thrilled! This dissertation is the result of three years of the lab works under the guidance of my GREAT supervisors, the discussion with colleagues and friends. I would like to take this opportunity to express my immense gratitude to all of them.

In particular, I am profoundly indebted to my supervisors, A/Prof. Dr. Marta Camps–Arbestain, Prof. Mike Hedley, and Dr. Miko U.F. Kirschbaum who are very generous with their time and knowledge and assist me in step–by–step to complete the thesis. Special thanks go to A/Prof Dr. Marta Camps–Arbestain, "Thank you for providing me with such a great opportunity to study under such an adorable and relaxed research and living environment. I have not been so enjoying my study before. And thank you for being so considerate and thoughtful, for all your encouragements and communications and kindness, and for culturing my writing skills of course. I know that the draft of my first manuscript was definitely a torture for you. Sorry for that." Thanks to Prof. Mike Hedley for all your optimistic comments on the results of each experiment and to Dr. Miko U.F. Kirschbaum who makes all this happen at the first step. Simple words cannot express my gratefulness and appreciation to you all!

My sincere appreciations are extended to Dr. Tao Wang, Dr. Roberto Calvelo–Pereira, Dr. Peter Bishop, Dr. James Hanly, A/Prof. Cory Matthew, Dr. Jeya Jeyakumar, and Dr. Saman Herath, Dr. Qianhe Liu etc. for their stimulating discussions and invaluable suggestions to my study and thesis writing.

I am grateful for the technical supports from staffs of soil science group, particularly Ms. Glenys Wallace, Mr. Bob Toes, Mr. Ian Furkert, Mr. Mike Bretherton, Mr. Lance Currie, A/Prof. Bob Stewart, Dr. Anja Moebis, and Mr. Ross Wallace etc..

Thanks also goes to Ms. Liza Haarhoff, Ms. Denise Stewart and Ms. Sandra Dunkinson for all your kind help with paperwork; and whomever help me during my study and stay in New Zealand.

Special thanks go to all my friends: Ainul Mahmud, Aldrin Rivas, Amandine Faury, Ahmed Elwan, Agneta Ghose, Helen Walker, Hamed Khan, Jingli Lu, Khadija Malik, Léa Carlesso, May Sasikunya, Neha Jha, Quang Mai Ngoc, Sue Gifford, Stephen Collins, Wei Zhang, Xiao–tian Li, Yan Li, Yuan–cheng Wang etc. (list in alphabetical order) for sharing happiness and making my life being oversea extremely enjoyable.

I gratefully acknowledge New Zealand Biochar Research Centre, Massey University whose research grant made the greenhouse and lab works possible.

However, I am the only person responsible for errors in the thesis if any.

I love my family, dad Pan–zhi Shen, mum Yan–rong Zhang, brother Jian–xing Shen and sister–in–law Xiu–ling Liu, and sister Jian–hua Shen and brother–in–law Qiu–long Tian, and nephews Bin–wei Tian and Hao Chen, the nieces Shi–ting Shen and Bin–xin Tian, God–parents Yan–kun Yang, and God–sister Xiu–fang Yang, back in China, thanks for all their supports and endless love.

Thanks you all!

This thesis is dedicated to—

Father Pan-zhi Shen

Mother Yan-rong Zhang

A/Prof. Dr Marta Camps-Arbestain

Prof. Mike J Hedley

Dr. Miko U.F. Kirschbaum

PUBLICATIONS AND PRESENTATIONS

Publication under review/to be submitted

1. **Qinhua Shen**, Miko U.F. Kirschbaum, Mike J. Hedley, Marta Camps–Arbestain (2016). Testing an alternative method for estimating the length of fungal hyphae using photomicrography and image processing. *PLoS ONE* (Accepted)

2. **Qinhua Shen**, Mike J. Hedley, Marta Camps–Arbestain, Miko U.F. Kirschbaum. A novel technique for evaluating the phosphorus transferred by arbuscular mycorrhizal fungi hyphae. *Soil Research* (To be submitted).

3. **Qinhua Shen**, Mike J. Hedley, Marta Camps–Arbestain, Miko U.F. Kirschbaum. Can biochar increase the bioavailability of phosphorus? *Journal of Soil Science and Plant Nutrition* (Accepted)

4. **Qinhua Shen**, Marta Camps–Arbestain, Mike J. Hedley, Miko U.F. Kirschbaum, Peter Bishop. Can Biochar Ameliorate Aluminium Phytotoxicity? *Geoderma* (To be submitted)

5. Huo–Yan Wang, **Qin-Hua Shen**, Jian–Min Zhou et al. (2011). Plants use alternative strategies to utilize non–exchangeable potassium in minerals. *Plant and soil* 343: 209–220

Book chapters

1. Balwant Singh, Michaela Mei Dolk, **Qinhua Shen,** Marta Camps–Arbestain (2015). Chapter 3 Biochar pH, electrical conductivity and liming potential. In: Balwant Singh, Marta Camps–Arbestain, Johannes Lehmann (Eds.), Methods of Biochar Analysis for Environmental Applications. CSIRO Publishing, Melbourne

2. Marta Camps–Arbestain, **Qinhua Shen**, Tao Wang (2015). Chapter 24 Biochar Available nutrients. In: Balwant Singh, Marta Camps–Arbestain, Johannes Lehmann (Eds.), Methods of Biochar Analysis for Environmental Applications. CSIRO Publishing, Melbourne

Abstracts/proceedings and posters/presentations in Conference/Worshop

1. **Qinhua Shen**, Marta Camps–Arbestain, Mike J. Hedley (2014). Use of Biochar to Reduce Soil Acidity and Ameliorate Aluminum Phytotoxicity. In "Proceedings of NZ Society of Soil Science Conference "Soil Science for Future Generations" (NZSSS: Halmiton, New Zealand).

2. **Qinhua Shen**, Mike J. Hedley, Marta Camps–Arbestain (2014). Can Biochar be Used to Increase the Bioavailability of Phosphorus Immobilized in Andisols? IDS 5. Biochar Soil Amendment for Environmental and Agronomic Benefits. In 'Proceedings of the 20th World Congress of Soil Science; Soils Embrace Life & Universe' (IUSS: Jeju, Korea).

3. **Qinhua Shen**, Mike J. Hedley, Marta Camps–Arbestain (2014). Can Biochar be Used to Increase the Bioavailability of Phosphorus Immobilized in Andisols? Nutrient Management for the Farm, Catchment and Community (Eds. L D Currie and C L Christensen). (FLRC, Massey University, Palmerston North, New Zealand).

4. **Qinhua Shen**, Marta Camps–Arbestain, Mike J. Hedley (2013). Influence of Biochar Application on the Availability of Phosphorus in Volcanic Ash soils. In "Proceedings of New Zealand 2013 Biochar Workshop of The Final Answer? (New Zealand Biochar Research Center:Palmerston North, New Zealand)

TABLE OF CONTENTS

LIST OF TABLES

LIST OF FIGURES

LIST OF ABBREVIATIONS

Al	Aluminium
Alox	Acid ammonium oxalate extractable aluminium
Alpy	Sodium pyrophosphate extractable aluminium
AMF	Arbuscular mycorrhizal fungi
C	Carbon
Ca	Calcium
Ca(OH)2	Calcium hydroxide
CaCO3	Calcium carbonate
CEC	Cation exchange capacity
Cl	Chloride
d	days
DGI	digital gridline intersection method
DM	dry matter
EC	Electrical conductivity
Fe	Iron
Feox	Acid ammonium oxalate extractable iron
Fepy	Sodium pyrophosphate extractable iron
FTIR	Fourier–transform infrared spectroscopy
GHG	Greenhouse gas
h	hours
H+	Hydrogen ions
HCl	Hydrogen chloride
K	Potassium
Mg	Magnesium
min	minutes
N	Nitrogen
Na	Sodium
NaHCO3	Sodium bicarbonate
NaOH	Sodium hydroxide
pH–BC	pH buffering capacity
PIP	photomicrography–ImageJ processing method
P	Phosphorus
RMSE	root mean square errors
VGI	visual gridline intersection method
wk	weeks
XPS	X–ray photoelectron spectroscopy

Chapter 1

GENERAL INTRODUCTION

This general introduction chapter provides (i) a general background of this research; (ii) the research objectives; and (iii) the outline of this thesis.

1.1. General background

Phosphorus deficiency and Al phytotoxicity have long been recognized as two main factors limiting crop yield in acid soils. Given the large coverage of these soils (ca 50% of the potentially arable lands of the world) (Bolan et al., 2003; Kochian et al., 2004)), they represent an important challenge for securing agricultural production worldwide. Attempts (e.g., heavy liming and P fertilization) have been made to manage these problems (Uchida and Hue, 2000; Curtin and Syers, 2001; Fardeau and Zapata, 2002). With the current ongoing agricultural production demand, and the fact that the decrease in mineable resources is expected to lead to a shortage of P rock (Cordell et al., 2009), other potential management practices should be considered. Organic residues resulting from composting and different types of digestion have been used as soil amendments to recycle nutrients (Haynes and Naidu, 1998; Haynes and Mokolobate, 2001; Mokolobate and Haynes, 2002; Xu et al., 2006; Hue et al., 1994; Berek et al., 1995; Butterly et al., 2013), but have also raised certain environmental concerns (e.g., eutrophication of water bodies and the presence of inorganic and organic pollutants and pathogens) after continuous application of these residues (Toor et al., 2006; Odlare et al., 2011; Lu et al., 2012).

Recently biochar has been proposed as an alternative option to overcome some of these limitations. Biochar is the solid product that results from thermally–treating biomass in the absence of or with limited amount of O_2 so that it can be added to soil for agronomic and environmental management (Lehmann and Joseph, 2015). Biochar mainly differs from charcoal in that the latter is intended to be used as fuel (Lehmann

and Joseph, 2015). Soil amended with biochar is advocated as a multiple–'win' strategy (Lehmann et al., 2006; Macías and Camps–Arbestain, 2010; Smider and Singh, 2014; Tammeorg et al., 2014; Jeffery et al., 2015) that includes:

(i) carbon sequestration;

(ii) waste disposal;

(iii) biofuel/bioenergy production;

(iv) pollutant immobilization;

(v) soil fertility enhancement

However, not all benefits can be maximized simultaneously and a compromise between them will inevitably occur (Jeffery et al., 2015). The application of biochar may enhance soil functions by modifying specific soil physical, chemical, and biological properties (Gul et al., 2015). A tailor–made biochar with high alkalinity may increase soil pH (Yuan and Xu, 2011; Yuan and Xu, 2012; Smider and Singh, 2014), and a biochar with high nutrient content (e.g., P and Ca) in the ash fraction may reduce soil fertility constraints (Mia et al., 2014). Subsequently, these effects result in an enhancement in soil functions, and thus, in crop performance (Jeffery et al., 2011; Smider and Singh, 2014; Tammeorg et al., 2014).

The impracticality of biochar removal once deployed, and the long–lasting nature of biochar implies the need for an in–depth understanding of the properties of the biochar to be applied to soil and a mechanistic knowledge of the response of the soil and the plant to this addition. This will depend on the types of feedstock, pyrolysis conditions (e.g., fast vs slow pyrolysis, final temperature of pyrolysis), and pre– and post–treatments (e.g., wet oxidation or steaming activation) (Singh et al., 2010a; Smith

et al., 2015; Yang et al., 2015), as well as the biochar application rate, its particle size, and the properties of the soil to be amended (Blackwell et al., 2010; Biederman and Harpole, 2013; Martinsen et al., 2015).

This technology caught the interest of the New Zealand Government (Winsley, 2007), given that more than half of greenhouse gas (GHG) emissions originate from the agriculture sector (Clark et al., 2011). Moreover, many New Zealand soils tend to be acidic in their pristine stage, and most pasture soils have pH values between 5.5 and 6.2 (Cornforth, 1998). It is also worth mentioning that in the North Island of New Zealand, soils developed from volcanic materials are dominant. In these soils, nanocrystalline minerals (e.g., allophane and ferrihydrite) prevail and have a high fixation capacity for phosphate anions causing the blockage of a relatively large fraction of P added as fertilizer (Parfitt, 1989). Thus, any possibilities to apply biochar to New Zealand acid soils in order to improve soil functions and sustainable agricultural production as well as C sequestration, should be considered and explored.

1.2. **Research objectives**

1.2.1 Main objective

This study intends to explore the possibility of using biochar for agronomic advantage beyond the service of C sequestration. Specifically, it intends to investigate the effect of biochars derived from willow woodchips and pine woodchips on (i) the

mobilization of residual P in sil–andic Andosols, and (ii) the amelioration of Al phytotoxicity in acid soils through changes in soil pH and AMF growth.

1.2.2 Specific objectives

Six sub–objectives are associated/derived from the main objectives, including:

Sub-objective 1 To develop specific analytical methods for biochar characterization, in particular, to establish an effective protocol for estimating the liming potential of biochars so that the biochar application rate can be determined when intending to increase soil pH to a specific value.

Sub-objective 2 To evaluate whether the current method intended to measure available N in biochars – originally developed using N–rich biochars (e.g., carbonized human– and animal wastes) – is suitable to characterize biochars low in N (e.g., woody biochars).

Sub-objective 3 To refine the established visual gridline intersection method by using the digital photomicrography technique and the available image processing software (e.g., ImageJ with/without NeuroJ) with the membrane filtration and staining (e.g., Typan blue) for measuring AMF hyphal length.

Sub-objective 4 To modify the common root study container by including a novel P diffusion barrier between contrasting P sources. This barrier should allow the transfer of P by AMF hyphae but impair P diffusion, thus making it possible to study

the influence of amendments prone to change P availability (e.g., fertilizers, lime, biochar) on the transfer of P by AMF hyphae.

Sub-objective 5 To test the effectiveness of specific biochars – produced from willow woodchips at 550^{o}C and pine woodchips at 450 ^{o}C and 550^{o}C – in improving the bioavailability of residual P in soils with high P–fixation (i.e., Andosols). In particular, to determine whether these biochars could enhance plant growth by mobilizing soil P through changing soil pH and/or facilitating the growth of AMF. The availability of P in biochar will also be investigated.

Sub-objective 6 To investigate the mechanisms involved in the amelioration of acid soils by the application of biochars of contrasting liming potential.

1.3. **Thesis outline**

The whole thesis includes 8 chapters described briefly as follows:

Chapter 1 (this chapter) is an introduction to the entire thesis and presents general background information and specifies the objectives of the current research and the outline of this dissertation.

Chapter 2 is a literature review that provides an overview on (i) acid soils and associated plant growth constraints; (ii) business–as–usual management practices intended to overcome soil acidity (e.g., inorganic liming amendments); (iii) the potential

for biochar to manage acid soils and, in particular, to alleviate P deficiency and Al phytotoxicity; and (iv) research gaps and priorities.

Chapter 3 tests current analytic methodologies for the measurement of the pH–buffering capacity and available N in biochars, and develops them further.

Chapter 4 presents two refined methodologies for measuring AMF external hyphal length in soil by deploying the photomicrography and image processing program (e.g., ImageJ software) in conjunction with the membrane filtration and staining techniques.

Chapter 5 presents a modified root study container involving a "P diffusion break" made of tephra soil in between two compartments – a root compartment to which root and AMF hyphae have full access and a root–free hyphal compartment to which only AMF hyphae can access – where soils with contrasting P status will be packed. This root study container will make it possible to evaluate the P transferred by AMF to the host plant while avoiding P diffusion.

Chapter 6 explores the possibility of using specific biochars (two produced from pine woodchip at 450 and 550^{o}C and a third one produced from willow woodchips at 550^{o}C) to increase the bioavailability of P immobilized in Andosols and thus increase the yield of *Lotus pedunculatus cv* barsille.

Chapter 7 compares the amelioration effects of two biochars (produced from willow woodchips and pine woodchips both at 550^{o}C) with those resulting from the addition of inorganic liming chemicals [$Ca(OH)_2$ and NaOH] to two acidic soils of

contrasting pH–buffering capacity. It also evaluates the responses of the alfalfa (*Medicago sativa* L.) to these amendments and investigates the underlying mechanisms.

Chapter 8 is a general summary of the whole thesis and a discussion on some future research recommendations.

Note that (1) The content of Chapter 3 will be published as part of two book chapters in: Balwant Singh, Marta Camps–Arbestain, Johannes Lehmann (2015). Methods of Biochar Analysis for Environmental Applications. CSIRO Publishing, Melbourne; (2) Chapter 4 – 7 have been submitted to or are in the process of submission for journal publications – this information is provided in each chapter. As these stand–alone chapters were written according to the format requirements from different journals, the structure of each chapter may differ slightly; and overlapping and repetition occur between some sections.

Chapter 2

LITERATURE REVIEW

This literature review provides an overview on (i) acid soils and associated plant growth constraints; (ii) business–as–usual management practices intended to overcome soil acidity (e.g., inorganic liming amendments); (iii) the potential for biochar to manage acid soils and, in particular, to alleviate P deficiency and Al phytotoxicity; and (iv) research gaps and priorities.

2.1 An overview on acid soils

2.1.1 Acid soil distribution

Acidity is measured on the pH. A pH of 7.0 is neutral, pH values below 7 are considered acidic. Von Uexküll and Mutert (1995), however, defined acid soils as soils with a pH < 5.5. Acid soils cover ca 30% of the total ice–free land area and ca 50% of the potentially arable lands of the world (Kochian et al., 2004); ca 75% of these areas are also affected by subsoil acidity (Sumner and Noble, 2003). On a global scale, there are two main geographical belts of acid soils: (i) the northern belt (cold and temperate climate) which is dominated by Podzols, and (ii) the southern tropical belt that consists largely of Acrisols and Ferralsols (Figure 2–1) (Herrera–Estrella, 1999). Acid soils also occur in Andosols, Arenosols, Alisols, Albeluvisols, Cambisols, Histosols, Leptosols, Plinthosols, Planosols, Fluvisols, Regosols and Umbrisols (IUSS Working Group, 2006) (Table 2–1).

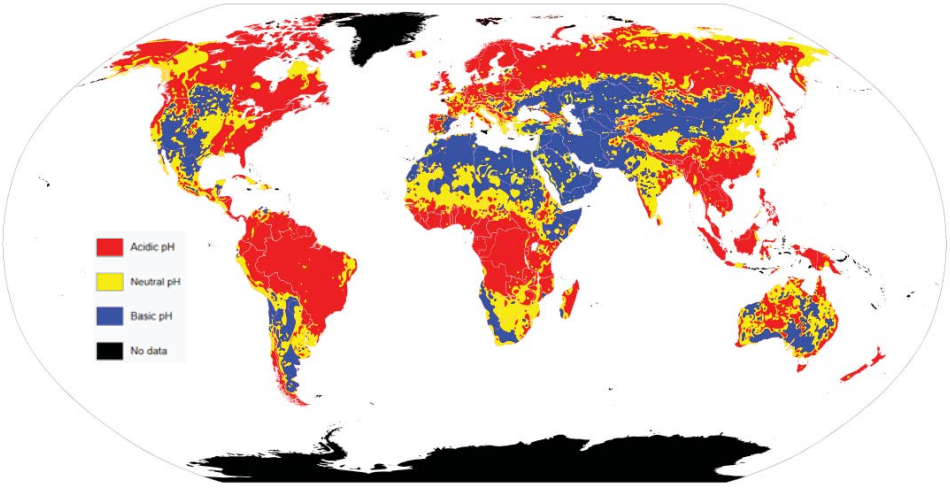

Figure 2–1 World acid soils distribution (Ninjatacoshell, 2015).

Table 2-1 Surface distribution of acids soils in the world (left column) and in the region of Australia and New Zealand (right column) by soil group (Von Uexküll and Mutert, 1995)

Soil group	World million ha	Australia and New Zealand million ha
Fluvisols	49,741	107
Gleysols	401,747	551
Regosols	293,166	97,399
Arenosols	280,291	83,473
Rankers	60,878	85
Andosols	33,975	1,751
Cambisols	299,539	11,874
Podzoluvisols	254.881	0
Podzols	415,186	11,427
Planosols	15,262	7,668
Acrisols	731,032	12,944
Nitosols	117,907	2,158
Ferralsols	726,592	9,414
Histosols	270,224	495
Total	3,950,421	239,346
% of area	30	30

2.1.2 Soil acidification

Acidification occurs primarily through agricultural product removal and/or increases in N and S inputs (e.g., legume pastures, fertilizer inputs, atmospheric deposition) in agricultural soils. These inputs are either directly converted into acid–generating compounds (e.g., NH_4^+ upon oxidation), and/or contribute to the loss of charge–balancing base cations (Ca^{2+}, Mg^{2+}, K^+ or Na^+) when either NO_3^- or SO_4^{2-} leaves the system in product removal or by leaching (Adams, 1981; Bolan et al., 2003). For instance, during nitrification two net H^+ ions are generated whereas one H^+ is the net balance from both ammonification and nitrification (Figure 2–2). This acidity can only be neutralized if NO_3^- can be completely transformed back into the original input forms. However, some NO_3^- is usually leached through the soil profile along with charge–balancing base cations and thus acidity tends to remain in the system (Haynes, 1983; Edmeades and Ridley, 2003). Rates of acidification vary from 0.7 kmol H^+ ha^{-1} $year^{-1}$ in pristine systems to as high as 40 kmol H^+ ha^{-1} $year^{-1}$ in production systems receiving high rates of ammonium–N fertilizers (Sumner and Noble, 2003). As animal–grazed pastures mainly relying on legumes dominates New Zealand's agriculture, particular attention has to be paid to the acidification of New Zealand soils (Bolan et al., 1991).

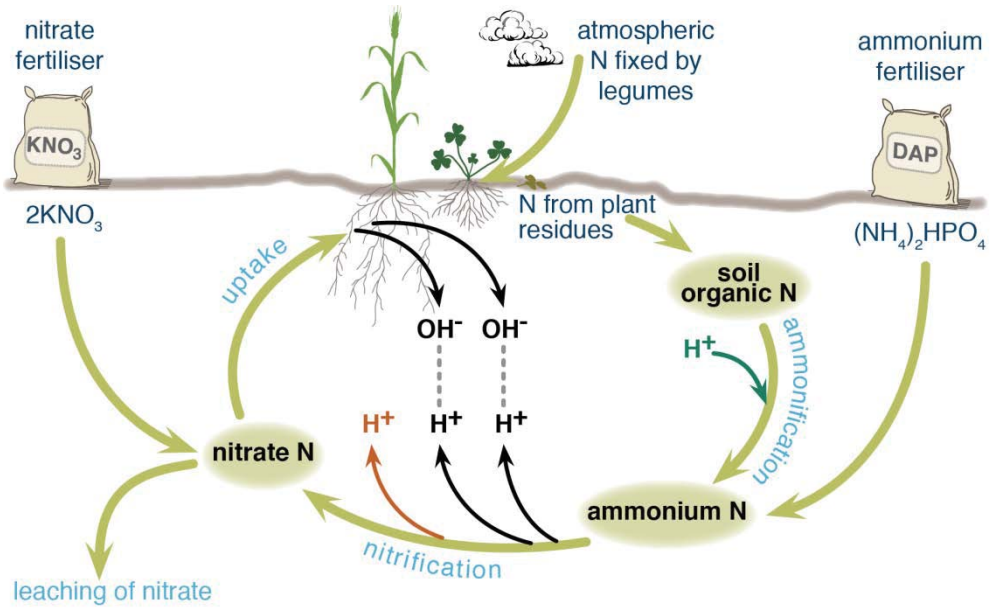

Figure 2–2 Different nitrogen fertilizers follow different pathways in the nitrogen cycle causing the release of different amounts of hydrogen ions (Government of Western Australia, 2015)

2.1.3 Constraints to plant growth in acid soil

The chemical nature of acid–induced constraints to plant growth – toxicity of specific metals (e.g., Al and Mn), nutrient deficiency (e.g., P and Ca) (Figure 2–3), decrease in cation exchange capacity by formation of hydroxyl–Al intergrades in expanding layer silicates – has long since been recognized (Adams, 1981).

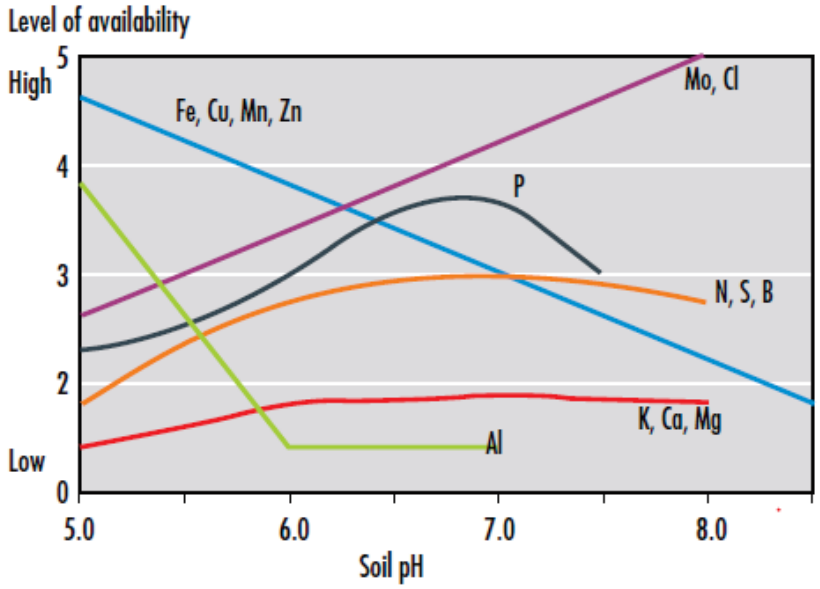

Figure 2–3 Relationship between the availability of elements and soil pH (Hede et al., 2001)

Aluminium phytotoxicity is governed by the amount and forms of Al present in soil solution, and this depends on soil pH, the solubility of Al–containing soil constituents, and organic matter content (given its chelating properties) (Adams, 1981; Barceló et al., 1995; Takahashi et al., 2007). Concentration of Al^{3+} in solution increases exponentially as soil pH decreases below 5 (Figure 2–3), as an increase in H_3O^+ in solution results in a more rapid diffusion of protons into the soil mineral structure and promotes hydrolysis (Robarge, 1999). Predominant Al species in acid soils are the mononuclear species ($AlOH^{2+}$, $Al(OH)_2^+$, $Al(OH)_3$, and $Al(OH)_4^-$) (Figure 2–4), and soluble complexes with inorganic ligands such as sulfate and fluoride, and also with many organic compounds. Larger polynuclear hydroxyl Al species also form as metastable intermediates during $Al(OH)_3$ precipitation. The mononuclear $A1^{3+}$ species seems to be most toxic at low pH, at which it exists as an octahedral hexahydrate

(Kinraide, 1991; Stass et al., 2006), inhibiting cell division and elongation (Kidd and Proctor, 2001; Edmeades and Ridley, 2003) and thus stunts root growth (Foy, 1988). This results in an inefficient nutrient uptake, including that of P (Kidd and Proctor, 2001).

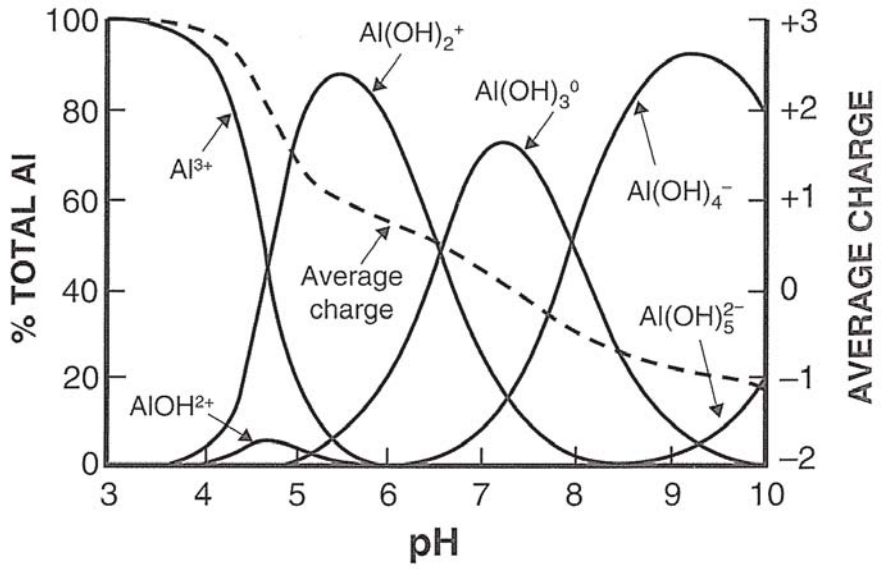

Figure 2–4 Relationship between pH and the distribution of soluble aluminium species (Sparks, 2003);

Retention of phosphate by soil particles is strongly related to binding on Al and Fe oxy–hydroxides and short–range ordered aluminosilicates (i.e., allophane). At low pH values, these amphoteric adsorbents become more positively charged due to protonation (Figure 2–5a) thus increasing their phosphate retention capacity (Saunders, 1959b; Bolan et al., 1999). Two major reactions − adsorption and precipitation − are involved in the process of P fixation on these surfaces (Parfitt, 1989). The former occurs mainly through ligand–exchange reactions (i.e., formation of inner–sphere complexes)

of P–OH groups with exposed –OH/OH_2 groups in Fe and Al oxy–hydroxides and short–range ordered aluminosilicates (Figure 2–5b) (Munns and Fox, 1976; Parfitt, 1978; Goldberg and Sposito, 1985; Beck et al., 1999), although outer–sphere type of interactions may also occur (Johnson et al., 2002). Over time, after this initial adsorption, local solutes may become concentrated causing the precipitation of Al/Fe phosphate (Munns and Fox, 1976; Imai et al., 1981), with some phosphate becoming occluded and isolated from solution (Li and Stanforth, 2000). These reactions depend on soil pH and the saturation of surface binding sites with P (Goldberg and Sposito, 1985). In the North Island of New Zealand, soils developed from volcanic materials are common. In soils formed from andesitic tephra allophane is a prevalent soil constituent along with ferrihydrite. These nanocrystalline minerals have a high affinity for phosphate anions causing the immobilization of a relatively large fraction of P added as fertilizer (Parfitt, 1989). This has led to an accumulation of up to almost 4 t P ha^{-1} in intensively farmed allophanic Andisols in New Zealand (Perrott and Sarathchandra, 1987; Perrott et al., 1989).

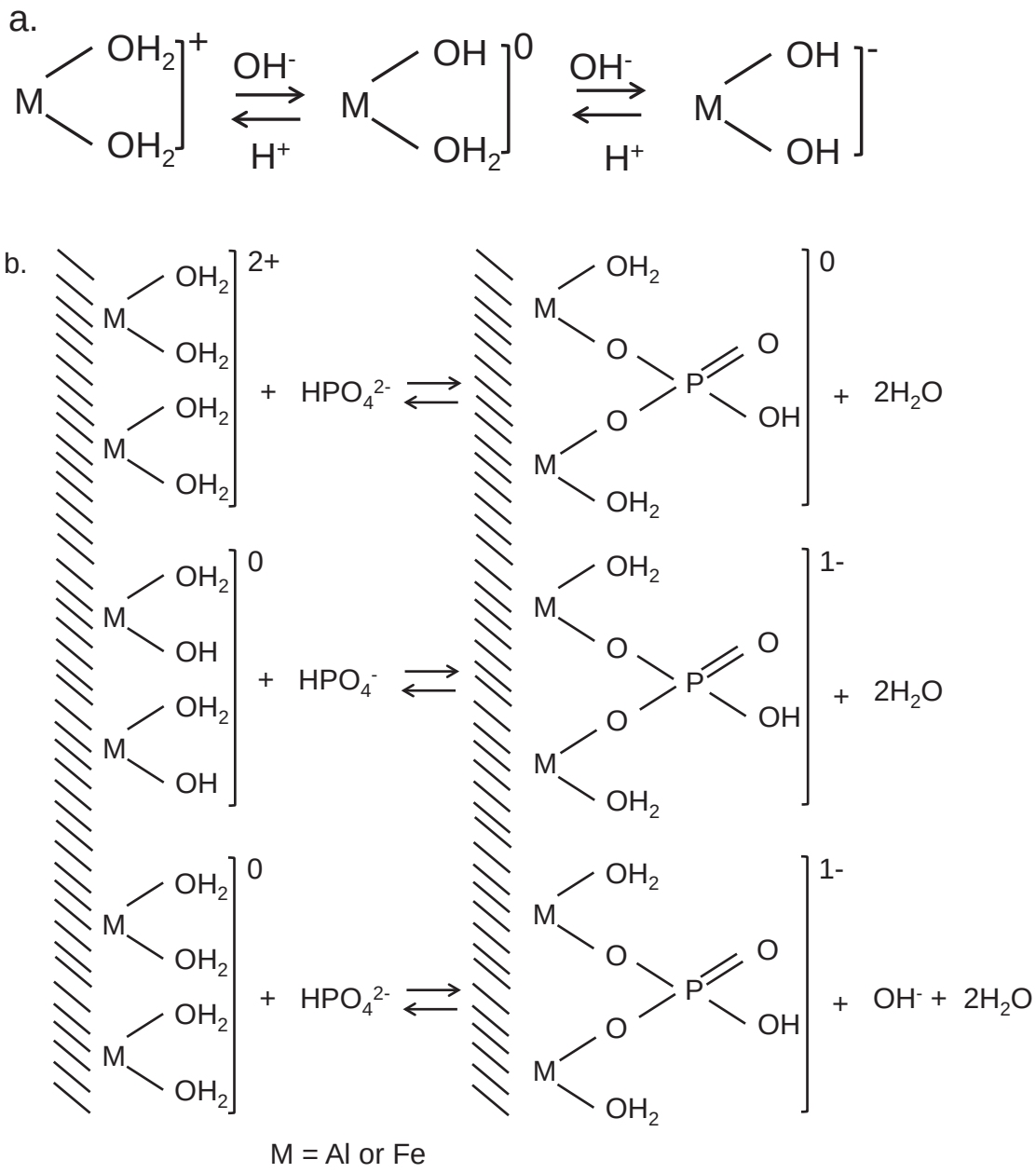

Figure 2–5 Schematic diagram of (a) the pH–dependent surface charge on an amphoteric metal oxide surface (Haynes, 1982) and (b) examples of ligand exchange reactions with phosphate (Cornforth, 2013)

2.2 Management of acid soils

2.2.1 Chemical liming

Liming materials (e.g., oxides, hydroxides, and carbonates of Ca or Ca–Mg mixtures) have long been used to manage acid soils (Bolan et al., 2003). Excess OH^- produced by the application of liming material favours the polymerization of Al in solution and this may precipitate whenever the solubility product is exceeded (Figure 2–6). The effect of excess OH^- on soil pH will depend on the pH–buffering capacity of the soil (Aitken, 1992; Nelson and Su, 2010). The increase in plant available Ca and/or Mg resulting from the addition of liming materials further alleviates Al toxicity to plants as these cations block Al absorption sites in plant roots (Kinraide and Parker, 1987), this effect being special effective in the case of Mg (Barceló et al., 1995; Silva et al., 2001; Bose et al., 2011; Hossain et al., 2014). The proposed mechanisms for Al^{3+} toxicity alleviation by Ca^{2+} and/or Mg^{2+} ions include (i) a reduction in Al^{3+} saturation at the apoplastic exchange sites on plant root; and (ii) a decreased Al^{3+} activity at the root cell plasma membrane surface (Kinraide, 1994, 1998; Bose et al., 2011).

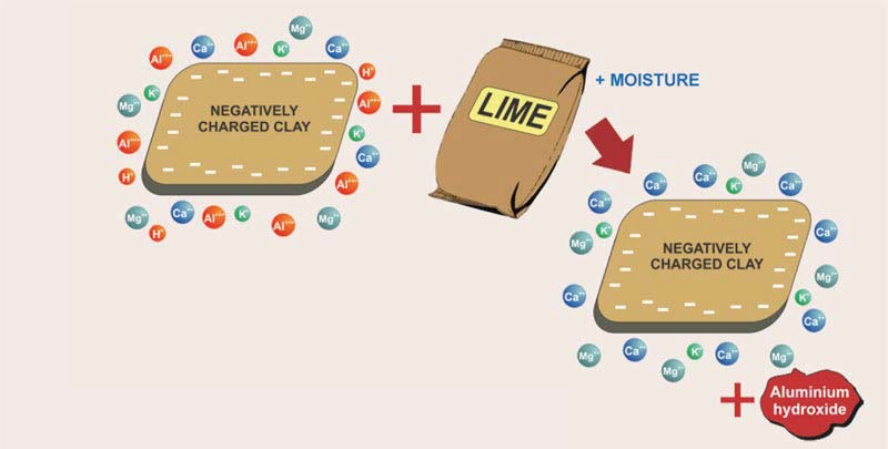

Figure 2–6 The reactions occurring as a result of soil liming (Grain SA, 2013)

The effect of liming on P availability is influenced by the existence/non–existence of Al phytotoxicity. In acid soils where Al toxicity is a major problem, lime decreases Al toxicity to roots and overcomes the associated stunted root growth; this subsequently increases P accessibility to plants and mitigates P deficiency (Bolan et al., 2003). Where Al content is not high enough to impair root growth, the effect of liming on P availability varies from negative, to neutral and positive. An enhanced P bioavailability is however often anticipated and it is ascribed to (i) a decrease in P adsorption on amphoteric soil surfaces caused by an induced pH increase in negative surface charge; (ii) an enhanced solubilisation of mineral P (e.g., strengite and variscite) and (iii) an enhanced mineralization of organic P as favoured by the increase in soil pH (Haynes, 1982). However, in some instances, the Ca/Mg commonly added to the system with the liming materials may precipitate with newly available P oxy–anions causing a decrease in P availability (Edmeades et al., 1984). Thus P fertilizers application may still be required alongside to improve soil fertility (Mansell et al., 1984).

2.2.2 Organic amendments

The incorporation of certain organic residues (e.g., anaerobic municipal sludges or manure) to acid soils has been proposed as a substitute for inorganic liming materials (Whalen et al., 2000; Petersen et al., 2003), as these may provide certain advantages: (i) the inherent P content of some of organic residues (e.g., poultry litter, sewage sludge) may contribute to plant available P (Larney and Angers, 2012); and organic acids in the residue or generated during its decomposition may (ii) enhance P solubilisation via metal complexation reactions (Iyamuremye and Dick, 1996) and (iii) block P sorption sites on Al and Fe (hydro)oxides (Jackman, 1964a, b); and/or (iv) contribute to Al detoxification (Hue et al., 1986; Mokolobate and Haynes, 2002; Camps–Arbestain et al., 2003).

The application of organic wastes (e.g., anaerobic municipal sludges) to acid soils has however been questioned in some instances because of: (i) the potential increase in the load of inorganic (e.g., As, Cd, Cr, Cu) and organic pollutants, as well as that pathogens to the environment (Odlare et al., 2011; Lu et al., 2012); and (ii) the potential of causing a net acidifying effect (e.g., through nitrification) (Egiarte et al., 2005) – the more chemically–reduced the waste and the smaller the acid–buffering capacity of the soil, the greater the risk of soil acidification (Egiarte et al., 2005)

2.3 Potential of biochar for alleviating P deficiency and Al toxicity in acid soils

Biochar is the solid product that results from thermally–treating biomass in the absence of, or with limited amount of O_2, with the intention to be added to soil for improved agronomic and environmental outcomes (Lehmann and Joseph, 2015). For a charred material to be referred to as biochar, it must comply with a series of requisites, including (i) a carbon content higher than 10% (dry mass basis), (ii) a $H:C_{org} < 0.7$, and (iii) the compliance of specific thresholds for heavy metals, metalloids, and organic contaminants (IBI, 2012). The greatest chemical difference between biochar and the feedstock (e.g. wood, litter, compost, manure and biosolids) from which biochar is produced is the much larger proportion of condensed aromatic C in the former, for which a greater activation energy is needed to decompose it compared with common soil organic matter constituents (Lehmann et al. 2015). Biochar technology has thus been proposed as a C sequestration approach to contribute to the mitigation of greenhouse gas (GHG) emissions (Lehmann et al., 2006; Macías and Camps–Arbestain, 2010).

In addition to C sequestration (Lehmann and Joseph, 2015), the use of biochar in soil can provide agronomic and environmental benefits, such as (i) the reduction in nutrient loss through increasing cation adsorption (Laird et al., 2010); (ii) the supply of plant–available nutrients (e.g., P) (Wang et al., 2013a); (iii) an improvement of soil structural properties (Herath et al., 2013); (iv) act as a liming agent (Rodriguez et al., 2009; Yuan and Xu, 2012); (v) enhance soil biological community abundance and functions (Pietikäinen et al., 2000; Anderson et al., 2011; Lehmann et al., 2011; Chen et

al., 2013; Gomez et al., 2013); (vi) contribute to remediate contaminated sites (Beesley et al., 2011; Gregory et al., 2014); and (vii) reduce non–CO_2 greenhouse gas emissions (Singh et al., 2010b; Anderson et al., 2011; Cayuela et al., 2013; Cayuela et al., 2014). However, given the variety of feedstocks and process conditions used to produce biochar, not all benefits can be simultaneously maximized and a compromise between them will inexorably occur (Jeffery et al., 2015). The next section attempts to explore the possibility of exploiting biochar for ameliorating problems associated with acid soils, mainly P deficiency and Al toxicity.

2.3.1 Liming potential of specific biochars

During pyrolysis, the acidity of the original feedstock tends to be preferentially removed (e.g., as CO_2, acidic functional groups), resulting in a residual accumulation of ash (Ueno et al., 2008; Yip et al., 2009; Fuertes et al., 2010; Singh et al., 2010a). This ash is enriched in salts that differ in their water solubility and includes (i) readily soluble salts, (ii) carbonates (either from CO_2 evolved during pyrolysis and trapped by alkaline material or carbonates originally present in the feedstock), (iii) sparingly soluble metal oxides and hydroxides (that will become enriched at temperature > 600 ^{o}C, at which carbonates thermally decompose), and (iv) silicates, the latter being especially the case when feedstock contain soil particles (Glaser et al., 2002; Okuno et al., 2005; Vassilev et al., 2013a, b; Wang et al., 2014). Most of these salts have significant liming value (Vassilev et al., 2013b; Smider and Singh, 2014). The ash fraction is feedstock– and pyrolysis process– dependent (Xie et al., 2014).

Acidic organic functional groups, such as carboxylic groups, are practically absent in freshly produced biochar, although they will tend to form over time as the subsequent exposure of biochar surfaces to an oxygenated atmosphere will lead to their oxidation and the formation of oxygen containing functional groups (e.g., carboxyl, hydroxyl, and carbonyl groups) (Cheng et al., 2006; Cheng et al., 2008; Calvelo Pereira et al., 2014). Carboxylic functional groups tend to be more abundant in those biochars produced at the lower temperature compared with high temperature biochars, as decarboxylation reactions increase with increasing pyrolysis temperature (Bourke et al., 2007; Singh et al., 2010a; Uchimiya et al., 2011; Calvelo–Pereira et al., 2015; Jiang et al., 2015). Acidic organic functional groups in biochar confer the biochar with a pH–dependent charge that contributes not only to buffer soil pH (Novak et al., 2009; Yuan et al., 2011b) but also to the retention of nutrient cations (Cheng et al., 2006). Biochars can be purpose–made so that they are enriched with surface charge (Nuithitikul et al., 2010). Pre-treatment of wood with alkaline tannery waste has been shown to increase the content of carboxylic functional groups (Hina et al., 2010). Others have been post–treated charcoals by steam activation (Uchimiya et al., 2011) and wet oxidation (e.g., HNO_3, H_2O_2, NaOCl, $(NH_4)_2S_2O_8$) for such purposes (Figure 2–7) (Moreno–Castilla et al., 2000; Tabti et al., 2014).

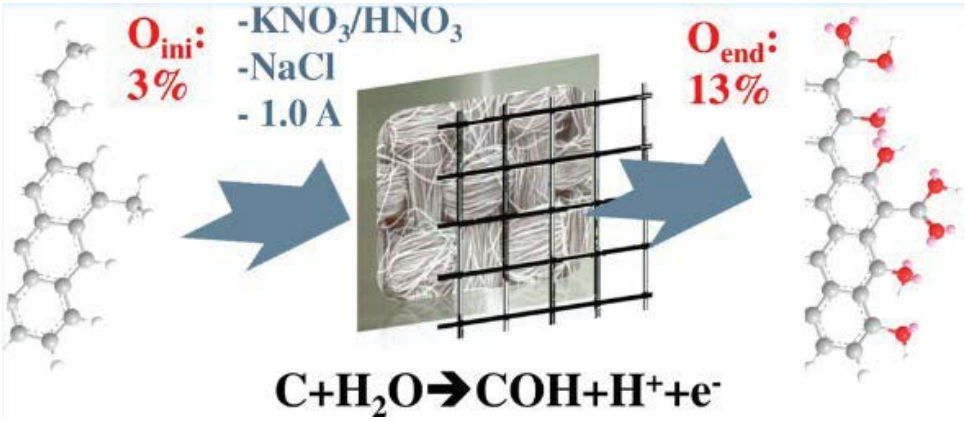

Figure 2–7 The wet–oxidation of activated carbon by adding KNO_3/HNO_3 to increase carboxylic functional groups (Tabti et al., 2014)

Several studies in the literature have reported an increase in soil pH and a decrease in exchange acidity and exchangeable Al upon biochar application (Rodriguez et al., 2009; Yuan et al., 2011a; Hass et al., 2012; Yuan and Xu, 2012; Chintala et al., 2013; Slavich et al., 2013; Masud et al., 2014; Wan et al., 2014; Martinsen et al., 2015; Zhao et al., 2015). For example, the addition of 2% pecan shell biochar produced at 700^{o}C to a sandy soil caused an 1.5–unit increase in pH, and a 50% and 38% reduction in exchangeable acidity and monomeric Al species on exchange sites, respectively (Novak et al., 2009). This has been attributed to the solubilisation of alkaline salts present in the ash fraction of biochars (Chan et al., 2007; Novak et al., 2009; Chintala et al., 2013) with the subsequent displacement of exchangeable Al^{3+} and H^{+} (Chan et al., 2008; Rezaul Karim, 2011; Hass et al., 2012; Chintala et al., 2013) and the formation of Al–hydroxyl ions and/or precipitates of displaced Al hydroxides (Ritchie, 1994; Masud et al., 2014). Moreover, the oxygen–containing functional groups on the biochar surface can complex Al^{3+} (Qian et al., 2013), thus further contributing to a decrease in Al in

solution (Yuan and Xu, 2012). Several studies have shown the decrease in exchangeable and soluble Al and precipitation of Al as hydroxy–Al species after the addition of biochar (Novak et al., 2009; Major et al., 2010; Van Zwieten et al., 2010; Yuan et al., 2011a). Yet specific studies on changes in the fractionation of soluble Al and its speciation upon the addition of biochar to soil have not yet been carried out.

2.3.2 Quantitative measurements of acidity and alkalinity of biochar

Several studies have characterized the surface acidic functional groups of biochar following different procedures, including boehm and potentiometric titrations, fourier–transform infrared spectroscopy (FTIR) and X–ray photoelectron spectroscopy (XPS) analyses (Calvelo–Pereira et al., 2015). Also, different methods to quantify the carbonate–C content in biochar have been tested including titrimetric methods, acid fumigation/acid wash prior to dry combustion and thermogravimetric analysis (Wang et al., 2014). The total alkalinity of biochar has been quantified by adding an acidic solution to the biochar let it stand for 24 h followed by titrating the resulting extracts to pH 7.0 with consumed base (Yuan and Xu, 2011), similar to the method proposed for the measurement of the liming potential of biochars by International Biochar Initiative (2012) following the method of Rayment and Lyons (2011) (originally used to measure soil carbonate content). In fact the latter, generally reported as the equivalent proportion of the liming effect that $CaCO_3$ would have (referred to as % $CaCO_3$–eq), has been used to classify biochars into the following classes: (i) Class 0 (< 1 %$CaCO_3$–eq), (ii) Class 1 (1 to 10 % $CaCO_3$–eq), (iii) Class 2 (10 to 20 %$CaCO_3$–eq); (iv) Class 3 (>

20 %$CaCO_3$–eq) (Camps–Arbestain et al., 2015). However, no studies to present have evaluated different methodologies to determine the pH–buffering capacity of biochars and compared with the proposed methodology to determine the liming equivalence. Therefore, further research in this area is required.

2.3.3 Effects of biochar on soil P bioavailability

During pyrolysis of organic material a complex mixture of P species are formed. This may include amorphous, semi–crystalline and crystalline constituents, along with organic constituents (Uchimiya and Hiradate, 2014; Uchimiya et al., 2015). However, organic P forms will tend to disappear while inorganic P forms will subsequently be formed, with crystallinity increasing as pyrolysis temperature increases (Zwetsloot et al., 2015). Phytate has been observed to be converted to inorganic P when pyrolysing at temperatures ≥ 350°C (Uchimiya and Hiradate, 2014). Orthophosphate (PO_4^{3-}) is the only P species observed in biochars produced from manures at temperatures ≥ 500°C (Wang et al., 2013a), whereas pyrophosphate ($P_2O_7^{4-}$) can still be found in biochars produced from plant residues at temperatures as high as 650°C (Uchimiya and Hiradate, 2014). Crystalline phosphorus minerals that have been identified in biochars include: whitlockite [$(Ca, Mg)_3(PO_4)_2$] in biochars produced from manure at 500°C (Cao and Harris, 2010), dehydrated struvite (NH_4MgPO_4) in biochars produced from cattle manure and sewage sludge (Wang et al., 2012b), and hydroxyapatite [$Ca_5(PO_4)_3(OH)$] in biochars made from mixtures of either wood or corn and slaughterhouse waste (Zwetsloot et al., 2015). A decrease in crystallinity of hydroxyapatite has been observed in the former biochars when biomass (e.g., wood,

corn residue) was added to these wastes prior to pyrolysis, thus increasing the soluble P fraction out of total P (although total P was diluted by doing so) (Zwetsloot et al., 2015).

In addition to pyrolysis conditions, the availability of P in biochars is related to (i) the amount of P originally present in the feedstocks, and (ii) the nature of the form of P. Biochars produced from lignocellulitic residues generally have a low amount of available P (< 1 g kg^{-1} as estimated using 2% formic acid proposed by Wang et al. (2012b), whereas considerable amounts of available P can be found in biochars derived from animal and human waste (> 4 g kg^{-1}) (Camps–Arbestain et al., 2015). Values of 2% formic acid extractable P > 100 g kg^{-1} have also been reported by Weber et al. (2014) when using meat and bone meal as feedstock, these representing > 90% of total P. The fraction of available P out of total P is also generally smaller in plant residue–derived biochars (< 40%) than in animal–waste–derived biochars (> 65%) (Camps–Arbestain et al., 2015). Uchimiya et al. (2015) detected a dominance of pyrophosphate over orthophosphate in biochars pyrolysis from cotton seed hulls under 350 and 650°C. They suggested that this form of P in these biochars might be stabilized through complexation of P with ash components or with organic C (e.g., electrostatic and H–bonding interactions) rendering it less available.

These stabilization mechanisms have been shown to become impaired when adding soda to the feedstocks prior to pyrolysis, as P extractable by 2% formic acid and 2% citric acid in biochars made from canola cake and dried distillers grain feedstocks increased from < 10% total P to > 60% total P (Weber et al., 2014). Alternative treatments to increase the fertilizer value of biochars, as shown in those produced from jarrah wood, including the activation with phosphoric acid and blending with high Fe–bearing kaolinite clay, chicken manure, phosphate rock, ilmenite and dolomite. This has

rendered products with up to 26 g kg^{-1} of P extracted by 1 M ammonium citrate at pH 7 (Nielsen et al., 2014).

2.3.4 Effects of biochar on AMF growth

More than 90% of plant species have a symbiotic association with arbuscular mycorrhizal fungi (AMF) (Schachtman et al., 1998). Fungal hyphae play an important role in the forage and acquisition of P for plant uptake (Bolan, 1991; Smith and Read, 2010). An extensive network of hyphae extends from plant roots, enabling the plant to explore a greater volume of soil, thereby overcoming the limitations imposed by the slow diffusion of P in the soil (Bolan, 1991). Biochar application has been found to effect soil microflora community and function (Kim et al., 2007; Grossman et al., 2010; Gomez et al., 2013), although this is soil– and biochar–dependent with potential impacts on: (i) nutrient status and C availability; (ii) soil pH; (iii) bacterial adhesion capacities; (iv) capacity for protecting bacteria from predators; and (v) effects of toxins and other environmental pressures, such as water stress (Lehmann et al., 2011; Wang et al., 2015a). In recent years several studies on the potential impact of biochar application on AMF growth in soil and its subsequent effect on plant P uptake have been carried out (Matsubara et al., 2002; Choi et al., 2009; Habte and Antal, 2010; Warnock et al., 2010), but a mechanistic understanding has not yet been attained. In addition to the different biochar and soil type combinations, the use of different experimental approaches, including different AMF and plant species, have made the comparison between studies difficult contributing to the lack of consistency.

To our knowledge, previous research has mostly focused on the quantification of root colonization by AMF and its influence on P uptake (Matsubara et al., 1995; Solaiman et al., 2010a; Warnock et al., 2010; Nzanza et al., 2012). Much less is known on the impacts that biochar addition has on the development of AMF external hyphae. In many instances, the effects of biochar on AMF hyphae growth and associated contribution to plant P uptake and growth have not been distinguished from those of root growth. Recently, Hammer *et al.* (2014) presented the first evidence that AMF could use biochar as a supporting matrix and nutrient source, and looked into the influence of biochar on the establishment of AMF attachments to plant root and its contribution to P foraging and acquisition. However, this study was conducted under soil–less conditions, which are likely to underestimate the potential effect of AMF on P uptake from a biochar–amended soil due to a more effective P movement in the absence of a soil matrix. This warrants the need for the design of an experimental setting able to distinguish the contribution of biochar on root growth from that on AMF development and the subsequent effect on P plant uptake and growth.

The method most frequently used to study the influence of biochar on AMF abundance or root colonization by AMF is the traditional gridline intersection method (Ishii and Kadoya, 1994; Solaiman et al., 2010b; Warnock et al., 2010; Vanek and Lehmann, 2014). This method utilizes specific stains (e.g., Typan blue) to visualize AMF and quantifies fungi by counting the intersections of the visualized hyphae with the gridline on the eye–piece under microscopy (Phillips and Hayman, 1970; McGonigle et al., 1990). This methodology is neither quantitative nor objective (Giovannetti and Mosse, 1980), and this may have to some extent contributed to above–mentioned inconsistences. Therefore, a more objective and comparable procedure is

needed to advance in the research on the extra–radical hyphal network of AMF (Green et al., 1994; Leake et al., 2004).

2.4 Current research gaps and priorities in biochar application to acid soils

The following research gaps and priorities related to the impact of biochar on P deficiency and Al toxicity in acid soils have been identified and listed below:

I. It is well–known that the characteristics and particularly the liming capacity and the fertilizer value of biochars will influence their use as soil amendment. The characterization of biochar is often carried out using inconsistent and sometimes unsuitable laboratory procedures. It is difficult to compare the results from different studies and draw useful conclusions. The analytical methods for biochar characterization need to be tested.

II. The traditional gridline–intersection methodology commonly used for measuring AMF abundance is observer–dependent and that may partially contribute to the varied range of responses of AMF growth to biochar addition reported in the literature. The possibility that advanced techniques (e.g., photomicrography and image processing techniques) can be used to develop a relatively observer–independent method to measure AMF external mycelium length for reliable comparison needs to be tested.

III. Reports indicate that certain biochars stimulate the development of AMF delivering an increase in plant P uptake. However, the extent to which the stimulation of biochar on AMF contributes to plant P acquisition is often confounded by the effect of biochar on plant root growth as well as the P diffusion. Thus, a design of an experimental setting able to excluding the P diffusion thus distinguish the contribution of biochar on AMF development from that on root growth and the subsequent effect on P plant uptake and growth is needed.

IV. The potential of biochar to increase soil pH and stimulate AMF growth as well as to supply P fertilization provides an interesting opportunity for this amendment to be used in P–deficient acid soils, such as allophanic Andosols, common in the North Island of New Zealand. To present no studies in this area have been yet carried out.

V. Biochar has been used as liming agent to ameliorate acid soils, yet, very little is known about the mechanistic principles through which biochar ameliorate the common Al toxicity affecting plants growing in these soils. An in–depth study on the effect of biochar liming properties on soil chemistry has not yet been reported.

Chapter 3

BIOCHAR CHARACTERIZATION

The characteristics of biochar, in particular, its liming capacity and fertilizer value, govern their use as soil amendment. An adequate knowledge of these biochar attributes is thus needed before their application to soil. The characterization of biochar is often carried out using inconsistent and sometimes unsuitable laboratory procedures, which makes the comparison of results from different studies and the drawing of useful conclusions difficult. This chapter aims to compare methodologies intended to measure the liming property and the available N content of biochar.

The content of this chapter will be published as part of two book chapters:

Balwant Singh, Michaela Mei Dolk, **Qinhua Shen**, Marta Camps–Arbestain (2015). Chapter 3 Biochar pH, electrical conductivity and liming potential. In: Balwant Singh, Marta Camps–Arbestain, Johannes Lehmann (Eds.), Methods of Biochar Analysis for Environmental Applications. CSIRO Publishing, Melbourne

Marta Camps–Arbestain, **Qinhua Shen**, Tao Wang, Lukas van Zwieten, Jeff Novak (2015). Chapter 24 Biochar Available nutrients. In: Balwant Singh, Marta Camps–Arbestain, Johannes Lehmann (Eds.), Methods of Biochar Analysis for Environmental Applications. CSIRO Publishing, Melbourne

---

3.1 Liming potential

Biochar results from thermally–heating biomass in the absence of or with limited amount of O_2 (Lehmann and Joseph, 2015). Most biochars are alkaline and have a range of liming potential values, these being feedstock– and pyrolysis process–dependent (Hossain et al., 2010; Laird et al., 2010; Xie et al., 2014). Biochars with liming properties could be used as liming agents in acidic soils (Novak et al., 2009; Yuan and Xu, 2011; Chintala et al., 2013; Masud et al., 2014). Prior to the application of biochar to soil with the intention to increase soil pH, knowledge of the pH–buffering capacity (referred to as pH–BC hereafter) of the soil and that of the biochar is needed so that the appropriate recommended application rate can be made.

The pH–BC of soils is commonly measured after adding incremental amounts of either a base ($Ca(OH)_2$ or NaOH) or an acid (HC1 or H_2SO_4) – depending on the initial soil pH – to the soil, then letting the soil incubate for a specific period of time (Bloom, 2000; Nelson and Su, 2010), and establishing a titration curve. Then the soil pH–BC is calculated from the slope of the titration curve and reported as the quantity of base/acid required to raise/decrease the soil pH by one unit (Thomas and Hargrove, 1984; Aitken and Moody, 1994). This technique is however very time–demanding (e.g., 5 d) and involves multiple acid/base additions. Simplified methodologies have been proposed, such as the 2–point titration (before and after a single addition of acid/base added) (Noble et al, 2002) that relies on the fact that the pH–BC curve of most soils is 'essentially linear' over the pH range 4.0–6.5 (Magdoff and Bartlett, 1985; Aitken et al., 1990). More recently, a statistical relationship between the pH–BC of a wide range of soils after a 30–min equilibration with a base ($pH–BC_{30min}$) and that obtained after a 5–d

equilibration (pH–BC_{eq}) has been established in order to invest less time in the measurement of this parameter (Liu et al., 2005; Kissel et al., 2007; Thompson et al., 2010; Kissel et al., 2012).

The liming potential of biochar is often reported as an equivalent proportion of the liming effect that $CaCO_3$ would have (referred to as % $CaCO_3$–eq). The International Biochar Initiative (2012) recommends the use of the method proposed by Rayment and Lyons (2011), originally intended to measure carbonate content in soil, for such purpose. In brief, this method involves an overnight incubation of the biochar sample with a known amount of acid, followed by a back titration of the excess acid with a standardized base. Yuan et al. (2011b) used the acid–base rapid titration – in which biochar is continually titrated (using an autotitrator) with acid to pH 2.0 while stirring – to estimate the total alkalinity of biochar and reported this as the amount of the acid being consumed by the biochar (cmol H^+ kg^{-1} biochar). However, with either method, it is possible that the sparingly soluble metal oxides and hydroxides have not yet completely reacted causing an underestimation of the liming properties of the biochar. Other methods thus may need to be tested in this regard.

In this study we propose to investigate whether the pH–BC methodologies originally developed for soils (Aitken and Moody, 1994; Liu et al., 2005; Kissel et al., 2007; Thompson et al., 2010; Xu et al., 2012) could be used to assess the liming potential of biochars so that appropriate recommended application rates could be made. Specifically we propose comparing the methods that use either single vs multiple acid addition, and short vs long equilibration times, along with the liming equivalence methodology described above.

3.1.1 Materials and methods

3.1.1.1 Biochar tested

Nineteen biochars were produced by different research groups using slow pyrolysis, and a range of feedstocks and temperatures (Table 3–1). Details on the production and selected characteristics of these biochars have been provided elsewhere (Novak et al., 2013; Slavich et al., 2013; Fang et al., 2014; Smider and Singh, 2014; Van Zwieten et al., 2014). Prior to their characterization, all biochar samples were dried at 60 $^{\circ}$C and ground to a particle size < 0.3 mm using a ring mill. The pH, ash content total N, C, H and S, and H/Corg molar ratio were present in Table 3-2.

Table 3-1 Feedstock and production temperature of the 19 biochar sample

ID	Code	Feedstock	HTT (°C)	Source	References/website
1	WS550	Wheat straw	550	UK Biochar Research Centre	http://www.charchive.org/record.php?record id=100
2	WS700	Wheat straw	700	UK Biochar Research Centre	http://www.charchive.org/record.php?record id=93
3	SG400	Switch grass	400	United States Department of Agriculture	(Novak et al., 2013)
4	SG550	Switch grass	550	United States Department of Agriculture	(Novak et al., 2013)
5	PI400	Pine chips	400	United States Department of Agriculture	(Novak et al., 2013)
6	PI550	Pine chips	550	United States Department of Agriculture	(Novak et al., 2013)
7	EU450	Eucalyptus	450	University of Sydney	(Fang et al., 2014)
8	EU550	Eucalyptus	550	University of Sydney	(Fang et al., 2014)
9	PL550	Poultry litter	550	Department of Primary Industries, New South	(Van Zwieten et al., 2014)
10	DG700	Digestate	700	Susteen Technologies Germany	(Teichmann, 2014)
11	GW550	Greenwaste	550	Department of Primary Industries, New South	(Slavich et al., 2013a)
12	RH550	Rice husk	550	UK Biochar Research Centre	http://www.charchive.org/record.php?record id=91
13	RH700	Rice husk	700	UK Biochar Research Centre	http://www.charchive.org/record.php?record id=92
14	MS550	Miscanthus	550	UK Biochar Research Centre	http://www.charchive.org/record.php?record id=97
15	MS700	Miscanthus	700	UK Biochar Research Centre	http://www.charchive.org/record.php?record id=96
16	MW550	Mixed	550	UK Biochar Research Centre	http://www.charchive.org/record.php?record id=94
17	MW700	Mixed	700	UK Biochar Research Centre	http://www.charchive.org/record.php?record id=95
18	TW550	Tomato	550	University of Sydney	(Smider and Singh, 2014)
19	DS400	Durian shell	400	Agriculture Department of Thailand	(Prakongkep et al., 2015)

Table 3-2 Selected properties of the 19 biochar sample

ID	Code	Volatiles %	Ash %	N %	C %	H %	S %	H/Corg
1	WS550	16.4	20.2	1.1	67.6	2.6	0.1	0.5
2	WS700	12.7	21.3	1.0	68.3	1.9	0.1	0.3
3	SG400	32.2	3.3	0.5	73.0	4.2	0.0	0.7
4	SG550	18.3	5.3	0.6	80.5	3.1	0.0	0.5
5	PI400	34.8	3.7	0.3	71.2	4.0	0.0	0.7
6	PI550	18.9	5.2	0.4	77.8	2.8	0.0	0.4
7	EU450	38.7	5.1	0.6	66.9	3.8	0.0	0.7
8	EU550	27.0	5.8	0.7	72.2	3.3	0.0	0.5
9	PL550	25.3	44.7	1.6	36.5	2.2	0.4	0.7
10	DG700	11.5	32.7	1.3	61.5	1.3	0.3	0.3
11	GW550	17.6	8.6	0.3	76.9	2.4	0.0	0.4
12	RH550	8.3	48.6	0.7	44.1	1.7	0.1	0.5
13	RH700	17.0	12.0	0.7	45.3	1.0	0.1	0.3
14	MS550	12.4	11.6	0.4	74.7	2.9	0.1	0.5
15	MS700	20.5	1.5	0.8	76.7	1.9	0.1	0.3
16	MW550	12.7	1.8	0.3	82.4	3.2	0.0	0.5
17	MW700	30.5	56.4	0.4	88.7	2.2	0.0	0.3
18	TW550	31.3	12.9	2.4	28.0	1.5	4.5	0.6
19	DS400	12.2	46.5	2.1	63.2	3.8	0.2	0.7

3.1.1.2 Calcium carbonate equivalence (% $CaCO_3$-eq)

Calcium carbonate equivalence, also referred to as liming equivalence, was determined using the method proposed by IBI (2012) after Rayment and Lyons (2011). For this, 10.0 mL standardized 1 M HCl solution was added to 0.5 g biochar, shaken with an end–over–end shaker for 2 h and let stand overnight. Then the slurry (without any separation procedure) was titrated using an autotitrator under vigorous stirring with standardized 0.5 M NaOH until a neutral pH (~7) was reached. The volume of NaOH solution consumed was recorded as *V*. A reference sample of $CaCO_3$ powder (previously dried at 105 ^{o}C for 1 h) was included in the batch. Liming equivalence (% $CaCO_3$–eq) was then calculated using equation [3–1].

Chemical reaction and calculations:

$$CaCO_3 + 2HCl \rightarrow CaCl_2 + H_2O + CO_2\ (g) \qquad [3–1]$$

In the above reaction for dissolving one mole of $CaCO_3$ (i.e. 100.09 g of $CaCO_3$) two moles of HCl are consumed. The number of moles of HCl consumed in the given biochar sample and blank was obtained from the titration and the % $CaCO_3$ equivalent was calculated as given below:

Calculations:

$$\%\ CaCO_3\ \text{equivalent} = \frac{M\times(a-b)\times10^{-3}\times100.09\times100}{2\times W} \qquad [3–1]$$

where:

M is standardized molarity of NaOH (mol L^{-1})

a is volume of NaOH being used (mL) for the blank

b is volume of NaOH being used (mL) for the biochar sample

10^{-3} is to convert the volume from mL to L

100.09 is molar mass of $CaCO_3$

100 is multiplier for obtaining % $CaCO_3$ equivalent

W is mass of biochar (g)

2 is one mole of $CaCO_3$ consumes two moles of HCl in the chemical reaction

3.1.1.3 pH buffering capacity at pH=7 (pH-$BC_{pH=7}$)

The pH–$BC_{pH=7}$ was measured following the method described by Yuan et al. (2011b). For this, 20 mL of deionized water was added to 1 g of each biochar. The pH of biochar at time 0 was measured after stirring the suspension for 30 min (pH_0). Then the suspension was titrated to pH 7 using continuous stirring using an auto–titrator at a minimal acid addition rate (standardized 0.01 M HCl) at room temperature (ca 20 ^oC). The volume of NaOH solution consumed was recorded as *V*. The pH–$BC_{pH=7}$ was calculated using equation [3–2].

Calculation

$$\text{pH–BC}_{\text{pH=7}}\ [\text{mmol H}^+\ \text{kg}^{-1}\ (\text{pH unit})^{-1}] = \frac{\text{the amount of H}^+\text{added}}{W \times 10^{-3} \times (\text{pH}_0 - 7)} \qquad [3\text{–}2]$$

where

M_{HCl} is standardized molarity of HCl (mol L^{-1})

V is volume of HCl being used (mL)

pH_0 is biochar pH

W is the mass of biochar (g)

3.1.1.4 pH buffering capacity determined in 5-d incubation (pH-BC_{5d})

The pH–BC_{5d} was determined following the single acid addition method as proposed by Thompson et al. (2010) after Liu et al. (2005) and Kissel et al. (2007) for measuring soil pH–BC with specific modifications. These involved the use of a soil: liquid ratio of 1:20 and that of an acid (HCl) instead of a base. For this, ca 0.5 g of each biochar was weighted to two 35–mL polypropylene (PE) urine specimen containers. Ten mL of deionized water were added to each container and the suspension was ultra–sonicated for 1 min to ensure the biochar was thoroughly wetted and then let stand for 30 min. Subsequently, based on the $CaCO_3$–eq of biochars measured above (either < 5%, 5 – 10%, 10 – 20%, or > 20 % $CaCO_3$–eq) 0.25, 0.5, 0.75, or 1 mL of standardized 0.5 M HCl were added to one of the containers whereas the other one was used as the control (without acid addition). Thereafter, the suspensions were incubated at a constant room temperature (ca 20 ^{o}C) for 5 d and the pH in both HCl–treated and control samples were measured at the end of the incubation and referred to as $pH_{HCl-treated}$ and $pH_{control}$, respectively. The pH–BC_{5d} was calculated using equation [3–3].

Calculation

$$\text{pH–BC}_{5d}\ [\text{mmol H}^+\ \text{kg}^{-1}\ (\text{pH unit})^{-1}] = \frac{\text{the amount of H}^+\text{added}}{W \times 10^{-3} \times (\text{pH}_{\text{control}} - \text{pH}_{\text{HCl-treated}})} \quad [3–3]$$

where

pH_0 is the initial biochar pH

$pH_{control}$ is the pH of the biochar suspension without acid addition.

$pH_{HCl-treated}$ is the pH of the biochar suspension with acid addition

W is the mass of biochar (g)

3.1.1.5 pH buffering capacity determined in 30-min incubation (pH-BC_{30min})

The pH–BC_{30min} was determined following the procedure described in section 3.1.1.4 except that the incubation time was reduced to 30 min after acid was added. The pH–BC_{30min} was calculated using equation [3–3].

3.1.1.6 pH buffering capacity predicted from pH-BC30min (Predicted pH-BC_{5d})

A relationship between the pH–BC_{5d} (considered here as the pH–BC measured under pseudo–equilibrium conditions) and pH–BC_{30min} was established in order to predict the pH–BC_{5d} as proposed by Liu et al. (2005), Kissel et al (2007), Thompson et al. (2010), and Kissel et al (2012). For this, the pH–BC_{5d} was regressed with the pH–BC_{30min} (results provided in the result section 3.1.2.1) so that an equation – with corrective factors intended to account for the lack of equilibrium in the pH–BC_{30min} determination –could be obtained (equation [3–4]) and the pH–BC_{5d} predicted.

$$\text{Predicted pH–BC}_{5d} = 2.2 \times \text{pH–BC}_{30min} + 20.4 \ (r^2 = 0.81) \qquad [3–4]$$

3.1.1.7 Validation of the use of predicted pH-BC_{5d} and % $CaCO_3$-eq values as biochar liming potential index

A 10–d incubation of soil amended with different amounts of biochar was conducted so that the suitability of the liming equivalence and the predicted pH–BC_{5d} (based on pH–BC_{30min}) to determine the application rate of biochar needed to raise the soil pH to a specific value. The pH–$BC_{pH=7}$ was not considered suitable (as described in the results section 3.1.2.1) as the application rates, calculated based on the results obtained below, were too high for feasible applications.

For this, two soils with contrasting alkaline–pH–buffering capacities were used: (1) Ramiha Silt Loam (Andic Umbrisol (IUSS Working Group, 2006)) and (2) Hautere Silty Clay Loam (Haplic Cambisol (IUSS Working Group, 2006)) (the detailed information on the two soils was provided in Chapter 7). Soil subsamples were separately amended with the 19 biochars under study at different application rates intended to target a pH of 6.5. These rates were calculated based on equations [3–5] and [3–6], which were in turn derived from equation [3–3] using the known pH–BC of the soils and the liming potential of the biochars based on either (i) the predicted pH–BC_{5d} (rate 1) or (ii) liming equivalence – % $CaCO_3$–eq (rate 2). In water, $CaCO_3$ dissolves according to the equation below:

$$CaCO_3 + H_2O \rightarrow Ca^{2+} + HCO_3^- + OH^- \qquad [3–2]$$

Thus one molecule of $CaCO_3$ dissolves neutralising one proton (Bohn et al., 1985). In very acidic soils, the HCO_3^- will further neutralise an additional proton and

form H_2CO_3 (pK = 6.4) and then CO_2 will be subsequently released (Liu et al., 2005; Kissel et al., 2007; Thompson et al., 2010; Kissel et al., 2012).

$$\text{Rate1 (\%)} = \frac{\text{pH}-\text{BC}_{\text{soil}} \times (\text{pH}_{\text{target}} - \text{pH}_{\text{soil}}) \times 100}{\text{pH}-\text{BC}_{\text{biochar}} \times (\text{pH}_{\text{biochar}} - \text{pH}_{\text{target}})} \qquad [3\text{–}5]$$

$$\text{Rate2 (\%)} = \frac{\text{pH}-\text{BC}_{\text{soil}} \times (\text{pH}_{\text{target}} - \text{pH}_{\text{soil}})/2 \times 100}{\%\ \text{CaCO}_3 - \text{eq}} \qquad [3\text{–}6]$$

The soils were then thoroughly mixed with the biochars (in duplicates) at the calculated application rates and wetted with deionized water to 70 % of field capacity. All treatments were incubated in a chamber at a constant room temperature of 20 ^{o}C for 10 d. Thereafter, the pH was measured.

3.1.1.8 Statistical analysis

All statistical analyses were conducted in the statistical software R version 3.2.2 (R Core Team, 2015). The pH, liming equivalence (% $CaCO_3$–eq) and different pH–BC (mmol H^+ kg^{-1} biochar (unit pH)$^{-1}$) measurements of 19 biochar samples were compared using the fitted linear models. Unless otherwise stated, results are expressed as means of two replicates.

3.1.2 Results and discussion

3.1.2.1 Comparison of the different methodologies intended to determine the biochar liming potential

The mean values of the liming equivalence (% $CaCO_{3–eq}$) and the pH buffering capacity – $pH–BC_{pH=7}$, $pH–BC_{30min}$, $pH–BC_{5d}$ and predicted $pH–BC_{5d}$ – of the biochar samples are presented in Table 3–2 and the boxplot comparing the different pH–BC values is presented in Figure 3–1. Values of $pH–BC_{5d}$ were higher than those measured by other methods, given the longer equilibration time provided by the former as this allowed the additional solubilisation of some of the slowly–soluble salts. Measurements of pH values at specific time intervals (data not shown) indicated that (i) an initial fast reacting phase (< 8 h) often was followed by a slow one, and (i) a maximum of 96 h was needed to reach pseudo–equilibrium. The predicted $pH–BC_{5d}$ values – obtained using equation [3–4] – were within similar range to the measured $pH–BC_{5d}$, as expected. The bivariate scatterplots (Figure 3–2) show the correlation between these indexes and also that with pH. The latter correlated poorly (r^2 = 0.05–0.13) with the liming equivalence and pH–BC values, showing that pH is a poor indicator of the liming potential of biochar. The liming equivalence, $pH–BC_{pH=7}$, $pH–BC_{30min}$, $pH–BC_{5d}$ and predicted $pH–BC_{5d}$ significantly correlated (r^2 = 0.66 – 0.83, $p < 0.001$) with each other, as expected. The closest correlation (largest r^2) of $pH–BC_{5d}$ with another index was provided by $pH–BC_{30min}$ (r^2 = 0.81) and this index, in turn, was highly related with liming equivalence (r^2 = 0.83). The liming equivalence and $pH–BC_{pH=7}$ provided r^2 of 0.55 and 0.43 when regressed with $pH–BC_{5d}$, respectively.

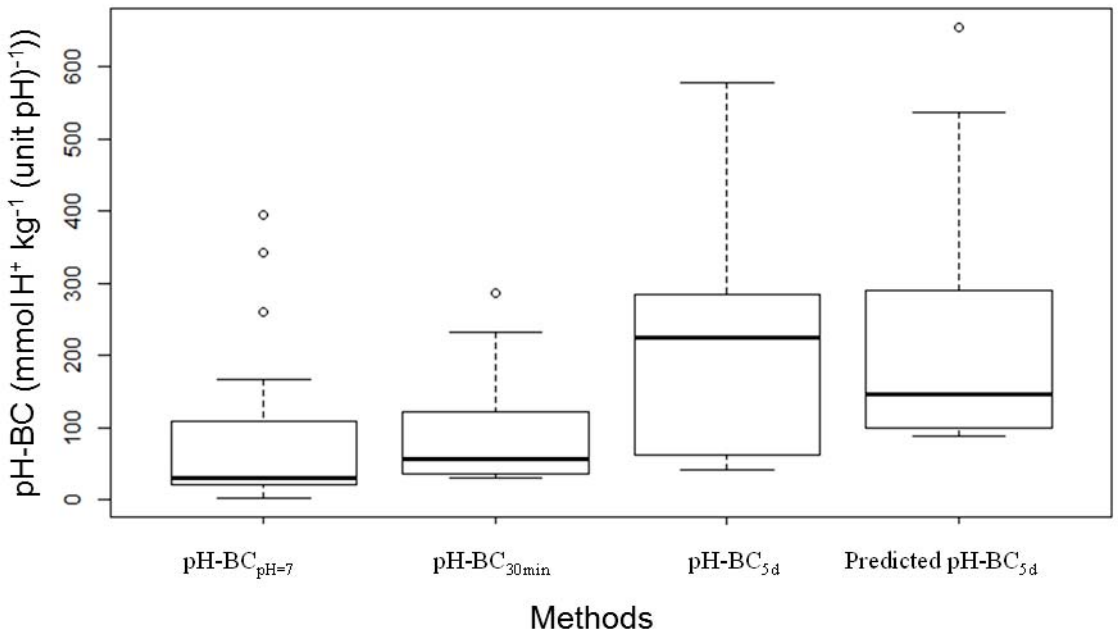

Figure 3–1 Boxplot of pH–BC (mmol H^+ kg^{-1} biochar (unit pH)$^{-1}$) measurements of 19 different biochar samples, grouped by method. Four methods were used (continual acid addition and auto–titrate until pH = 7, single acid addition and incubation (30 min), single acid addition and incubation (5 d) and the prediction from the 30 min incubation with single acid addition base on the relation exist between the values obtained in methods of single acid addition and incubation (30 min) and single acid addition and incubation (5 d).

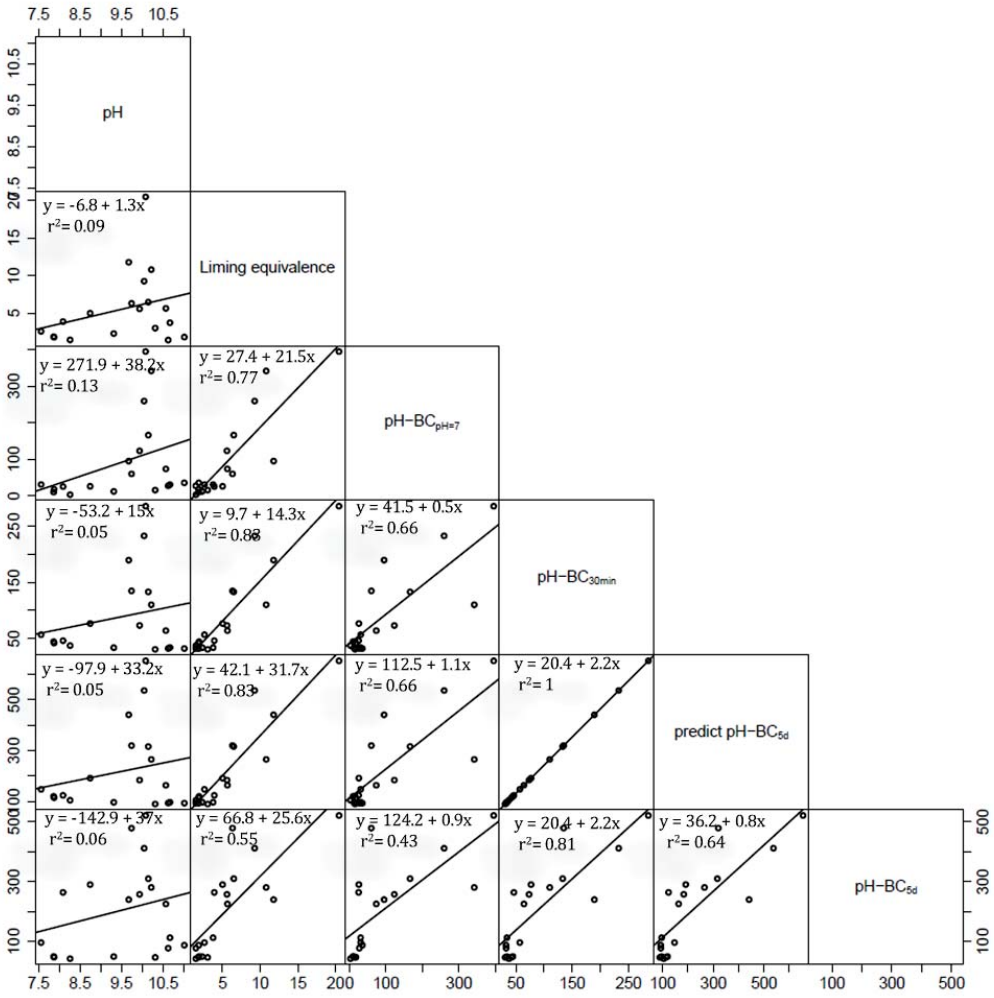

Figure 3–2 Relationship between pH, liming equivalence (% $CaCO_3$–eq) and different pH buffering capacity (pH–BC) (mmol H^+ kg^{-1} biochar (unit pH)$^{-1}$) measurements of 19 biochar samples. Equations of relationships between results of different methods are displayed along with r^2 values.

The greatest liming potential (either liming equivalence, pH–$BC_{pH=7}$, pH–BC_{30min}, or predicted pH–BC_{5d}) was found in TW550 biochar (Table 3–3). This was attributed to the large amount of ash (56.2%) in this biochar containing calcite and other carbonate minerals (e.g., magnesite and ankerite) (Smider and Singh, 2014). Biochars

made from poultry litter (PL550), digestate (DG700), durian shell (DS400), wheat straw (WS550, WS700), pine and eucalyptus wood carbonized at 550°C (PI550, EU550), and miscanthus carbonized at 700°C (MS700) had a liming equivalence of % $CaCO_3$–eq > 5% and pH–BC_{5d} >200 mmol H^+ kg^{-1} biochar (unit pH)$^{-1}$); while the rest of biochars had liming equivalence < 5% $CaCO_3$–eq and pH–BC_{5d} < 100 mmol H^+ kg^{-1} biochar (unit pH)$^{-1}$. In general, this reflected the ash content of the biochars for poultry litter (45% ash content) and digestate (33% ash content), but not that of the rice husk biochars, as they had an ash content above 45% (mostly silica, data not shown), but a low liming potential. The composition of the ash has therefore a key role; rice husk has a predominance of silica (SiO_2) (Shackley et al., 2012; Liu et al., 2013; Prakongkep et al., 2015), which does not contribute to the alkalinity of the biochar (Yuan and Xu, 2011). Also, it was observed that biochars produced using the same feedstock but at higher temperature tend to have greater liming potential than the ones produced at lower temperature irrespective of the methods (Table 3–3). This is often explained by the increase in the ash content and the removal of the organic functional group with the increasing temperature (Yuan et al., 2011b).

Table 3-3 Means of pH, liming equivalence (% $CaCO_3$ – eq) and pH buffering capacity [pH–BC (mmol H^+ kg^{-1} biochar (unit pH)$^{-1}$)] of biochar samples measured by different methods.

ID	Biochar	pH	% $CaCO_3$–eq	pH–$BC_{pH=7}$	pH–BC_{30-min}	pH–BC_{5-d}	Predicted pH–BC_{5d}
1	WS550	11	5.7	74	64	225	163
2	WS700	10	6.5	166	133	309	316
3	SG400	8	1.9	10	45	49	120
4	SG550	10	3.0	16	31	46	89
5	PI400	8	3.9	25	46	263	123
6	PI550	9	5.0	26	77	290	191
7	EU450	8	2.6	31	57	96	147
8	EU550	10	6.3	60	135	578	320
9	PL550	10	11.8	95	189	239	441
10	DG700	10	10.8	342	110	280	265
11	GW550	8	1.8	18	42	47	114
12	RH550	11	1.5	27	33	77	93
13	RH700	11	1.9	36	32	87	92
14	MS550	11	3.8	31	34	112	96
15	MS700	10	5.6	123	73	257	183
16	MW550	8	1.5	3	38	42	104
17	MW700	9	2.3	12	34	49	96
18	TW550	10	20.5	395	285	520	654
19	DS400	10	9.3	259	233	411	537

3.1.2.2 Validation of the use of predicted pH-BC_{5d} and % $CaCO_3$-eq values as biochar liming potential indexes

The pH values of the soils amended with biochar at rates 1 and 2 (based on either predicted pH–BC_{5d} or % $CaCO_3$–eq values, respectively, Table 3-4) after a 10–d incubation were plotted in Figure 3–3a and b, respectively. The results indicate that, when the rates of the amendments were estimated using predicted pH–BC_{5d}, (i) 63% of the pH values fell within ± 0.25 pH units of the target pH = 6.5, (ii) 92% were located within ± 0.5 pH units of the target, and (iii) the final pH values ranged between 5.5 and 7.6 (Figure 3–3a). When the rates of the amendment were estimated using % $CaCO_3$–eq, the results indicate that (i) 21% of the amended soil pH values located ± 0.25 pH units of the target pH = 6.5, (ii) 55% were located ± 0.5 pH units of the target, and (iii) the final pH values ranged between 5.6 and 6.5 (Figure 3–3b). Therefore, the data obtained using predicted pH–BC_{5d} was more precise (average closer to the targeted value) but less accurate (wide range of final pH values) than that using % $CaCO_3$–eq. Several reasons may explain the results obtained (all of them being interlinked): (i) the $CaCO_3$–eq measures the potential liming equivalence whereas the predicted pH–BC_{5d} provides a more realistic value (within the time frame considered), as it was determined at pH values closer to the conditions of the soil (i.e., the amount of H^+ used to determine the pH–BC was smaller than that used for the liming equivalence): (ii) as soil pH increases and approaches the pK value of 6.3 (at which concentrations of HCO_3^- equal those of H_2CO_3), the use of an equivalence of one (only one H^+ becomes neutralized by additionally dissolving carbonate molecules) instead of two becomes more realistic; i.e. the amount of biochar needed for liming purposes was therefore underestimated; (iii)

the dissolution of alkaline salts in soils takes longer than 10 d and a longer term incubation should provide a more realistic response. More research would be needed before selecting a method to determine the liming properties of biochars. For the purpose of this thesis though, the predicted pH–BC_{5d} method was chosen.

Table 3-4 The soils (1) Ramiha Silt Loam and (2) Hautere Silty Clay Loam amended with the 19 biochars under study at application rates (g biochar per 100 g soil) calculated based on either (i) the predicted pH–BC_{5d} (rate 1) or (ii) liming equivalence – % $CaCO_3$–eq (rate 2) intended to target a pH of 6.5

		Rate 1 (g biochar per 100 g soil)		Rate 2 (g biochar per 100 g soil)	
ID	Biochar	Ramiha Silt Loam	Hautere Silty Clay Loam	Ramiha Silt Loam	Hautere Silty Clay Loam
1	WS550	9.5	5.7	5.4	3.2
2	WS700	5.4	3.3	4.7	2.8
3	SG400	40.4	24.2	16.1	9.6
4	SG550	18.0	10.8	10.0	6.0
5	PI400	15.5	9.3	7.8	4.7
6	PI550	23.5	14.1	6.1	3.6
7	EU450	19.0	11.4	11.7	7.0
8	EU550	5.9	3.5	4.8	2.9
9	PL550	4.2	2.5	2.6	1.5
10	DG700	22.8	13.7	2.8	1.7
11	GW550	16.6	9.9	16.7	10.0
12	RH550	20.2	12.1	20.9	12.5
13	RH700	18.9	11.3	16.4	9.8
14	MS550	39.6	23.7	8.1	4.9
15	MS700	8.1	4.9	5.4	3.3
16	MW550	13.2	7.9	20.6	12.4
17	MW700	15.7	9.4	13.2	7.9
18	TW550	2.8	1.7	1.5	0.9
19	DS400	5.2	3.1	3.3	2.0

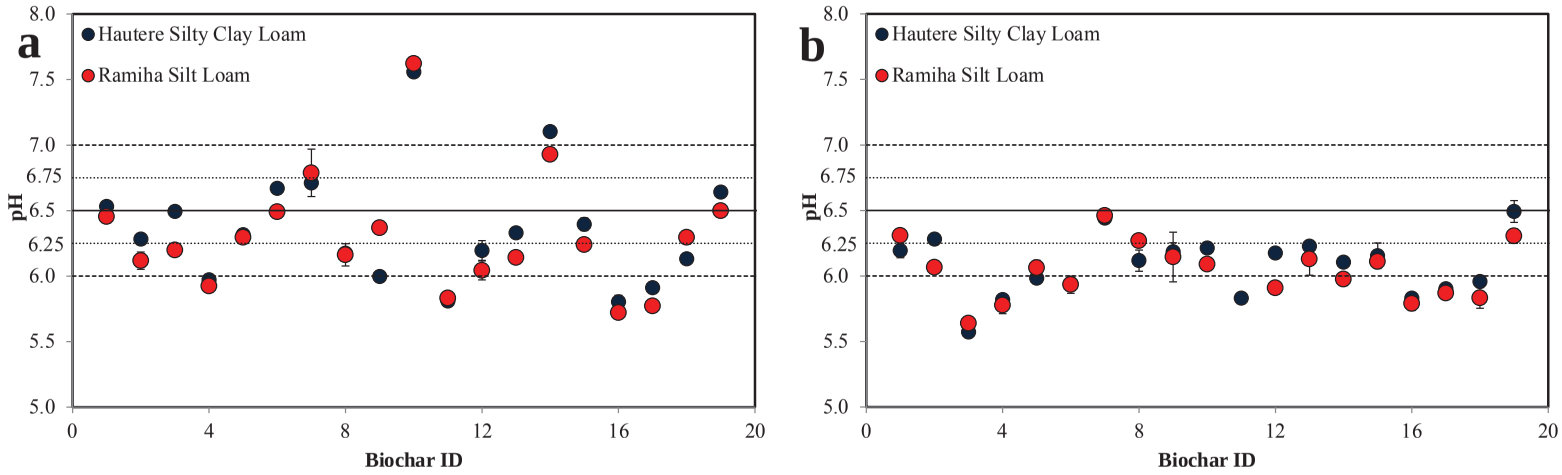

Figure 3–3 The distribution of pH values of Ramiha Silt Loam and Hautere Silty Clay Loam after 10–days incubation of soils amended with biochar at rate 1 calculated from the predicted pH–BC_{5d} (a) and at rate 2 calculated from liming equivalence (% $CaCO_3$–eq) to achieve a pH of 6.5 (b).

3.1.3 Recommended protocol for measuring the liming potential of biochar

The recommended final protocol followed for measuring the biochar liming potential was predicting pH–BC_{5d} from a 30 min incubation of biochar with single acid addition with correction factors accounting the lack of equilibrium as follows:

Ca 0.5 g of biochar was weighted to two 35–mL polypropylene (PE) urine specimen containers. In each, added 10 mL of deionized water and Ultra–sonicate the mixture for 1 min to ensure the biochar becomes thoroughly wetted and then let stand for 30 min. Then, based on the $CaCO_3$–eq of biochars measured (either < 5%, 5 – 10%, 10 – 20%, or > 20 % $CaCO_3$–eq) add 0.25, 0.5, 0.75, or 1 mL of standardized 0.5 M HCl to one of the containers and use the other one as the control (without acid addition). Then, the suspensions were incubated at a constant room temperature (ca 20 ^oC) and the pH in both HCl–treated and control samples after 30 min were recorded as $pH_{HCl–treated}$ and $pH_{control}$, respectively. The pH–BC_{30min} was calculated using equation [3–3] and then inserted into equation [3–4] to calculate the predicted pH–BC_{5d}.

3.2 Available nitrogen

When N–containing organic materials are exposed to high temperature (as in pyrolysis), an enrichment in heterocyclic N forms, such as pyrrole–type N, pyridine–type N and indole N, occurs along with a decrease in amide N (Knicker et al., 1996; Almendros et al., 2003). This enrichment is not only the result of a residual

accumulation of heterocyclic N forms but also of the formation of new ones. Almendros et al. (2003) suggested as possible reactions (i) the auto–condensation of aromatic compounds with NH_3 released from amide–containing constituents, (ii) the cyclisation of aliphatic chains in the presence of amino groups or NH_3, and (iii) the cyclisation of peptide chains. Amide structures have been reported to be more resistant to thermal degradation than O–alkyl and carbonyl groups possibly due to stabilizing cross–linking reactions or steric hindrance in organic domains (Almendros et al., 2003). Effective protein thermal decomposition generally begins ca 300°C (Barreto et al., 2003; Thipkhunthod et al., 2007). However, the thermal stability of N–containing compounds has been reported to vary widely. While some amino acids completely degrade after heating above 400°C (e.g., glutamic acid, β–alanine) others are still detectable at temperatures above 700°C (Douda and Basiuk, 2000).

Nitrate (NO_3^-) and ammonium (NH_4^+) are the major sources of inorganic N taken up by the roots of higher plants, and are often referred to as soil mineral N (nitrite – NO_2^- – does not contribute to it substantially). Acid hydrolysis using 6 M HCl is frequently used to characterise organic N in soil (Kelley and Stevenson, 1995) and has also been used to hydrolyse N forms in biochar (Wang et al., 2012a). The acid hydrolysate N can be further fractionated into: (i) NH_4^+–N, (ii) amino acid–N, (iii) amino sugar–N, and (iv) unknown–hydrolysable–N (HUN fraction) (Kelley and Stevenson, 1995). Non–hydrolysable N in soil is mostly associated with heterocyclic N in soils, although some peptide structures have also been reported to be non–hydrolysable due to entrapment within soil mesopores (Hedges and Keil, 1995) and/or encapsulated within macromolecular organic matrices (Knicker and Hatcher, 1997).

Heterocyclic N compounds are relatively recalcitrant to microbial decomposition and limit the conversion of organic N to forms available to plant uptake (Almendros et al., 2003; Wang et al., 2012a). Wang et al. (2012a) measured hydrolysable N in biochars made from protein–rich feedstocks (manure and sewage sludge) and found that, at temperature of pyrolysis of 450°C and above, values ranged between 0.9 and 2.6 g kg^{-1}. No amino acid–N was detectable in the acid hydrolysates of those biochars, whereas some NH_4^+ was observed and suggested to derive from (i) that originally present in the biochar, and (ii) that generated from hydrolysis of amides that resisted pyrolysis (Wang et al., 2012a). Amino sugars were detected in biochar hydrolysates although in low amounts; these authors attributed the resistance of these N compounds against thermal degradation to their possible association with inorganic constituents (Solomon et al., 2001; Buurman et al., 2002).

As mentioned earlier, acid hydrolysis using 6 M HCl, which is frequently used to characterise organic N in soil (Kelley and Stevenson, 1995), has also been used to hydrolyse N forms and to estimate the available N in biochar (Wang et al., 2012a). Two procedures were described Wang et al. (2012a) for determining the available N: (1) by calculating the difference in the total N in the biochar before and after treated with 6 M HCl; and (2) by digesting the 6 M HCl hydrolysates of biochar and measure the N in the digestion. It should be noted that the biochars being used in the study by Wang et al (2012a) were produced from manure and sewage sludge and rich in total N (> 13.5 g kg^{-1}) and available N (> 2 g kg^{-1}). However, the suitability of the procedure described therein was not tested on biochars low in available N (e.g., woody biochar). In this section, which 19 biochars have a wide range of N content, were used to test both procedures and assess their suitability.

3.2.1 Materials and methods

3.2.1.1 Biochar used

See section 3.1.1.1

3.2.1.2 Total N

Total N contents were determined using a TruSpec CHNS analyser (LECO Corp. St. Joseph, MI).

3.2.1.3 Method 1-Difference in total N in biochar before and after treated with 6 M HCl

Method 1 determines available–N by calculating the difference in total N in biochar before and after treated with 6 M HCl, as described by Wang et al. (2012a)**.** Ca 0.5 g (W_1, g) biochar was weighed into a 50 mL Pyrex® cation digestion tube. Acid mixture (25 mL; 6 mol L^{-1} HCl and 0.1% phenol plus drops of octyl alcohol) was added. The suspension was mixed using a vortex mixer and sonicated for 5 min to ensure complete wetting of the biochar. The tubes were covered with reflux funnels and placed on an Al digestion block set at 105°C for 24 h. The hydrolysates were filtered through a pre–weighed dry Whatman® 542 filter paper (W_2, g). The filter paper with non–hydrolysable residue was rinsed with deionized water and oven dried at 60°C until

constant weight was obtained. The weight of residue + filter paper was recorded (W_3, g). Total N content of the original biochar and the non–hydrolysable residue were determined using a Tru–Spec CHNS analyser (LECO Corp. St. Joseph, MI, USA). Total hydrolysable N (available–N) was calculated according to the equation [3–7].

Calculation

$$\text{available N (g kg}^{-1}) = \frac{N_1 \times W_1 - N_2 \times (W_3 - W_2)}{W_1 \times 10^{-3}} \quad [3–7]$$

where

N_1 is N content in biochar before treated with 6 M HCl (%)

N_2 is N content in biochar after treated with 6 M HCl (%)

W_1 is dried mass of biochar before treated with 6 M HCl (g)

W_2 is dried mass of filter paper (g)

W_3 is dried mass of filter paper + biochar after treated with 6 M HCl (g)

3.2.1.4 Method 2- Hydrolysable N content in the digestion of the 6 M HCl hydrolysate

Method 2 determined available N by digesting the 6 M HCl hydrolysate of biochar and measured the N in the digestion, as described by Wang et al. (2012a) after Pansu and Gautheyrou (2006). The digestion procedure as in *method 1* was followed. The filtrate was collected into a 100 mL volumetric flask and the residue on the filter paper was then rinsed with small aliquot of deionised water until 100 mL of total filtrate

was collected. Then 2.5 mL of hydrolysate was neutralised with 5 M NaOH (~ 0.75 mL) in a 10 mL polypropylene tube and total volume was topped up to 5 mL with deionised water. Thereafter, 2.5 mL of alkaline potassium peroxodisulfate reagent was added. Tubes were capped tightly and autoclaved (at 121°C and 205 kPa for 1 h) (Maher et al., 2002). During this process, inorganic N and organically–bound N in the hydrolysate were converted to NO_3^-–N. Nitrate–N was then determined using a Technicon NH_4^+/NO_3^- Auto–Analyser. Total hydrolysable N (available–N) was calculated according to the equation [3–8]:

Calculation

$$\text{Available N (g kg}^{-1}) = \frac{\frac{N_{cont.} \times 7.5 \times 10^{-3}}{2.5} \times 100}{W_1} \quad [3–8]$$

where

$N_{cont.}$ is Nitrate–N concentration in the 6 M HCl hydrolysate of biochar (mg L^{-1})

7.5 is the total volume of the digestion solution (mL)

2.5 is the volume of the 6 M HCl hydrolysate of biochar used for digesting (mL)

100 is the total volume of the 6 M HCl hydrolysate of biochar (mL)

W_1 is dried mass of biochar before treated with 6 M HCl (g)

3.2.1.5 Modified method 2 - hydrolysable-N content in the digestion of the 6 M HCl hydrolysate

Modification of method 2 with a smaller dilution factor for measuring biochars low in available N (the justification for this modification is provided in the Results section). The digestion procedure as in *method 2* was followed. The filtrate was collected into a 50 mL volumetric flask and the residue on the filter paper was then rinsed with small aliquot of deionised water until 50 mL of total filtrate was collected. Then 3 mL of hydrolysates was pipetted into a 10 mL polypropylene tube and 5 M NaOH is added (~1.8 mL) to raise the pH to 6.5. Thereafter, 2.5 mL of alkaline potassium peroxodisulfate reagent was added. Tubes were capped tightly and autoclaved and the nitrate–N was determined as described in *Method 2*. Total hydrolysable N (available–N) was calculated according to the equation [3–9]:

Calculation

$$\text{Available N } (\text{g kg}^{-1}) = \frac{\frac{N_{cont.} \times 7.3 \times 10^{-3}}{3}}{W_1} \times 50 \qquad [3–9]$$

where

$N_{cont.}$ is Nitrate–N concentration in the 6 M HCl hydrolysate of biochar (mg L^{-1})

7.3 is the total volume of the digestion solution (mL)

3 is the volume of the 6 M HCl hydrolysate of biochar used for digesting (mL)

50 is the total volume of the 6 M HCl hydrolysate of biochar (mL)

W_1 is dried mass of biochar before treated with 6 HCl (g)

3.2.1.6 Statistical analysis

All statistical analyses were conducted in the statistical software R version 3.2.2 (R Core Team, 2015). Correlation between hydrolysable N determined by difference in N content of biochar before and after treatment with 6 M HCl (Hydro–N by difference) (*method 1*) and digesting the 6 M HCl hydrolysate of biochar (Hydro–N by digestion) (*method 2*) and *modified method 2* were compared using the fitted linear models. Unless otherwise stated, results are expressed as means of two replicates.

3.2.2 Results and Discussion

Results shown in Table 3–4 and Figure 3–4 reveal that hydro–N values obtained by calculating the difference in total N in biochar before and after treated with 6 M HCl following *method 1* were several folds (~7) of those obtained by digesting the hydrolysate following either *method 2* or modified *method 2*, as indicated by a slope of 0.14, although they correlated significantly ($P < 0.001$) ($r^2 = 0.83$ and 0.77 respectively; Figure 3–4). This is in disagreement with the results obtained by Wang et al. (2012a) when developing the methodology for a range of carbonised human– and animal wastes. It should be noted that Wang et al. (2012a) included fresh and poorly carbonised material, which contained high hydrolysable N (in some instances above 6 g kg^{-1}), and thus the measurements were less prone to error when determining hydro–N either by calculating the difference in total N in biochar before and after treatment with 6 M HCl (following *method 1*) or by digesting the 6 M HCl hydrolysates of the same (following *method 2*). *Method 1* is an indirect approach and the final result includes the summed

experimental errors from each analysis. This may explain the inconsistencies found, at least to some extent.

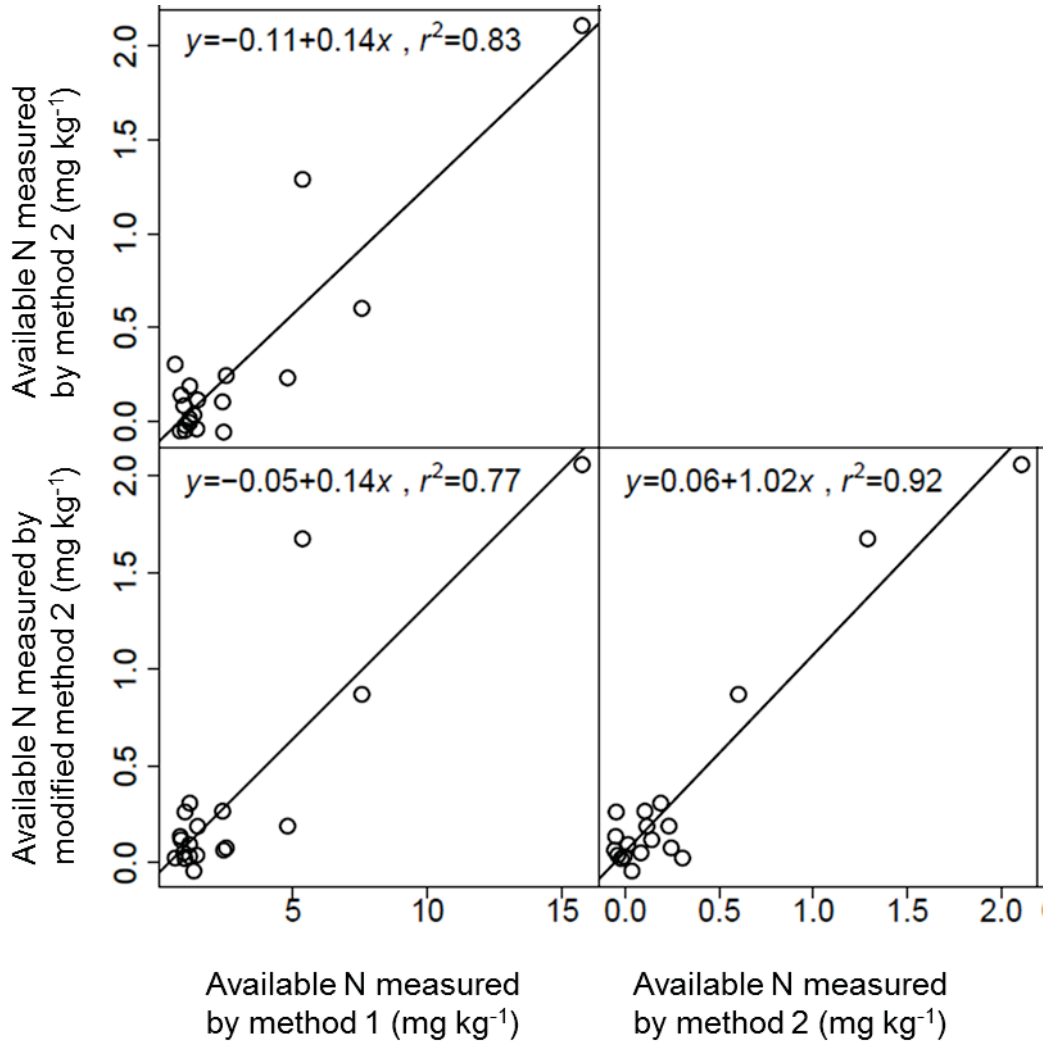

Figure 3–4 Correlation between hydrolysable N determined by calculating the difference in N content of biochar before and after treatment with 6 M HCl (Hydro–N by difference) (*method 1*) and digesting the 6 M HCl hydrolysate of the same biochar (Hydro–N by digestion) (*method 2*) and *modified method 2*.

According to Patton and Kryskalla (2003), high chloride concentrations (> 10 g L^{-1}) and dissolved organic C concentrations (> 150 mg L^{-1}) could react with persulfate and thus decrease the digestion efficiency. Moreover, Cl^- also interferes with the colorimetric determination of NO_3^-. Therefore, *method 2* was originally developed with dilution steps to avoid these interferences. However, this can produce N concentrations below the detection limit due to over–dilution in samples low in N, and is not appropriate for biochars produced from woody materials (e.g., WS770, GW550, RH700, MS550, MW550 and MW700; Table 3–5). A compromise should thus be made to minimize the interferences from Cl^- and dissolved organic C and to avoid over–dilutions of the hydrolysate. An additional test suggested that up to ~ 51 g L^{-1} of Cl^- could be acceptable for persulfate digestion of ammonium and determination of nitrate (data not shown). Therefore, we propose to modify *method 2* using a smaller dilution factor (242 vs 600) when biochars with low N content are to be characterised using this procedure. This has shown more consistent results for low N biochars (Table 3–5). The modified version showed similar results as obtained from *method 2* (r^2=0.92, and slope = 1.02), especially for the biochar high in N. The available N in the three biochars used in Chapter 6 and 7 was analysed following the *modified method 2*.

The results obtained (Table 3–5) indicate that whereas available N in biochars decreased as temperature of pyrolysis increased, the opposite pattern was observed for total N. The greatest amounts of total N were found in biochars derived from relatively protein–rich feedstocks, specifically TW550 (25.4 g kg^{-1}), DS400 (21.5 g kg^{-1}), PL550 (17.1 g kg^{-1}), and DG700 (11.6 g kg^{-1}) biochars (Table 3–5). Hydrolysable N measured by either *method 2* or *modified method 2* was < 1 g kg^{-1} for all biochars, except for the TW550 and DS400 biochars, which had values of 2.06 and 1.67 g kg^{-1}, respectively.

Wang et al. (2012a) also found values of hydrolysable N within this range (1–2 g kg^{-1}) in biochars made from manure and sewage sludge produced at 450 and 550°C. Camps–Arbestain et al. (2015) reported values of hydrolysable N of 1.9 g kg^{-1} for poultry litter biochar produced at 550°C, whereas woody biochars had values always < 1 g kg^{-1}.

Table 3-5 Means of available N (g kg^{-1}) analysis carried followed different methods

ID	Biochar	Total N	Available N		
			Method 1	*Method 2*	*Modified method 2*
1	WS550	10.5	2.39	0.10	0.27
2	WS700	10.2	2.43	–0.06	0.07
3	SG400	4.9	0.85	0.14	0.12
4	SG550	5.4	0.95	0.08	0.05
5	PI400	2.1	0.63	0.30	0.02
6	PI550	2.5	1.32	0.04	< d.l.
7	EU450	5.9	1.17	0.19	0.31
8	EU550	6.0	1.46	0.12	0.19
9	PL550	17.1	7.56	0.60	0.87
10	DG700	11.6	4.81	0.23	0.19
11	GW550	1.9	1.16	< d.l.	0.03
12	RH550	7.1	1.16	0.01	0.09
13	RH700	6.2	1.43	< d.l.	0.04
14	MS550	4.3	0.99	< d.l.	0.02
15	MS700	6.7	2.53	0.24	0.08
16	MW550	1.9	0.81	< d.l.	0.14
17	MW700	2.1	0.99	< d.l.	0.26
18	TW550	25.4	15.75	2.11	2.06
19	DS400	21.5	5.36	1.29	1.67

3.2.3 Recommended protocol for measuring the available N of biochar

Based on the results and discussion above, the protocol followed for measuring available N in biochar in this thesis was the *modified method 2,* which is consistent in the following steps. .

Ca 0.5 g of biochar was weighed into a 50 mL Pyrex® cation digestion tube. Acid mixture (25 mL; 6 mol L^{-1} HCl and 0.1% phenol plus drops of octyl alcohol) was added. The suspension was mixed using a vortex mixer and sonicated for 5 min to ensure complete wetting of the biochar. The tubes were covered with reflux funnels and placed on an Al digestion block set at 105°C for 24 h. The hydrolysates were filtered through a Whatman® 542 filter paper. The filtrate was collected into a 50 mL volumetric flask and the residue on the filter paper was then rinsed with small aliquot of deionised water until 50 mL of total filtrate was collected. Then 3 mL of hydrolysates was pipetted into a 10 mL polypropylene tube and 5 M NaOH is added (~1.8 mL) to raise the pH to 6.5. Thereafter, 2.5 mL of alkaline potassium peroxodisulfate reagent was added. Tubes were capped tightly and autoclaved (at 121°C and 205 kPa for 1 h) (Maher et al., 2002). During this process, inorganic N and organically–bound N in the hydrolysate were converted to NO_3^-–N. Nitrate–N was then determined using a Technicon NH_4^+/NO_3^- Auto–Analyser. Total available N (hydro–N) was calculated according to the equation [3–9].

Chapter 4

TESTING AN ALTERNATIVE METHOD FOR ESTIMATING THE LENGTH OF FUNGAL HYPHAE IN SOIL USING PHOTOMICROGRAPHY AND IMAGE PROCESSING

This methodology chapter is to develop and test an objective and rapid methodology for estimating the length of external arbuscular mycorrhizal fungal (AMF) hyphae in soil. The method involved the photomicrography and the image processing technology. This method will be used to estimate the response of the AMF hyphae development to biochar additive in Chapter 6.

A paper from this study has been submitted for publication: **Qinhua Shen**, Miko U.F. Kirschbaum, Mike J. Hedley, Marta Camps–Arbestain. Testing an alternative method for estimating the length of fungal hyphae using photomicrography and image processing (2016). *PLoS ONE* (Accepted)

Abstract

This study aimed to develop and test an unbiased and rapid methodology to estimate the length of external arbuscular mycorrhizal fungal (AMF) hyphae in the soil. The traditional visual gridline intersection (VGI) method was refined, first by using a digital photomicrography technique, referred to as "digital gridline intersection" (DGI) method, and secondly by processing the images using ImageJ software, which was referred to as the "photomicrography–ImageJ processing" (PIP) method. The DGI and PIP methods were tested using known grade lengths of possum fur. Then they were applied to measure the hyphal lengths in soils with contrasting phosphorus (P) fertility status. Linear regressions were obtained between known lengths (L_{known}) of possum fur and those values determined by using either the DGI (L_{DGI}) [$L_{DGI} = 0.37 + 0.97 \times L_{known}$ ($r^2 = 0.86$)] or PIP (L_{PIP}) methods [$L_{PIP} = 0.33 + 1.01 \times L_{known}$ ($r^2 = 0.98$)]. There were no significant ($p > 0.05$) differences between the L_{DGI} and L_{PIP} values. While both methods provided accurate estimation (slope of regression being 1.0), the PIP method was more precise, as reflected by a higher value of r^2 and lower coefficients of variation. The average hyphal lengths (6.5 – 19.4 m g^{-1}) obtained by the use of these methods were in the range of those typically reported in the literature (3 – 30 m g^{-1}). Roots growing in P deficient soil developed 2.5 times as many hyphae as roots growing in P–rich soil (17.4 vs 7.2 m g^{-1}). These tests confirmed that the use of digital photomicrography in conjunction with either the grid–line intersection principle or image processing is a suitable method for the measurement of AMF hyphal lengths in soils for comparative investigations.

Keywords

Arbuscular mycorrhizal fungi (AMF), Extra–radical mycelium, Gridline intersection, Hyphal length, ImageJ software, Photomicrography

4.1 Introduction

The extra–radical mycelium of arbuscular mycorrhizal fungi (AMF) increases the exploration of soil volume making positional–unavailable nutrients (e.g., P) available thus supporting host–plant growth. In particular, in a P–deficient soil, AMF may contribute up to 90% of plant P uptake (Pacovsky and Bethlenfalvay, 1982; Sylvia, 1992). In addition, external hyphae are involved in the stabilization of soil aggregates (Wright and Upadhyaya, 1998; Rillig, 2004; Rillig and Mummey, 2006; Wilson et al., 2009) and can represent a significant proportion (up to 15%) of soil organic carbon (C) (Staddon et al., 2003; Zhu and Michael Miller, 2003). Hence, the abundance of the AMF external mycelia in soils can strongly affect the performance of their host plants as well as other soil ecosystem services. However, mycelia are known as the "hidden half" of this symbiosis (Leake et al., 2004) due to the small diameter of individual hyphae (< 5 μm) and their dispersed growth pattern (Staddon et al., 2003). This makes the identification and quantification of extra–radical mycelia exceptionally difficult and highly uncertain (Boddington et al., 1999), which has held back research on the extra–radical hyphal network of AMF (Bardgett, 1991; Green et al., 1994; Leake et al., 2004; Camenzind and Rillig, 2013).

Conventionally, the total length of AMF hyphae in soils has been determined by aqueous extraction, followed by membrane–filtration, staining (e.g., with trypan blue), and then visually examining the frequency of hyphal intersections with gridlines on a microscope eyepiece (Elmholt and Kjøller, 1987; Vilariño et al., 1993; Brundrett, 1994; Miller et al., 1995; Camenzind and Rillig, 2013). This is the so–called visual gridline intersection (VGI) method, which has become a well–acknowledged reference method as it is low–cost and readily implemented. However, counting the intersections of stained hyphae with gridlines under a microscope is laborious, time–consuming and induces fatigue that can lead to observer subjectivity (Morgan et al., 1991; Dodd, 1994; Green et al., 1994) and this has been shown to contribute up to 15% variation in measured results (Stahl et al., 1995).

Thanks to the availability of digital microscopes it has now become possible to take digital microscope images (referred to as photomicrography) at reasonably high magnification. This allows the electronic recording of hyphal images that can later be processed at the convenience of the operator. For this, a square grid layer can be designed and positioned on top of the image so that the intersection of gridlines and stained hyphae can be scored on a computer monitor. This uses the same principles as scoring the frequency of hyphal intersections with gridlines incorporated into a microscopes eyepiece under a microscope, but can save observers from fatigue and eye pain. This procedure has already been shown to be more accurate and efficient than the visual one for estimating hyphal length (Hynes et al., 2008), but to present has been scarcely used probably due to a lack of assessment of its accuracy and precision. Such a test has been conducted in the current study. In order to differentiate it from the

traditional visual gridline intersection (VGI) method, the new method is here referred to as the digital gridline intersection (DGI) method.

We also tested whether further advances could be made through employing modern imaging–processing software. ImageJ is a Java–based image processing program developed at the National Institute of Mental Health (USA) by Wayne Rasband (Sheffield, 2008). The software is available license–free and can run on any operating system. The program is a useful tool for biological image processing and analysis because it can perform a full set of image manipulations, such as scale setting, length and area measuring, image cropping (Collins, 2007; Sheffield, 2008) on digital images obtained from many sources (e.g., cameras and confocal systems).

This software, while useful for the length measurement of straight structures, does require additional support when the measured structures have bent or irregular shapes (e.g., hyphae). For this, the NeuronJ plugin (Abràmoff et al., 2004) can be used. This plugin is based on recently developed and validated algorithms specifically to detect and link elongated image structures of neurons and dendrites. Therefore, we investigated the application of ImageJ with NeuronJ plugin in measuring hyphal lengths, which is referred to as the photomicrography – ImageJ processing (PIP) method. The two proposed methodologies – DGI and PIP – were tested by using known length of possum fur and were compared for a measurement of hyphal lengths from two soils with contrasting P fertility.

4.2 Materials and Methods

4.2.1 Calculations involved in the digital methodologies

(1) *Digital gridline intersection (DGI) method.*

The Tennant (1975) equation [4–1], which was originally developed for determining root lengths, has subsequently also been applied to determine hyphal lengths (Miller et al., 1995). It was further modified for the DGI method to equation [4–2] to calculate the total length (L_{DGI}, mm) of samples (possum fur or hyphae) on each filter paper.

$$\text{Root length} = \left(\frac{11}{14}\right) \times g \times \text{N} \qquad [4–1]$$

$$L_{DGI} = \frac{\sum(C_1 + C_2 + \cdots C_{50}) \times \left(\frac{11}{14}\right) \times g \times A_f}{A_g \times N_i} \qquad [4–2]$$

where

$\frac{11}{14}$ is a constant

N is the count of the number of intersections across vertical and horizontal lines

$C_1, C_2, \cdots C_{50}$ are the counts of samples crossing the gridline in images #1, #2, #3, ….., #50

A_f is the area of filter paper (e.g., $A_f = \pi \times 12.31^2 = 476$ mm^2)

A_g is the area grid net (e.g., $A_g = 0.05 \times 0.05 \times 12 \times 9 = 0.27$ mm^2)

N_i is the number of images (e.g., 50)

g is the grid unit (e.g., 0.05 mm)

(2) *Photomicrography – ImageJ processing (PIP) method*

The total length measured by the PIP method (L_{PIP}, mm) of samples (possum fur or hyphae) on each filter paper was calculated using equation [4–3].

$$L_{PIP} = \frac{\sum(L_1 + L_2 + \cdots L_{50}) \times A_f}{A_i \times N_i} \quad [4–3]$$

where,

L_1, L_2, ⋯ L_{50} are the measured sample lengths in images #1, #2, #3, ….., #50 (mm)

A_f is the area of filter paper (same as above)

A_i is the size of the image (e.g. $A_i = 0.64 \times 0.48 = 0.31$ mm^2)

N_i is the number of images (same as above)

4.2.2 Testing the digital methodologies using possum fur

Brushtail possum (*Trichosurus vulpecula* Kerr) fur (D < 16 μm) was used to mimic hypha when testing the accuracy, precision and effectiveness of the two proposed methodologies. We prepared possum fur for microscopic observation by placing a range of known lengths of possum fur on filter paper. Possum fur sections of total lengths of 4, 8, 12, 16 and 20 mm were used. Their actual lengths were measured with a vernier caliper (± 0.01 mm). The total lengths of possum fur were chosen to cover the typical range of hyphal length observed using the filter paper technique.

Thereafter, in order to more closely reflect actual hyphae distribution, the possum fur on each filter paper was further cut into smaller sections (< 1 mm) under a microscope and placing them on cellulose nitrate filters (0.45 μm, D = 24.62 mm). While the lengths of individually–cut sections were not known, the total length of

smaller sections was known from the prior length determination. Each measurement method was evaluated against the known total length of fur in each sample.

The filter papers loaded with the possum fur pieces were mounted on slides using a low–viscosity, non–fluorescent immersion oil. For each grade length, four replicates were prepared. The slides were placed under a microscope (Nikon ECLIPSE E600 POL) and examined at × 200 magnifications. Fifty images (2560 x 1920 pixels) of the fields of view were randomly taken by a connected digital camera (Nikon Digital sight DS–U1) for each membrane filter and named in sequence (1 to 50).

The length (L) of possum fur on the images were measured using –

(1) *Digital gridline intersection (DGI) method.* A 12 × 9 square grid (size 0.05 ×0.05 mm) was created (Microsoft PowerPoint 2010) according to the scale displayed on the image and placed on the top of the image (Figure 4–1a). The horizontal and vertical intersections of possum fur that crossed the edges of each square on each image were counted (C_1, C_2, .., C_{50}) and insert to the equation [4–2] to calculate the length of the possum fur (L_{DGI}).

(2) *Photomicrography - ImageJ processing (PIP) method.* Each image was analysed using the ImageJ software (1.47 bundled with 64–bit Java) that can be freely download from http://imagej.nih.gov/ij/. The analysis consisted of scale setting (400 pixels = 100 μm), manually tracing and measuring the length (L_1, L_2, ..., L_{50}) of possum fur (Figure 4–1b) and inserting into equation [4–3] to calculate the length of the possum fur (L_{PIP}).

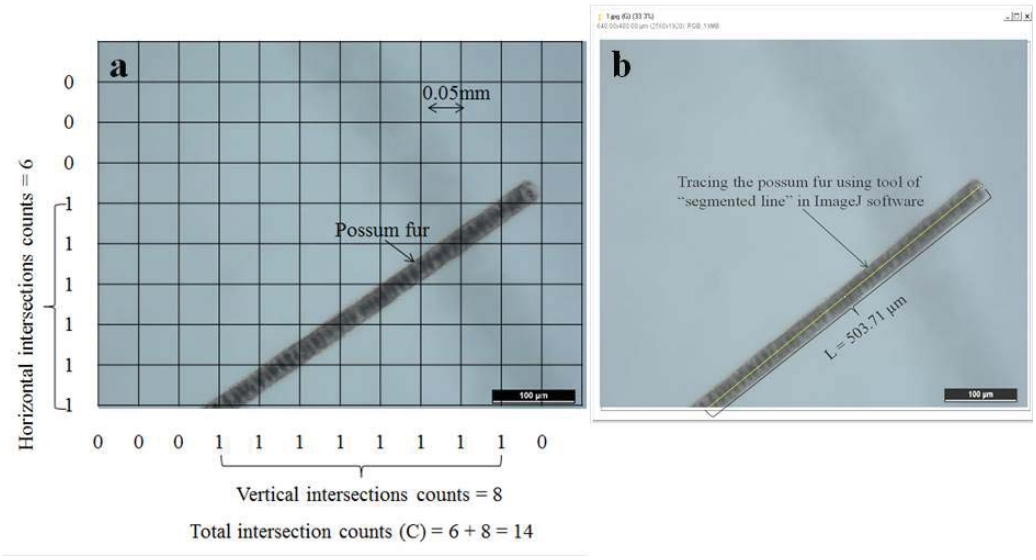

Figure 4–1 The measurement of possum fur on an image taken under a microscopy at ×200 magnification by using (a) the DGI method – A grid layer (12 × 9, grid size 0.05mm × 0.05mm) was placed on the top of the same image and the horizontal and vertical intersections of possum fur that crossed the edges of each square were counted and recorded (e.g., C = 14, the possum fur length calculated using the Tenant equation was 0.550 mm) and (b) the PIP method – the possum fur in the same image was traced (yellow line) manually and measured by the ImageJ software (e.g., L = 0.503 µm)

4.2.3 Measuring hyphal lengths in soils

Two soils with contrasting P status (Olsen P of 4.3 and 33.3 mg kg^{-1}, referred to as LP and HP soil, respectively) were prepared to grow *Lotus pedunculatus* cv barsille in a root study container for 32 wk to establish *rhizosphere* soils with native AMF populations. The root study containers established two soil zones, one with full root and hyphal access and a second that was root–free and could only be colonized by hyphae (Chapter 5). The detailed information on the two soils was provided in Chapter 6. After

the plants had been harvested, the soils were taken from the root–free hyphal compartment for measuring native AMF hyphal lengths.

We prepared hyphae for microscopic observation following the method described by Brundrett (1994) with certain modifications. Briefly, ca 0.40 g of moist soil was thoroughly swirled with 30 mL deionized water and 2 mL 35.7 g L^{-1} sodium hexametaphosphate (Calgon) solution intended to break up aggregates and release the hyphae. Thereafter, 10 mL of the suspension was filtered through a 250–µm sieve to remove large and heavy particles followed by re–suspension with another 30 mL deionized water and 2 mL Calgon solution and letting it settle for 30 seconds. Then, a 10 mL aliquot was filtered with a 20–µm nylon mesh to retain the hyphae, which subsequently were stained in 5 mL 0.6 g L^{-1} trypan blue in 1:2:2 lactic acid: glycerol: deionized water (v:v:v) for 1.5 h. The stained solution was then filtered with cellulose nitrate filters (0.45 µm, D = 24.62 mm) to collect the stained hyphae.

Filters with the stained hyphae were mounted on slides. Hyphae which were angular, aseptate in appearance, and between 1.0 – 13.4 µm in diameter (Figure 4–2) were deemed to be of AMF origin (Boddington et al., 1999) and only those were considered for the measurements and their length were determined following the above–described DGI (Figure 4–2a) and PIP (Figure 4–2b) methodologies. As mentioned before, we installed the NeuronJ plugin (http://www.imagescience.org/meijering/software/neuronj/) of the ImageJ software to facilitate the tracing and quantification of sinuous structures, like hyphae, on the images (Figure 4–2b). Total hyphal lengths (L, mm) on filter papers were obtained from either equation [4–2] or [4–3] and insert to equation [4–4] to calculate total hyphal length (L_{hyphae}, m g^{-1} moist soil) in each soil sample.

$$L_{hyphae}\text{, m g}^{-1}\text{ moist soil} = (L \times f)/(m \times 1000) \quad [4–4]$$

where

L (mm) is total hyphal length on filter paper,

f is the dilution factor (13.44 in the present study)

m (g) is the weight of soil (0.4 g in the present study)

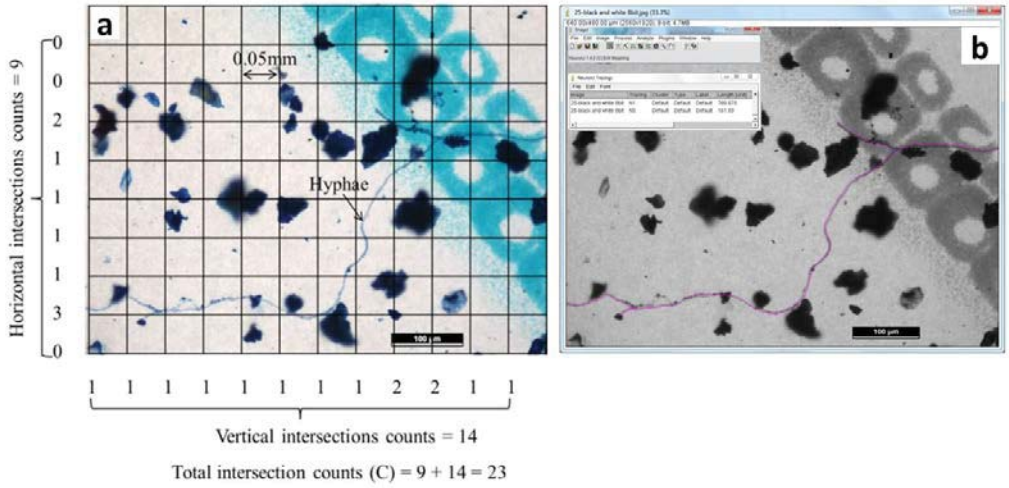

Figure 4–2 AMF hyphae on an image taken under a microscopy at ×100 magnification measured by using (a) the DGI method – a grid layer (12 × 9, grid size 0.05mm × 0.05mm) was placed on the same image, and the horizontal and vertical intersections of hyphae that crossed the edges of each square were counted and recorded (e.g., C = 23, the hyphal length calculated using the Tenant equation was 0.904 mm); and (b) the PIP method – the hyphae in the same image were traced (pink line) and measured by the ImageJ software with NeuronJ plugin (e.g., L = 0.931 mm).

4.2.4 Statistical analysis

All statistical analyses were conducted in the statistical software R version 3.2.2 (R Core Team, 2015). The possum fur lengths measured by the digital gridline intersection (DGI) and photomicrography – ImageJ process (PIP) methods and the known length of possum fur were compared using the fitted linear models. One–way ANOVA with a Tukey post–hoc test was used to evaluate statistical differences ($P < 0.05$) between the possum fur or hyphal lengths measured by the digital gridline intersection (DGI) and photomicrography – ImageJ process (PIP) methods, and between the hyphal lengths measured in two soils with contrasting P status (Olsen P of 4.3 and 33.3 g kg^{-1}). Unless otherwise stated, results are expressed as means of four replicates with their 95% confidential intervals.

4.3 Results

4.3.1 Calibration of the proposed methodologies using possum fur

A scatterplot matrix (Figure 4–3) showed that the results obtained by both testing methods (DGI and PIP methods) were comparable, as indicated by a highly significant ($p < 0.001$) linear relation between the two measurements: $L_{PIP} = 1.72 + 0.89 \times L_{DGI}$ ($r^2 = 0.84$). Also, the lengths of possum fur measured by both the DGI (L_{DGI}) and PIP methods (L_{PIP}) regressed significantly ($p < 0.001$) with the corresponding known lengths (L_{known}). Linear regression equations were $L_{DGI} = 0.37 + 0.97 \times L_{known}$ ($r^2 = 0.86$)

and $L_{PIP} = 0.33 + 1.01 \times L_{known}$ ($r^2 = 0.98$), respectively. The slope of the PIP method regression was 1.01, i.e. it overestimated the true lengths by 1%, while the slope of 0.97 of the DGI method suggests a 3% underestimation. Estimates made by both methods were well within their uncertainty ranges (Figure 4–4).

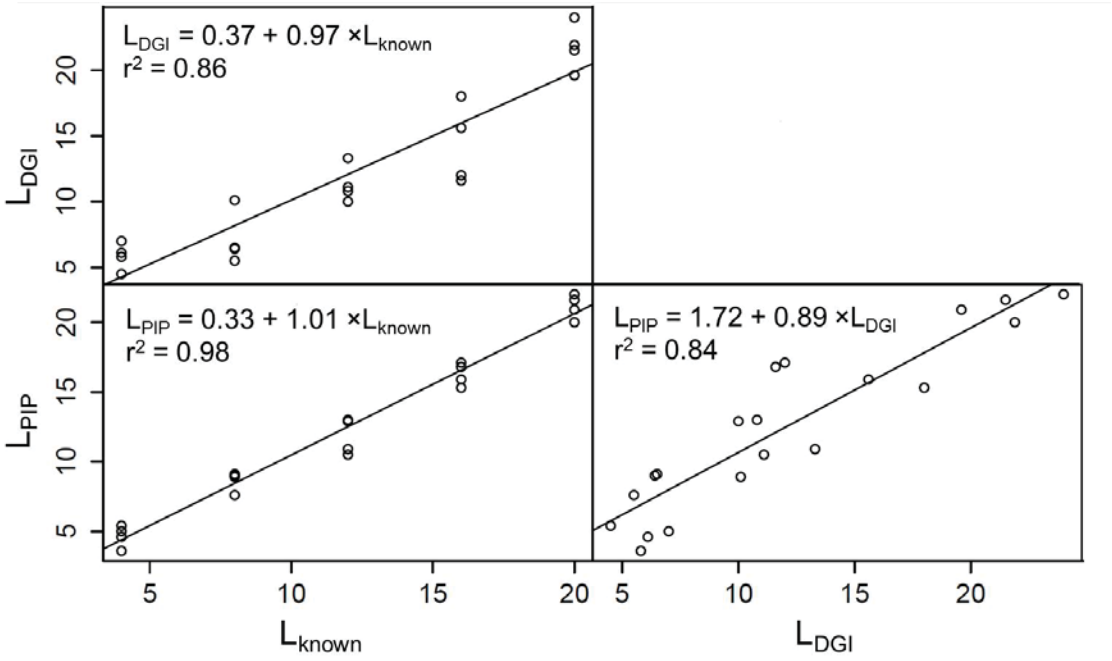

Figure 4–3 A scatterplot matrix with linear regressions amongst the lengths of possum fur measured by both the DGI (L_{DGI}) and PIP methods (L_{PIP}) and the known lengths of possum fur (L_{known})

Despite possum fur lengths as measured by the two methods were both similar to their known values, the coefficients of variation were much lower for the PIP (3.1–8.3%) than the DGI estimates (4.1–14.3%). So, the PIP method tended to be more precise than the DGI method, and this further supported by a higher r^2 value (0.98 vs

0.86). Furthermore, the root mean square errors (RMSE) of the difference between the measured and known lengths of possum fur were calculated as 0.96 and 2.37 mm for the PIP and DGI methods, respectively. Correspondingly, the PIP method resulted in much smaller confidence intervals (Figure 4–4). The 95% confidence interval for the DGI method ranged from –61 to 50% of the mean, whereas for the PIP method, the confidence interval was narrower (from –29 to 17%).

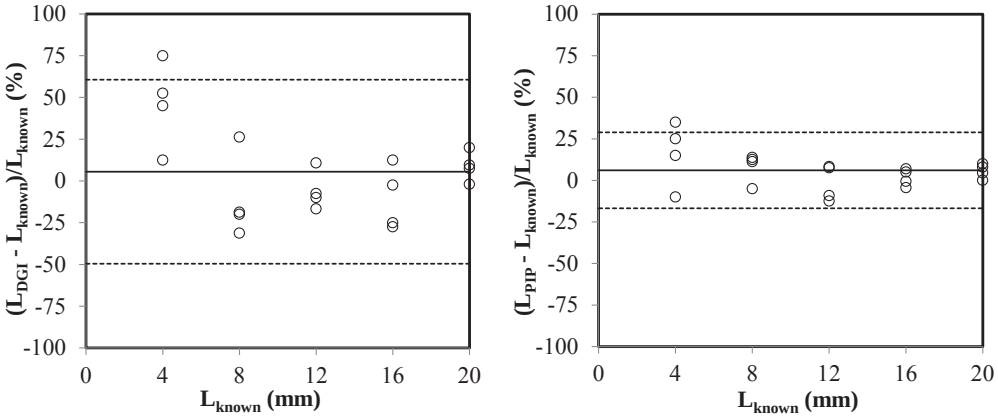

Figure 4–4 The distribution of the 95% confidence limits (dashed lines) of the mean lengths (solid lines) of possum fur measured by both the DGI (L_{DGI}) and PIP methods (L_{PIP}) and the known lengths of possum fur (L_{known})

4.3.2 Measurement of hyphal lengths in soils

The AMF hyphal lengths in soil measured using the DGI and PIP methods ranged from 7.1 to 24.1 m g^{-1} and 6.5 to 19.4 m g^{-1}, respectively (Figure 4–5), both being within the typical of values (3 – 30 m g^{-1}) reported in the literature (e.g. see Table 2 in the review of Leake et al., 2004). Mean hyphal lengths in the same soil samples measured by these two methods were not significantly ($P > 0.05$) different from each

other, with mean values of 17.1 vs 17.4 m g^{-1} in the low–P soil and 7.1 vs 7.2 m g^{-1} in the high–P soil. However, the PIP method gave much smaller uncertainty bounds than the DGI method (Figure 4–5). This was particularly true for the soil with higher AMF hyphal abundance where the confidence intervals were 14.8 – 20.1 mm vs 8.2 – 26.1 mm for the PIP and DGI methods, respectively.

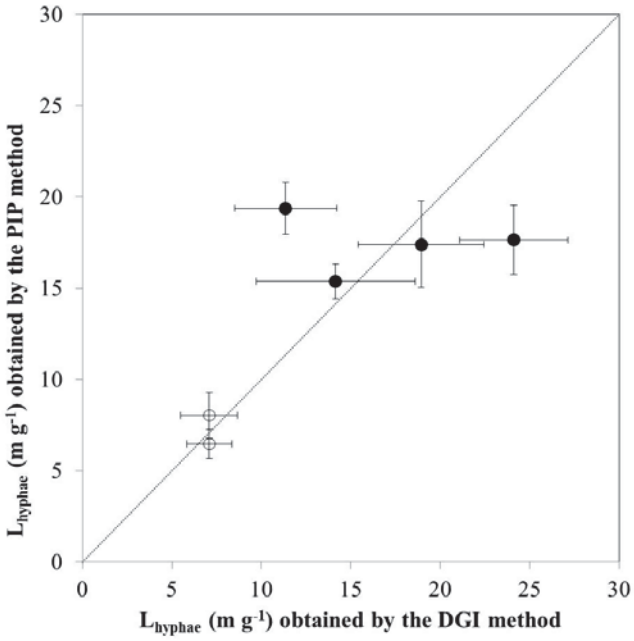

Figure 4–5 The lengths (means ± 95% confidence intervals) of hyphae in soils with low P fertility (solid circles) and high P fertility (open circles) measured by the digital gridline–intersection (DGI) method plotted against measurements by the photomicrography – ImageJ processing (PIP) method. The 1:1 line is shown as a dashed line.

4.4 Discussion

An initial test done on pieces of possum fur which ranged from 4 to 20 mm in length showed linear regressions between the known lengths and the measured lengths of possum fur by using the DGI and PIP methods with no significant ($p > 0.05$) differences between the results obtained using these two methods. There was good agreement between known fur lengths and those estimated by the PIP and DGI methods and no indication of any systematic biases. The digital analysis methods could therefore be considered as suitable alternative methods to the traditional visual gridline intersection method for measuring the lengths of any randomly distributed objectives in soils or other media (e.g., possum fur or mycorrhizal hyphae).

Both methods were then used to measure the length of the AMF mycelia in two soils with distinct P fertility. The hyphal lengths obtained by either the DGI or the PIP methods were consistent with values reported in the literatures (Abbott et al., 1984; Camenzind and Rillig, 2013; Leifheit et al., 2015). The mean hyphal lengths in the same soil sample measured by these two methods were very similar (17.1 vs 17.4 m g^{-1} in the low–P soil and 7.1 vs 7.2 m g^{-1} in the high–P soil, respectively). In previous work, Green et al. (1994) also found no significant differences ($P < 0.05$) between the lengths of AMF hyphae estimated using an image analysis system and those estimated by a trained observer using a modified grid–line intersection method.

Although possum fur length values measured by both methods were close to their known values, the coefficients of variation were much lower for the PIP (3.1–8.3%) than the DGI estimates (4.1–14.3%). Likewise, the standard errors of the estimates of hyphal lengths in soils were approximately 4.3% and 16.3% of their means obtained by

the PIP and DGI methods, respectively. This indicated greater accuracy and reproducibility of the PIP method. Green et al. (1994) also suggested that an image analysis system can facilitate the collection of hyphal data by being faster and less subjective than manual methods, as it is less observer–dependent. Using digital microscope images in conjunction with Tennant's equation was found to be a more accurate and efficient way of estimating hyphal biomass than using a direct visual approach (Hynes et al., 2008).

Although the time spent in measuring the length of hyphae using the two methodologies was similar, the PIP method tended to be more precise than the DGI method. The greater uncertainty of the DGI estimates can be partly attributed to the underlying principle of the DGI method. Any structures on the images were only counted when they intersected the defined gridlines which introduced an extra element of randomness into the counting procedure. Specifically, different results can be obtained when measuring the same length of hyphae by the DGI method since the intersections of the gridline with a stained hyphae can vary with the different random arrangements (i.e. an underestimation by 21% would be obtained when this was arranged perpendicular to one axis (Figure 4–6a) and an overestimation by 23% would be obtained when arranged in diagonal (Figure 4–6b)).

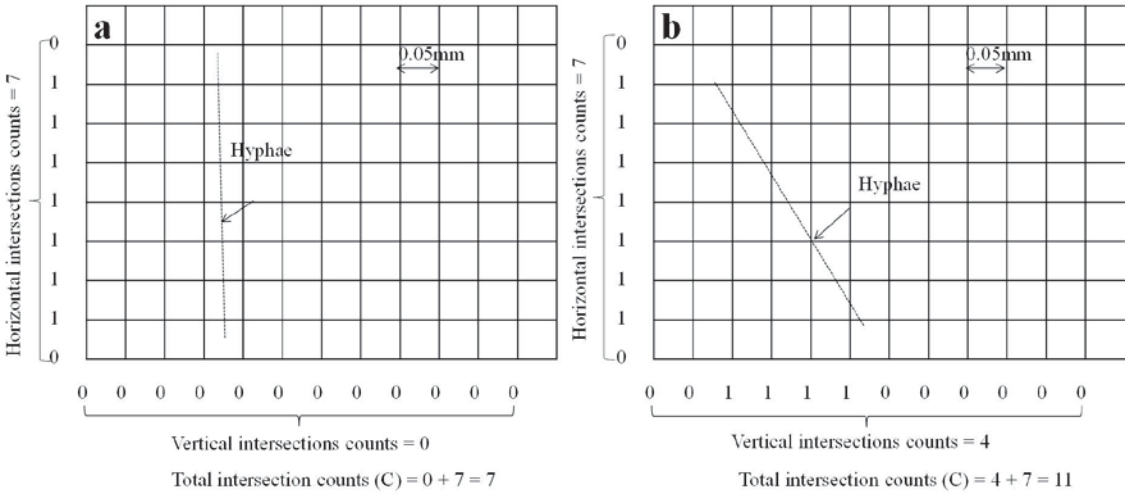

Figure 4–6 Illustration of the intersection of gridlines with a stained hypha and the different number of counts that can be obtained with different random arrangements of these structures. A given length of 0.35 mm hyphae if distributed as (a) intersection count recorded C=7, then a estimated legnth of 0.28 mm was calculated using Tennant equation, and as (b) intersection count as C= 11, its corresponding estimated length was 0.43 mm.

We estimated the extent of that uncertainty by simulating line intersections of straight lines over a large number of random angles starting locations within a grid square. It showed that of the randomness of image angles and starting positions alone introduced a standard deviation of estimates ranging from 10% to 18% (data not shown). Variance was greater for shorter sample lengths, with sample lengths greater than about 10 gridline units, standard deviation became less than about 11%. This kind of random error is unavoidable when the gridline intersection method is used, but can be overcome by the PIP procedure where the whole structure present on the image is traced and measured regardless of its position or distribution on the image.

4.5 Conclusions

Given the effectiveness, accuracy, and ease of processing large data sets by both photomicrography image processing methodologies (DGI and PIP methods), we concluded that both are suited for large–scale and routine measurement of the external mycelia of mycorrhizal fungi under diverse conditions. Among the two digital photography methods, the ImageJ with NeuronJ plugin analysis allowed a semi–automated analysis of the whole elongation structure and minimized observer biases, leading to smaller uncertainty than the digital gridline intersection method. ImageJ is a user–friendly, freely available software that is readily adaptable to different computer platforms. As the photomicrography–ImageJ processing technique is efficient and less prone to error (e.g., associated not only to user bias but also to that caused by how hyphae distributes on the grid), it is a suitable and easy method to study the density and distribution of AMF hyphae in the soil.

4.6 Acknowledgements

The authors acknowledge financial support for Qinhua Shen from the New Zealand Biochar Research Centre. The authors are also deeply grateful to Drs Bob Stewart, Anja Moebis and Xiong Zhao He for their guidance on the principles and use of digital microscopy, and to Mr Bob Toes for providing the possum fur.

Chapter 5

A NOVEL TECHNIQUE FOR EVALUATING THE PHOSPHORUS TRANSFERRED BY ARBUSCULAR MYCORRHIZAL FUNGAL HYPHAE

This chapter aims to evaluate whether the root study container designed by Hedley et al. (1982b) that divides the soil to two sections – *root zone* and *hyphal zone* – can be modified so that phosphorus (P) diffusion between the two compartments is impaired. This root study container will be used in Chapter 6 for testing the hypothesis that the application of biochar increases P bioavailability in soils via stimulating AMF hyphae development in soils.

A paper from this study will be submitted for publication: **Qinhua Shen**, Mike J. Hedley, Marta Camps–Arbestain, Miko U.F. Kirschbaum. A novel technique for evaluating the phosphorus transferred by arbuscular mycorrhizal fungi hyphae. Soil Research (To be submitted).

Abstract

Root study containers that separate soils into *root plus hyphal zone* (also called *root zone*), *rhizosphere* and *hyphal zone* have demonstrated how phosphorus (P) diffusion plays an important role in its bioavailability and so does P uptake by plant roots and arbuscular mycorrhizal fungi (AMF). Potential diffusion of P from the *hyphal zone* to the *rhizosphere zone* makes it difficult to accurately assess the contribution to plant P uptake made by AMF in the *hyphal zone*. This study tested whether a layer of tephra with high P sorption characteristics (referred to as 'P diffusion break') can be used to halt P diffusion between the *root zone* and *hyphal zone* of soils with contrasting P fertility in a root study container. Phosphate sorption studies were conducted on tephra to show that a 3 mm thick layer of tephra was adequate to break P diffusion from a soil with an Olsen P of 33.3 g kg^{-1} (referred to as HP soil) to a soil with an Olsen P of 4.3 mg k^{-1} (referred to as LP soil) for a plant growth period of 1 year. After an 8–month plant growth experiment there was no significant ($P > 0.01$) P accumulation in Resin–P (< 5 mg kg^{-1}) and total P in the middle slice of the 'P–diffusion break' tephra layer in treatment $\frac{\text{LP}}{\text{HP}}$ ($\frac{\text{root zone}}{\text{hyphal zone}}$) when compared with that in treatment $\frac{\text{LP}}{\text{LP}}$, so that there was no P diffused from HP soil to LP soil. Plant P uptake was greater (ca 2 mg pot^{-1}) in the former than in the latter and with a subsequent increase in plant yield by 56%. Given that (i) the aforementioned inability of P to diffuse across the tephra layer; (i) the incapability of roots to penetrate through the mesh to *hyphal zone* to take up P from the HP soil; and (iii) microscopic analysis detected AMF hyphae in the tephra layer, we concluded that by including a layer (e.g., 3 mm) of tephra soil in root study container

the contribution of AMF hyphae to plant P accumulation can be accurately determined. This experimental design can then be applied to study the influence of soil amendments prone to change P availability (e.g. fertilizers, lime, biochar) on P transfer by AMF hyphae.

Key words:

Arbuscular mycorrhizal fungi, Langmuir adsorption – isotherm, Lotus pedunculatus *cv barsille*, P diffusion, Root study container, Tephra

5.1 Introduction

Historically, the prototype 'root study container' consisted of two–round waxed cardboard cartons originally devised by Stanford and DeMent (1957) for measuring nutrient absorption by plants during short periods of time. In the 1980's further development of root study containers was undertaken to measure nutrient depletion profiles in *rhizosphere* soil utilizing nylon or polyester mesh to create a distinct boundary between the rhizoplane and rhizosphere soil (Grinsted et al., 1982; Kuchenbuch and Jungk, 1982; Hedley et al., 1994; Trolove et al., 2003). Studies using these containers facilitated an understanding of how specific processes (e.g., root–induced P depletion and pH changes) occurring in the *rhizosphere* soil are different from those of the *bulk* soil (Trolove et al., 1996; Zoysa et al., 1999). This combined with the soil P fractionation studies (Hedley et al., 1982a) has accelerated the understanding on how crop roots utilize soil P in the glasshouse and field (e.g. Zoysa et

al., 1997; Trolove et al., 2003). The root excluding nylon mesh (*e.g.*, range 20– to 80–μm opening) also provides a root–free compartment into which only AMF mycelia can grow, which has been referred to as a *hyphal zone* or *hyphal compartment* (e.g. Schüepp et al., 1987). This greatly increased the understanding of the abundance and the function of external mycelia in soil (Leake et al., 2004).

The upper compartment in a root study container (e.g. Figure 5-1) has full root and hyphal access (referred to as *root zone*) and lower compartment beneath the fine nylon mesh, is a root–free zone only penetrated by hyphae (referred to as *hyphal zone*). This physical separation allows soil amendments (e.g., fertilizer, or lime, or biochar) to be added to either the *root zone* or the *hyphal zone* separately. Hence, the impacts of these soil additives on root activity and/or on AMF hyphal growth and the contribution of which to plant P uptake can be discriminated (Marschner and Rengel, 2012). However, if a gradient in P status is generated between the two compartments the intended discrimination between hyphal and root P– uptake could be masked by the occurrence of P diffusion between these two compartments.

A modification of the root study container would then be needed so that a 'P diffusion break' was provided and the contribution of hyphal P translocation/uptake from that of P diffusion could be distinguished. The 'P diffusion break' could be made up of a thin layer of subsoil, such as andesitic volcanic tephra, with very high P sorption characteristics through which AMF hyphae could grow to mobilize and transport P from the soil below the 'P diffusion break'. Weathered tephra has reported to have a P fixation capacity of 80–97% (Ryden and Syers, 1975; Hanly et al., 2008) and been used to remove excess P from the wastewater and sewage prior to discharging to an aquatic system (Hanly et al., 2008; Liesch, 2010; Su et al., 2015).

Thus, a layer of this tephra with high P affinity, applied between a P source and roots in conjunction with a root excluding mesh, is expected to provide a barrier for P diffusion in root study containers. Plants growing with such a barrier would be expected to show low P uptake unless AMF mycelia can grow through the layer of tephra, acquire P and transfer it via hyphae to the host plant root. Treatments that stimulate AMF mycelia growth may be expected to increase P uptake, whereas diffusion of P through the barrier will be unaffected.

The objectives of this study were to (i) evaluate the experimental value of adding a layer of tephra between two compartments of a root study container to provide a 'P–diffusion break' (ii) to determine the required specific thickness of the tephra layer; and (iii) to test its effectiveness in halting P diffusion between two soils of contrasting P status.

5.2 Materials and Methods

5.2.1 Soil sampling and characterization

The tephra soil used for the 'P–diffusion break' was collected from a quarry in the Ruapehu district, New Zealand (39°21'39.81"S, 175°19'28.08"E) and characterized with a high P retention capacity (99%) (Table 5–1). Two top soils (0–10 cm depth) were collected from two sites 250 m apart in Mokoia, Taranaki, New Zealand. Both soils were classified as Egmont black loam (Hewitt and Dymond, 2013) − sil–andic Andosols (IUSS Working Group, 2006) − and characterized by having a high allophane content (> 7%, as estimated following the method of Mizota and Van Reeuwijk (1989)) derived from andesitic tephra. The two soils had strongly contrasting Olsen P levels, however

Table 5-1 Selected characteristics of the studied materials

Soil	pH	Bulk density g cm^{-3}	Water holding capacity % (w/w)	Resin P mg kg^{-1}	Olsen P mg kg^{-1}	Total P mg kg^{-1}	P retention capacity[a] %
Tephra soil	6.0	0.79	65	3.8	0.5	649	99
LP soil	6.2	0.74	71	34	4.3	1981	97
HP soil	6.2	0.78	65	164	33.3	4144	99

[a]

the high Olsen P soil (33.3 mg kg^{-1}, referred to as 'HP') was sampled in an area of grazed permanent ryegrass/clover pasture (39°37'11.30"S, 174°21'41.94"E), while the low Olsen P soil (4.3 mg kg, shorted as 'LP') was taken from an undisturbed area under rough pasture that had not received any fertilizer for the last 20 years (39°37'18.02"S, 174°21'38.73"E). The detailed information on the two soils is provided in Chapter 6.

After removing roots and plant debris, fresh soil samples were sieved through a 2–mm sieve and stored in a cold room (< 4°C) for further use. Most of the soil passed through the sieve, given the typical micro–aggregation of these soils. Subsamples were taken, air–dried and characterized for chemical and physical properties using standard methods.

Soil pH (1:2.5, soil: water w/w) was determined using a glass electrode in a 1:2.5 soil: deionized water suspension. The water holding capacity was measured using a pressure plate apparatus at –0.3 bar (Dane and Hopmans, 2002). Total P was determined using a Technicon Auto–Analyser after Kjeldahl digestion (McKenzie and Wallace, 1954). Olsen P was extracted by shaking 1 g of air–dried soil with 20 mL of 0.5 M $NaHCO_3$ solution (pH = 8.5) for exact 30 min (Olsen et al., 1954). Extracts were centrifuged at 25,155 × *g* for 15 min and filtrated through Whatman No. 42; then the pH was adjusted to ca 4 prior to determining P using the ammonium molybdate (blue) method (Murphy and Riley, 1962). Resin–P was determined using the procedure of Saggar et al. (1990). Phosphorus retention capacity (PRC) was determined by shaking 5 g of air–dried soil with 25 mL of 1000 mg L^{-1} KH_2PO_4–P solution for 16 h (Saunders, 1959b). Phosphorus concentration was determined following the vanadomolybdate (yellow) method (Kitson and Mellon, 1944) at 420 nm.

5.2.2 Tephra soil P absorption experiment

Prior to assembling the root study container, the thickness (x mm) of the tephra layer as needed to provide a P diffusion barrier between two Andosols with contrasting P status (HP and LP soils) was determined. For this, a P absorption experiment was conducted so that the P–buffering capacity of the tephra was defined. This was required in order to calculate the effective diffusion coefficient of phosphate in the tephra.

Ca 2 g tephra was shaken overnight (16 h) with 10 mL of 0.01 *M* $CaCl_2$ solution spiked with KH_2PO_4 (previously dried at 105 ^oC for 1 h) to give 11 different P concentrations (5, 10, 20, 40, 60, 80, 100, 200, 400, 800, 1000 mg L^{-1}). The suspension was thereafter centrifuged at 25,155 × *g* for 15 min and filtered through Whatman No. 42. Phosphorus was determined according to the ammonium molybdate (blue) method (Murphy and Riley 1962) at 712 nm after adjusting solutions pH to ca 4.

5.2.3 The concept of the root study container

The root study container consisted of 2 cylindrical containers to provide an upper and a lower compartment. The top cylindrical compartment had an internal diameter of 82.5 mm and a 25 mm effective soil depth, whereas for the basal cylindrical compartment, these were 75 mm and 50 mm, respectively (Figure 5–1). A layer of nylon mesh (30 μm, openings) was arranged in–between the top and basal cylinders to prevent root penetration. Thus, in the section above the mesh both root and hyphae accessed the soil (*root zone*) but the section below the mesh was a root–free zone only penetrated by hypha (*hyphal zone*). The 7–mm thick layer of soil immediately below the

nylon mesh was referred to as *rhizosphere soil* (Zoysa et al., 1999). Below this 7–mm thickness *rhizosphere* soil, a layer of tephra soil was arranged between two soils of contrasting P status in order to perform as a "P–diffusion break". The thickness of this layer was determined after investigating the P adsorption capacity of the tephra and described in the Result and Discussion section 5.3.

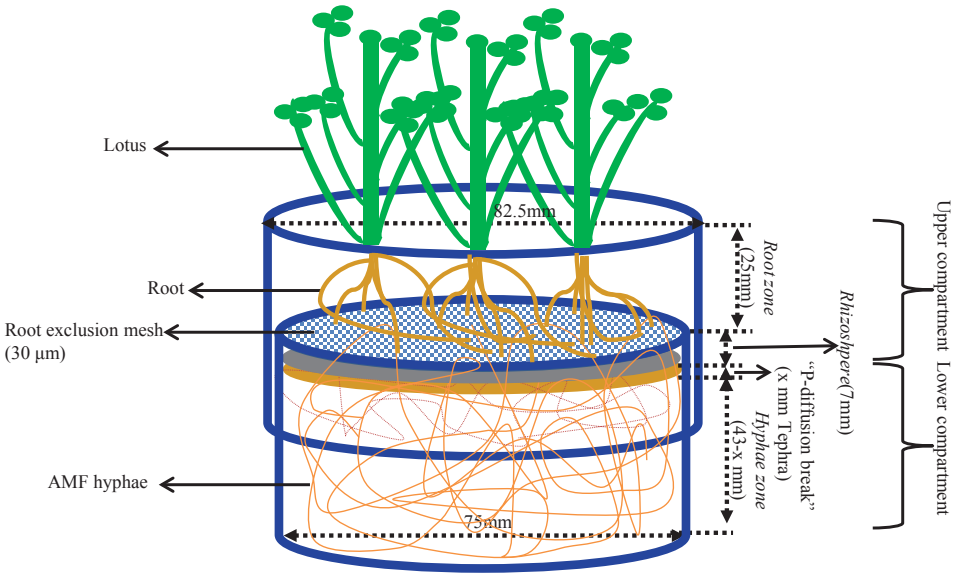

Figure 5–1 Schematic representation of the root study containers

5.2.4 Validation of the 'P diffusion break'

5.2.4.1 Bioassay experiment setup

Lotus pedunculatus cv barsille was grown in root study containers packed with different combinations of soil P treatments in the upper and lower compartments ($\frac{LP}{LP}$ and $\frac{LP}{HP}$, ($\frac{\text{upper compartment}}{\text{lower compartment}}$)) to test the success of 'P diffusion break' (packed at a

bulk density of 0.78) (Figure 5–1). Four replications for each treatment were established. The root study container was then moistened with distilled water until the soils reached a volumetric water content of 70% of soil water holding capacity. The soil was pre–incubated for 2 wk and then thirty seeds of *Lotus pedunculatus cv barsille* (inoculated with *Rhizobium* sp.) were sown per root study container. Since abundant indigenous propagules (e.g., spores and hyphae in the soils) AMF were identified (Figure 5–2), no external inoculum was introduced. Two wk after germination, the seedlings were thinned to five plants per pot.

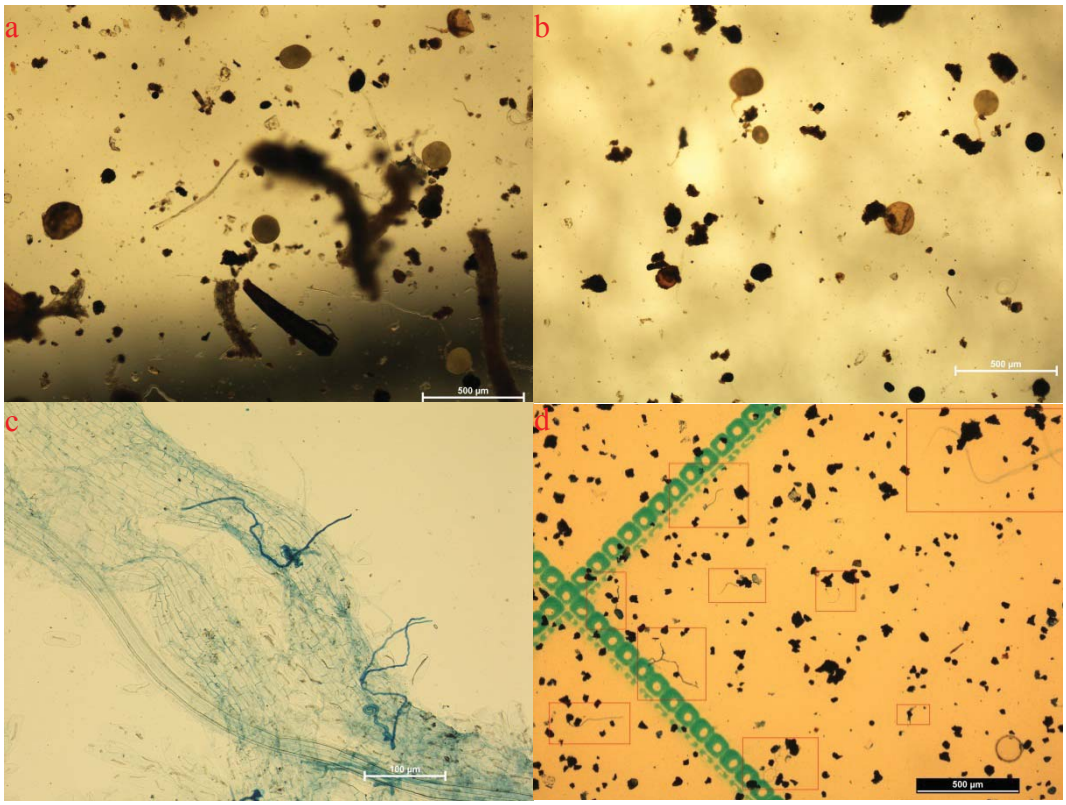

Figure 5–2 Identification of abundant indigenous AMF spores in (a) HP and (b) LP soils before plant growth, (c) AMF colonized in plant root and (d) hyphae in tephra layer after plant growth.

All pots were arranged in a completely–randomized design and kept in a glasshouse. Natural light was supplemented by four growth lights (F58W–GRO–LUX, 1500 mm*26 mm) to provide 16 h of light per day. An N– and P–free nutrient solution (Middleton and Toxopeus, 1973) was applied regularly to maintain plant growth. At harvest, visual inspection showed that *Rhizobium* sp. nodules had developed adequately and maintained adequate N supply to plants. This ensured that P was the principal element limiting plant growth. Water content was maintained at 70% of field water holding capacity throughout the trial period by weighing the pots daily and adding water to reach the corresponding weight.

5.2.4.2 Plant harvests and final harvest

Plants were harvested on four occasions when the height of most plants reached 15 cm. For this, the aboveground biomass was cut down to 2–3 cm above the soil surface, then dried at 75°C to constant weight and weighed to determine the aboveground DM. Subsamples were ground using a ball mill and analysed for P concentration in shoots on a Technicon Auto–Analyser after Kjeldahl digestion (McKenzie and Wallace 1954). The P accumulated in the aboveground plant shoot was calculated by multiplying with the aboveground DM weight. The relative P uptake was expressed relative to the P accumulated in the shoot of plant growth in the $\frac{\text{LP}}{\text{LP}}$ treatment.

After 8 months, the root study containers were destructively separated. The *rhizosphere* soil (directly under the mesh) and the tephra layer were sliced (0.5 mm thickness) using a piston microtome (Trolove et al., 1996). All the slices were kept separately and stored in a chilled room (< 4 ^{o}C) for further analysis. Total P and P

fractionation in the pure tephra slices at different distances (0.5, 1.0, 1.5 mm) away from the *rhizosphere* compartment were determined as described below.

5.2.4.3 P fractionation in tephra

Phosphorus in the first slice of tephra under the *rhizosphere* compartment was divided into four different fractions following Hedley et al. (1994). The different soil P fractions corresponded to differences in chemical solubility:

1. Resin–P (fraction 1) – plant–readily available P_i extracted by shaking ca 0.5 g sample with 30 mL deionized water (suspension #1) containing an anion (HCO_3^- saturated) and a cation (Na^+ saturated) exchange resin strips (6.25*2.5 cm; BDH Chemicals Ltd., England, Saggar et al, 1990) for 16 h and shaking the resin strips in 30 mL 0.5 M NaCl solution for 30 min to recover P;
2. NaOH–P_t including inorganic P associated with Fe and Al hydrous oxides and labile organic P. For this, 3.3 mL of 1 M NaOH were added to soil suspension #1 and re–shaken for 16 h (suspension #2). Thereafter, suspension #2 was centrifuged (Sorvall Centrifuge, with an S34 rotor) at 25,155 × *g* for 10 min and the supernatant #2 was filtered through a Whatman No. 41 filter paper. Then total NaOH extractable P (NaOH–P_t) was determined in a 10 mL aliquot of this supernatant #2 using an Auto–analyser after Kjeldahl digestion (McKenzie and Wallace 1954).
3. H_2SO_4–P (fraction 3) − which predominantly corresponds to calcium phosphates or apatite–like P, was extracted by shaking the soil residue from step (2) with 30

mL 0.5 M H_2SO_4 for 16 h. Thereafter, suspension #3 was centrifuged and filtered as described above for P measurement;

4. Residual–P (fraction 4) − recalcitrant inorganic and organic P, was determined using an auto analyser after Kjeldahl digestion of the soil residual from step (3) (McKenzie and Wallace 1954).

In order to avoid overestimating P, the residue from each step was shaken with 30 ml deionized water for 30 min and centrifuged as described above and the supernatant was discarded before adding the next extraction solution. Phosphorus was determined according to the ammonium molybdate (blue) method (Murphy and Riley 1962) at 712 nm after adjusting solutions pH to ca 4 unless otherwise mentioned.

5.2.5 Statistical analysis

Unless otherwise stated, results are expressed as means of four replicates with their standard errors. One–way ANOVA with a Tukey post–hoc test was used to evaluate statistical differences ($p = 0.05$) in total P in tephra slices by SPSS software (IBM SPSS Statistics 20). The equilibrium $H_2PO_4^-$ concentration and $H_2PO_4^-$ sorbed in tephra were fitted in the Langmuir adsorption – isotherm in RStudio (RStudio Team 2015) using the nls package.

5.2 Result and discussion

5.3.1 Langmuir adsorption – isotherm of tephra soil

The amount of P removed by the tephra from the solution (mg P kg^{-1} tephra) was calculated from the decrease of P concentration in the solution (mg P L^{-1}). Data of P sorbed was plotted against the equilibrium P concentrations in solution (Figure 5–3) and were well fitted (R = 0.99) by the *Langmuir adsorption - isotherm* equation [5–1].

$$\frac{q}{Q} = \frac{b \times C}{1 + b \times C} \qquad [5–1]$$

The resultant fitting equation was

$$\frac{q}{5337} = \frac{0.9465 \times C}{1 + 0.9465 \times C} \qquad [5–2]$$

where,

C is the equilibrium P concentration (mg L^{-1});

q is the mass of P per mass unit of tephra at equilibrium (mg kg^{-1});

Q is maximum P–adsorption capacity – the maximum mass adsorbed at saturation conditions per mass unit of tephra (5337 mg kg^{-1});

b is the P–binding energy constant – the empirical constant with the unit being the inverse of concentration (0.9465 L mg^{-1}).

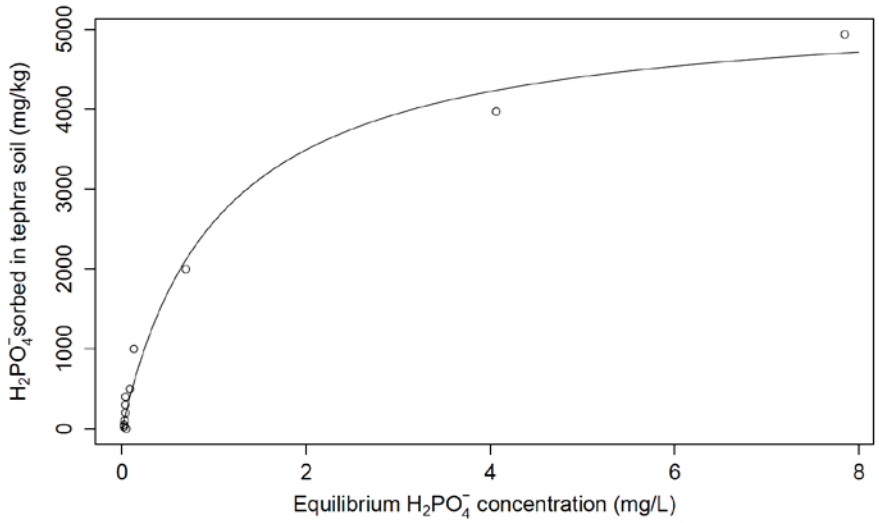

Figure 5–3 Relationship between equilibrium $H_2PO_4^-$ concentration and $H_2PO_4^-$ sorbed on tephra.

5.3.2 P-diffusion break' thickness calculation

The sufficient thickness (x mm) of the tephra layer to prevent P diffusing from the HP soil to the LP soil within the studied period (ca 1 year) was estimated using the following equations:

$$D_e = D_1 \times \theta \times \frac{1}{f} \times \frac{dCl}{dCs} \quad [5–3]$$

$$d = \sqrt{2 \times D_e \times t} \quad [5–4]$$

where,

D_e is the effective diffusion coefficient of P in the soil (m^2 s^{-1});

D_1 is the diffusion coefficient of $H_2PO_4^-$ in water;

θ is the volumetric water content of the soil (m^3 m^{-3});

f is the impedance factor which takes into account the tortuous pathway of ions and other solutes through water–filled soil pores, increasing the path length;

$\frac{dCl}{dCs}$ is the reciprocal of the soil buffer power for the $H_2PO_4^-$ concerned;

C_l is the concentration of $H_2PO_4^-$ in the soil solution;

C_s is the sum of $H_2PO_4^-$ in the soil solution and that desorbable from the solid phase.

All parameters as used to calculate the thickness of the tephra layer are presented in Table 5–2. Briefly, D_l was reported by Marschner and Rengel (2012). θ was calculated based on the fact that the water content was hold at 70% water holding capacity throughout the experiment. The initial C_l – the concentration of $H_2PO_4^-$ in the soil solution– at the soil–tephra boundary was estimated based on the relationship between soil P release (determined by $CaCl_2$ extraction in a 5:1 solution to soil ratio for 30 min) and the Olsen P values established by McDowell et al. (2001), that the corresponding soil P release (C_l) of an Olsen P value of 33.3 mg kg^{-1} (in HP soil) was 0.15 mg L^{-1}. The C_s value was calculated by inputting C_l into the equation [5–2] resulting is a value of 664 mg kg^{-1} (Table 5–2). A tephra thickness of 2.39 mm was obtained by entering the parameters in Table 5–2 to the equations [5–3] and [5–4]. Therefore, the results indicate that a 2.39 mm layer of tephra separating the HP and LP soil should be enough to prevent P diffusion between the layers for a time period of at least 1 year.

Table 5-2 Parameters for calculating the thickness of the tephra P diffusion break

Parameters	Unit	Formula	Values
θ			0.46
f			0.68
C_l	mg L^{-1}		0.15
C_s	mg L^{-1}	$C_s = \frac{5337 \times 0.9465 \times C_1}{1 + 0.9465 \times C_1}$	664
b		$b = \frac{dC_s}{dC_l}$	4423
1/b		$\frac{1}{b} = \frac{dC_l}{dC_s}$	2.26E–04
T	sec		2.07E+07
D_l	m^2 s^{-1}		9.00E–10
De	m^2 s^{-1}	$D_1 \times \theta \times \frac{1}{f} \times \frac{dC_l}{dC_s}$	1.38E–13
d	m	$d = \sqrt{2 \times D_e \times t}$	2.39E–03
d	mm		2.39

5.3.3 Validation of the 'P-diffusion break'

After 8 months of plant growth, total P concentration in the tephra slices sampled ranged from 682 to 716 mg kg^{-1} (Figure 5–4). The values were marginally higher than that of tephra at time 0 before plant growth (649 g kg^{-1}, Table 5–1). Total P in pure tephra slices of the $\frac{LP}{HP}$ treatment were generally higher the corresponding values in the $\frac{LP}{LP}$ treatment, but differences were not significant ($P > 0.05$). Furthermore, differences in total P concentrations with increasing depth away from the *rhizosphere* compartment were not significant ($P > 0.05$). Phosphorus concentrations in the 0.5, 1 and 1.5 mm slices bore no relationship to the proximity of the HP soil indicating that P diffusion from HP to LP soil did not impact on the P concentration in the tephra layer close to the *rhizosphere*.

In addition, when looking at the P fractionation in the first pure 0.5 mm thick tephra slice adjacent to under the *rhizosphere* (Table 5–3) there were no significant ($P > 0.05$) differences between treatment $\frac{LP}{LP}$ and $\frac{LP}{HP}$ in any of the P fractions studied (Resin–P, NaOH–P, H_2SO_4–P, and Residual–P). Resin–P values (the most readily P form for plant to uptake) of these treatments were < 5 mg kg^{-1} and there were no significant ($P > 0.05$) differences between the two treatments. The tephra resin–P concentrations ranged from 3 to 5 mg P kg^{-1} soil, whereas the LP and HP soils had resin P values of 34 and 164 mg P kg^{-1} (Table 5–1), respectively. It was also noted that there was a slight increase in H_2SO_4–P and Residual–P in the tephra of the $\frac{LP}{HP}$ treatment compared with that of the $\frac{LP}{LP}$ treatment, this being 94 vs 73 mg P kg^{-1}, and 170 vs 166 mg P kg^{-1}, respectively, which indicates a possible movement of P from the HP soil upwards, but a subsequent

conversion into recalcitrant P forms. In contrast to the tephra, the NaOH, H_2SO_4–P and Residual–P pools in the LP and HP soils were 1255, 219, and 473 and 2687, 652, and 641 mg P kg^{-1}, respectively. The overall increase in the different P fractions of the whole tephra layer (3 mm) represented < 0.7% and 2.1% of the resin P fraction and NaOH P fraction of a 4–mm HP soil depth, respectively. Thus, it is highly unlikely that P diffusion from the HP soil to the LP soil was observed.

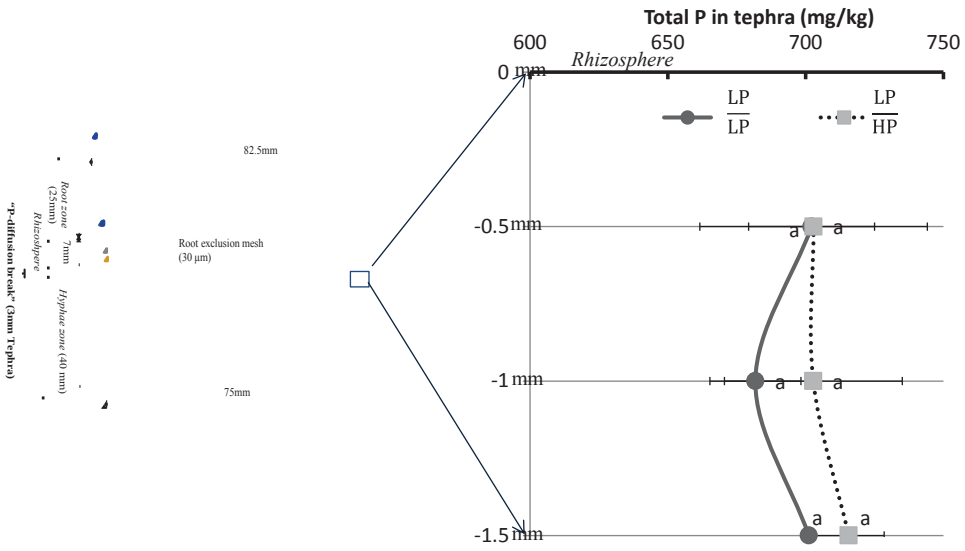

Figure 5–4 Total P content in the pure tephra slices of different depth (0.5, 1.0, 1.5 mm) away from *rhizosphere.*

Table 5-3 The P fractionation (mg kg^{-1}) in the first pure 0.5 mm thick tephra slice adjacent to under the *rhizosphere.*

Treatments	LP / LP	LP / HP
Resin–P	3.7 ± 0.8	4.5 ± 0.2
NaOH–P_t	467 ± 19	471 ± 18
H_2SO_4–P	73 ± 12	94 ± 6
Residual–P	166 ± 5	170 ± 3
Total P	710	739

*Different letters indicate significant differences ($P < 0.05$, n = 4) as determined by one–way ANOVA

AMF hyphae were detected in the tephra layer (Figure 5–2d). Phosphorus uptake by plant shoot in the $\frac{\text{LP}}{\text{HP}}$ treatment was doubled of that in the $\frac{\text{LP}}{\text{LP}}$ treatment (Figures 5–5a, b), resulting in a significant ($P < 0.05$) 56% increase in shoot DM accumulation (Figure 5–5c). Given that (i) upward P diffusion from HP soil in the hyphal zone soil was unlikely and (ii) the inability of roots to take up P from the HP soil (as a mesh impeded their penetration), the increase in P uptake can only be ascribed to P transferred from the HP soil in the hyphal compartment to the LP soil in the root compartment (*Rhizophere zone*) by AMF hyphae growing through the tephra layer. This allows assess the extent to which P taken up by AMF hyphae from a soil of high P fertility contribute to the total P uptake by the host plant growing in a P deficient soil. This experimental design can then also be applied to study the influence of soil amendments prone to change P availability (e.g. fertilizers, lime, biochar) on P transfer by AMF hyphae

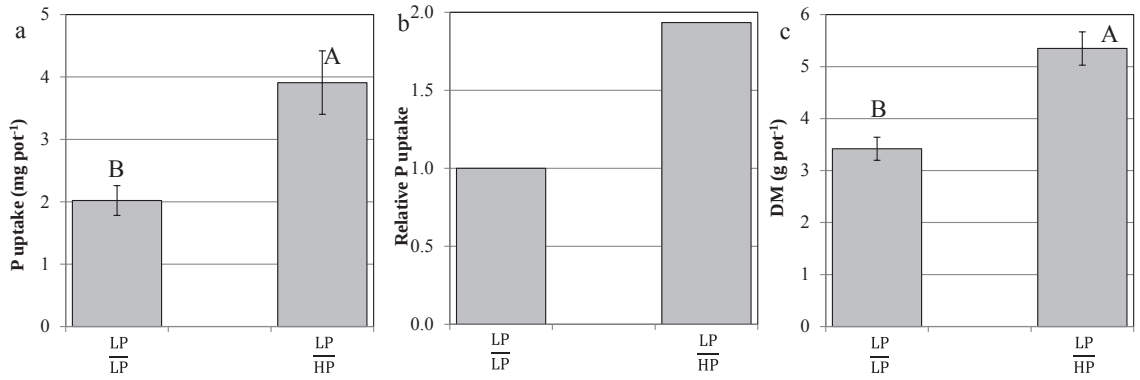

Figure 5–5 Effect of the presence of the HP soil (to which only hyphae had access) below the *root zone* of LP soil on the plant growth (shoot dry mass) (a), the P uptake (b) and the relative P uptake was expressed relative to the P uptake of plants grown in the treatment $\frac{\text{LP}}{\text{LP}}$ (c).

5.4 Conclusion

We determined that a 3 mm thickness tephra layer was sufficient to break the P diffusion between the HP soil and the LP soil within the study period. Indeed, there was no diffusion between two investigated soils during the 8–month experiment. Thus, any increase in P uptake by plant growth in the $\frac{\text{LP}}{\text{HP}}$ treatment compared with that in the $\frac{\text{LP}}{\text{LP}}$ treatment can be only attributed to acquisition of P by AMF hyphae from the HP soil present in the lower compartment. We propose that by including a layer of tephra soil in root study containers will allow to evaluate the contribution of AMF hyphae in P uptake by the host plant and distinguish from that originated from P diffusion and root P uptake. This can be used to study the influence of soil amendments intended to change P solubility (e.g. fertilizers, lime, biochar) on P transfer by AMF hyphae.

5.5 Acknowledgements

The authors acknowledge financial support for Qinhua Shen from the New Zealand Biochar Research Centre. The authors are also deeply grateful to Dr James Hanly for providing the tephra. We are also grateful for the technical support from Mr Ian Furkert, Mr Bob Toes, and Ms Glenys Wallace.

Chapter 6

CAN BIOCHAR INCREASE THE BIOAVAILABILITY OF PHOSPHORUS?

This chapter is reporting an experiment been conducted to test whether the biochars can be used to increase the availability of P to plant in sil–Andosols and the main achievements. The biochar investigated here were made from willow woodchips and pine woodchips, which in turn have contrasting characteristics (e.g., porosity, liming potential, and fertilizer values). The biochars were selected based on the hypothesis that the increase in soil pH and the stimulation of biochar as well as the self–contained P will increase P uptake and yield of plant growing in such Andosols amended with these very biochars.

A paper from this study will be submitted for publication: **Qinhua Shen**, Mike J. Hedley, Marta Camps–Arbestain, Miko U.F. Kirschbaum. Can biochar increase the bioavailability of phosphorus? (2016). Journal of Soil Science and Plant Nutrition (*Accepted*)

Abstract

A large proportion of phosphate (P) fertilizer applied to Andosols reacts with reactive aluminium (Al) and iron (Fe) to become unavailable for plant uptake. We investigated whether biochar could enhance plant growth by (i) mobilizing soil P through changing soil pH or facilitating the growth of arbuscular mycorrhizal fungi (AMF), and/or (ii) introducing additional P.

We grew *Lotus pedunculatus cv* barsille in two Andosols of contrasting P status amended with three biochars (with distinct porosity, nutrient and liming properties) at an application rate of 10 t ha^{-1} for 32 wk. The growth medium was divided into a *root* and a *hyphal zone* through a nylon mesh and a tephra layer that allowed the P in the hyphal zone to be transferred only by AMF hyphae.

The addition of a relative nutrient–rich biochar (e.g. made from willow woodchips) with liming properties to the *root zone* of a P–deficient soil increased plant growth by 59% and P uptake by 73% while pine–based biochar provided no extra nutrients and no growth stimulation. None of the tested biochars conferred advantages in the *root zone* of a high–P soil. However, biochar produced from pine woodchips at 450 ^{o}C enhanced P uptake by AMFs from the *hyphal zone* of a high–P soils by 76% and increased plant growth by 40%.

We concluded that the benefits from biochar addition to nutrient uptake and plant growth are biochar– and soil– specific. Thus, biochars need to be tailored for certain soils by optimizing feedstock and pyrolysis conditions before application.

Keywords

Arbuscular mycorrhizal fungi, Andosols, Biochar, Lotus, Phosphorus bioavailability, Rhizosphere

6.1 Introduction

Andosols are generally formed from volcanic parent materials at early stages of weathering, although they have also been identified in young soils developed from basic and meta–basic rocks under humid and per–humid climates (Garcia–Rodeja et al., 1987; IUSS Working Group, 2006). These soils are characterized by having high organic matter content, low bulk density, good aeration, and adequate moisture retention (Dahlgren et al., 2004; Lowe and Palmer, 2005). Even though these distinctive properties make them suitable for agricultural use (Nanzyo, 2002), the considerable presence of reactive Al (and to a lesser extent Fe) surfaces (e.g., allophane, imogolite, organo–Al complexes, ferrihydrite) generates a high affinity for P, which commonly leads to low agronomic P use efficiency (Saunders, 1959a, b, 1965; Parfitt, 1989; Nanzyo, 2002).

Two major reactions − adsorption and precipitation − are involved in the process of P fixation in Andosols (Parfitt, 1989). The former occurs mainly through ligand–exchange reactions of P–OH groups with exposed –OH/OH_2 groups in Fe and Al oxy–hydroxides (Parfitt, 1978; Goldberg and Sposito, 1985) and surface–bound silicates and bisulphates (Munns and Fox, 1976; Beck et al., 1999). Over time, after this initial adsorption, local solutes may become concentrated causing precipitation of Al

phosphate to occur (Munns and Fox, 1976; Imai et al., 1981). These reactions depend on soil pH and P saturation on surface binding sites (Goldberg and Sposito, 1985).

In sil–andic Andosols – those with reactive Al being predominantly inorganic Al constituents (i.e. allophane) rather than organo–Al complexes − most of the non–available P is locked up with allophane (Parfitt, 1989; Parfitt et al., 1989). This has led to an accumulation of up to almost 4 t P ha^{-1} in intensively farmed sil–andic Andosols top–soils in New Zealand (Perrott and Sarathchandra, 1987; Perrott et al., 1989). Moreover, many sil–andic Andosols in New Zealand have been under (mainly legume–based) permanent pasture for a long time, which has led to soil acidification ((Bolan et al., 1991; Bolan and Hedley, 2003) and references therein), which is likely to cause a further increase in reactive Al surfaces and thus P sorption (Bolan et al., 1999).

Consequently, a relatively high input of P fertilizer is essential for maintaining pasture production in these soils. We used the nutrient budget model OVERSEER$^{(R)}$ version 6.1.2 to estimate fertilizer requirements for a typical dairy farm of sil–andic Andosols with a stocking rate of 2.8 cows ha^{-1} and a milk solids production of 980 kg ha^{-1} in the Taranaki region (New Zealand) (LIC, 2013–14). We found that the farm required P fertilization rates of up to 59 kg P ha^{-1} $year^{-1}$ to maintain a soil Olsen P value of 35 mg kg^{-1} and sustain ongoing milk production at the set rate. Given that ongoing agricultural demand and diminishing mineable resources are expected to lead to a shortage of P (Cordell et al., 2009), it is necessary to consider management practices that can make the large pool of unavailable P in Andosols more available.

Biochar technology has been proposed as a carbon (C) sequestration strategy to contribute to the mitigation of greenhouse gas emissions (Lehmann et al., 2006; Macías and Camps–Arbestain, 2010). Additionally, purpose–made biochars hold promises in

improving soil physical properties (Herath et al., 2013; Quin et al., 2014), reducing soil fertility constraints (Mia et al., 2014) and stimulating soil biological processes (Anderson et al., 2011; Quilliam et al., 2013), and thereby enhance crop performance (Smider and Singh, 2014; Tammeorg et al., 2014). Several studies have been undertaken to understand how P availability to plants can be directly or indirectly influenced by biochar addition and these are described below.

Certain biochars have liming properties and are thus likely to modify the soil pH, the extent of this effect being dependent on the pH–buffering capacity of both biochar and the soil (Anderson et al., 2011; Yuan et al., 2011a; Xu et al., 2012). An increase in pH can reduce P adsorption and precipitation on reactive Al surfaces and also help overcome Al toxicity in acid soils (Haynes, 1982; Uchida and Hue, 2000; Curtin and Syers, 2001; Alleoni et al., 2010). This, together with potential soil physical improvements following biochar incorporation, may provide plant roots with a better environment to grow and take up nutrients (Prendergast–Miller et al., 2014; Ventura et al., 2014). The effect of biochar on P availability will also be influenced by the available P content of biochar (Slavich et al., 2013a; Wang et al., 2013a, b).

Furthermore, the addition of biochar may stimulate the activity of AMF (Warnock et al., 2007) by facilitating their abundance and functionality with the provision of a suitable environment through modifications of (i) soil pH (Solaiman et al., 2010a); (ii) soil micro–porosity (Nzanza et al., 2012; Hammer et al., 2014); (iii) mineral nutrient availability (Hammer et al., 2014), and/or (iv) root – fungi signalling path [as suggested by Warnock *et al*. (2007) and Vanek and Lehmann (2014)]. Nonetheless, the magnitude of these effects will also depend on (i) biochar characteristics; (ii) biochar placement (e.g., distance from plant root); (iii) soil type and (iv) soil P status (i.e., in a

case study where biochar raised the soluble P supply in the soil, there was lower root AMF colonization than in non–amended soils (Vanek and Lehmann, 2014)).

Although Vanek and Lehmann (2014) indicated that biochar enhanced the access of AMF to sparingly–soluble P in the *rhizosphere*, neither their study nor previous ones (to our knowledge), attempted to distinguish between the effects of biochar on the contribution of the roots and the AMF mycelium to P uptake. Hence, the specific objectives of this study were to (i) investigate the effect of different biochars (all derived from wood, but with different nutrient contents, porosity, and liming properties) on soil P bioavailability when added to two *root zone* soils of contrasting P status; and (ii) examine whether the effect of biochar on AMF growth, if any, was dependent on its placement (e.g., in a P–rich soil patch within a low P soil). We hypothesize that: (i) a soil of high P status, either inherent of the soil or resulting from biochar addition, would discourage AMF mycelium branching; (ii) in a soil with low P availability, AMP hyphal growth would be stimulated to explore the soil at a further distance from the plant root in order to increase P supply; (iii) plant roots would play a more prominent role in P uptake over that of AMF hyphae when sufficient P was available in the system.

6.2 Materials and Methods

6.2.1 Soil sampling and characterization

Two top soils (0–10 cm depth) were collected from two sites 250 m apart in Mokoia, Taranaki, New Zealand. Both soils were classified as Egmont black loam

(Landcare Research Centre, 2013) − sil–andic Andosols (IUSS Working Group 2006) − and characterized by having a high allophane content (> 7%, as estimated following Mizota and Van Reeuwijk (1989)) derived from andesitic tephra. The two soils had strongly contrasting Olsen P levels, however: the high Olsen P soil (33.3 mg kg^{-1}, referred to as 'HP') was sampled in an area of grazed permanent ryegrass / clover pasture (39°37'11.30"S, 174°21'41.94"E), while the low Olsen P soil (4.3 mg kg^{-1}, referred to as 'LP') was taken from an undisturbed area under rough pasture that had not received any fertilizer for the last 20 years (39°37'18.02"S, 174°21'38.73"E). After removing roots and plant debris, fresh soil samples were sieved through a 2–mm sieve and stored in a cold room (< 4°C) for further use. Most of the soil passed through the sieve, given the typical micro–aggregation of these soils. Subsamples were taken, air–dried and characterized for chemical and physical properties (Table 6–1) using standard methods.

Table 6-1 Selected properties of the two Andosols [a]

Properties	Units	LP soil	HP soil
Bulk density	g cm^{-1}	0.74	0.78
$pH_{1:2.5}$		6.2	6.2
pH_{NaF}		10.4	11.1
CEC [b]	cmol(+) kg^{-1}	13.5	13.9
P retention capacity	%	97	99
Olsen P	mg kg^{-1}	4.3	33.3
Resin–P	mg kg^{-1}	34	164
Total P	mg kg^{-1}	1981	4144
Total C	%	8.0	10.6
Al_{py} [c]	%	0.56	0.82
Al_{ox} [d]	%	2.50	3.16
$Al_{ox}+1/2Fe_{ox}$	%	3.02	3.72
Al_{py}/Al_{ox}		0.23	0.26
Allophane content	%	7.5	9.3
Exchangeable Al	cmol kg^{-1}	0.03	0.09

[a] All concentrations are expressed on an oven dry weight basis

[b] Cation exchangeable capacity

[c] Subscript py referred to sodium pyrophosphate–extractable

[d] Subscript ox referred to acid (pH=3) ammonium oxalate–extractable

The soil $pH_{1:2.5}$ was determined using a glass electrode in a 1:2.5 soil: water suspension. The pH_{NaF} at t = 2 min was measured in a 1:50 soil: saturated NaF suspension, a pH_{NaF} > 9.5 indicates the presence of reactive Al (allophane and/or organo–Al complexes) (Fieldes and Perrott, 1966). The CEC was determined by 1 M ammonium acetate (pH=7) (Rayment and Lyons, 2011). Aluminium (Al), Fe and Si from short–range order materials were extracted by acid ammonium oxalate (pH=3) (Al_{ox}, Fe_{ox} and Si_{ox}); Al and Fe from organic complexes were extracted by sodium pyrophosphate (Al_{py} and Fe_{py}), although this reagent can also extract relatively small amounts from short–range order inorganic constituents, and exchangeable Al was extracted by 1 M KCl solution (Al_{ex}) following the procedure outlined by García–Rodeja et al. (2004; 2007). The concentrations of Al, Fe and Si in all extractants were determined by Atomic Absorption Spectroscopy (AAS, GBC 904 Avanta Ver 1.33, Australia).

Total P was determined using a Technicon Auto–Analyser after Kjeldahl digestion (McKenzie and Wallace, 1954). Olsen P was extracted by shaking 1 g of air–dried soil with 20 mL of 0.5 M $NaHCO_3$ solution (pH = 8.5) for exact 30 min (Olsen et al., 1954). The suspension was then centrifuged at 25,155 × g for 10 min and filtrated through Whatman No. 42. The Resin–P was extracted by shaking ca 0.5 g sample with 30 mL deionized water containing an anion (HCO_3^- saturated) and a cation (Na^+ saturated) exchange resin strips (6.25*2.5 cm; BDH Chemicals Ltd., England, Saggar et al., 1990) for 16 h and shaking the resin strips in 0.5 M NaCl solution for 30 min to recover P (Hedley et al., 1994). The P in $NaHCO_3$ and NaCl solutions were then determined according to the ammonium molybdate (blue) method (Murphy and Riley, 1962). Phosphorous retention capacity was determined by shaking 5 g of air–dried soil

with 25 mL of 1000 mg L^{-1} P solution with respect of KH_2PO_4 (pre–dry at 105 ^oC for 1.5 h) for 16 h (Saunders, 1965). The P in the solutions after centrifugation and filtration as described above were then determined according to the vanadomolybdate (yellow) method (Kitson and Mellon, 1944).

6.2.2 Biochar production and characterization

Two types of feedstock were used for biochar production: (a) chipped pine (*Pinus radiata* D. Don) branches and (b) chipped weeping willow (*Salix matsudana* L.) branches. Pine wood chips were pyrolysed at 450°C or 550°C and willow wood chips only at 550°C in a 27–L gas–fired rotating drum kiln with an average heating rate of 10°C min^{-1}. The resultant solid pyrolytic products were referred to as BP450, BP550 and BW550, respectively. Biochars were ground to pass through a 2–mm sieve before mixing with soil for the bioassay trial. Subsamples were further ground to a particle size less than 0.3 mm using a ring mill for characterization (Table 6–2).

Table 6-2 Selected properties of biochars [a]

Biochar	Units	BP450	BP550	BW550
pH $_{1:20}$		7.5	8.9	9.4
EC[b]	µS cm^{-1}	212	283	1165
Liming equivalence	% $CaCO_3$–eq	≈0[c]	≈0[c]	18.2
Ash	%	1.1	1.6	10.8
Total N	g kg^{-1}	3.5	4.8	17.8
Available N [d]	mg kg^{-1}	56.5	41.3	383.5
Total P	mg kg^{-1}	443	490	4234
Available P [e]	mg kg^{-1}	92	97	1588
Available K [f]	g kg^{-1}	3.59	4.60	12.84
Available Mg [g]	g kg^{-1}	0.38	0.21	2.95
Available S [h]	mg kg^{-1}	69	59	2606
Resin – P	mg kg^{-1}	69	61	268

[a] All concentrations are expressed on an oven dry weight basis

[b] Electrical conductivity

[c] < Detection limit

[d] 6 M HCl hydrolysable N

[e] 2% formic acid extractable P

[f, g, h] 1 N HCl–extractable K, Mg, S

The pH and EC were measured following a modification of the method of Rajkovich *et al*. (2012) in a suspension of biochar in deionized water (ratio of 1:20; w/w) recommended by IBI (2012). Calcium carbonate equivalence (liming equivalence, % $CaCO_3$–eq) was determined according to IBI standards modified from the method proposed by Rayment and Higinson (1992). For this, 10 mL of 1 M HCl solution (standardized) to 0.5 g of biochar. The suspension was then shaken on an end–to–end shaker for 2 h and stood overnight. The excess HCl was then titrated against 1 M NaOH solution (standardized) under vigorous stirring using an autotitrator (TIM 865 Titration Manager, Radiometer Analytical).

Available P (2% formic acid extractable P) was measured according to the method proposed by Wang *et al*. (2012b, a), and available N (6 M HCl hydrolysable N) was measured following the protocol described in section 3.2.3, respectively. Available K, S and Mg were determined after filtering 1 M HCl extraction (following the method used for the liming equivalence determination) with Whatman No 42 filter paper. Total C, H, N and S contents were determined using a TruSpec CHNS analyser (LECO Corp. St. Joseph, MI). Total P was determined using a Technicon Auto-Analyser after Kjeldahl digestion (McKenzie and Wallace 1954). The ash content was determined by thermal analysis using a TG analyser (SDT Q600, TA Instruments, Melbourne, Australia).

6.2.3 Bioassay experiment setup

A root study container devised by Hedley et al. (1994) that further modified in Chapter 5 (Figure 5–1) by adding a thin layer of high P sorbing tephra layer below the

root exclusion mesh to provide a 'P–diffusion break'. Once P diffusion to roots was halted, P supply to plant roots from the soil in the lower compartment to which plant root cannot penetrate could only be mediated by fine hyphal growth. This allows to evaluate the contribution of AMF hyphae in P uptake by the host plant and distinguish from that originated from P diffusion and root P uptake and to study the influence of soil amendments intended to change P solubility (e.g. fertilizers, lime, biochar) on P transfer by AMF hyphae.

The root study containers were packed with soils and biochar mixture according to the experimental design: $\frac{LO}{LO}$, $\frac{LB}{LO}$, $\frac{HO}{LO}$, $\frac{HB}{LO}$, $\frac{LO}{HO}$, $\frac{LB}{HO}$, $\frac{LB}{HB}$ ($\frac{\text{upper compartment}}{\text{lower compartment}}$; L = LP soil, H = HP soil, B = with biochar and O = without biochar) (Figure 6–1). Biochar was added into the soils at an application rate of 4.5% (w/w, which was equivalent to a field deep–banded rate of 10 t ha^{-1}, assuming a fertilizer band of 25 cm within a row of 80 cm). Four replications for each treatment were established and pre–incubated at a soil volumetric water content of 70% of field water holding capacity for 2 wk (time 0).

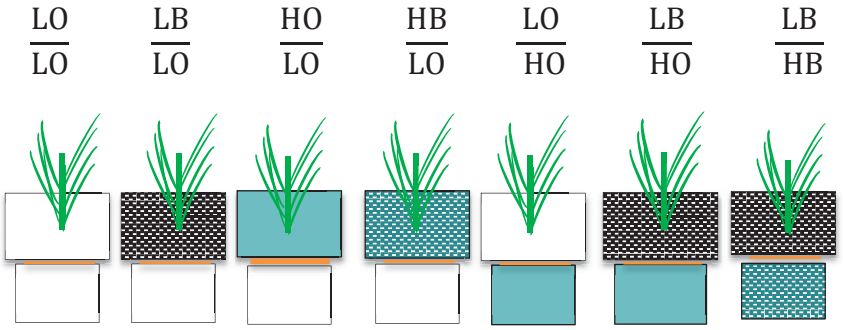

Figure 6–1 Experimental treatments design (LP soil, HP soil, LP soil with biochar, HP soil with biochar)

6.2.4 Plant growth and harvesting

Thirty seeds of *Lotus pedunculatus* cv barsille (inoculated with *Rhizobium*) were sown per root study container after 2 wk of pre–incubation. Since abundant indigenous AMF were identified (Figure 5–2 in Chapter 5), no external inoculum was introduced. Two wk after germination, the seedlings were thinned to five plants per pot. All pots were arranged in a completely–randomized design and kept in a glasshouse. Natural light was supplemented by four growth lights (F58W–GRO–LUX, 1500 mm*26 mm) to provide 16 h of light per day. An N– and P–free nutrient solution (Middleton and Toxopeus, 1973) was applied regularly to maintain plant growth. Visual inspection showed that *Rhizobium* nodules had developed adequately and maintained adequate N supply to plants. This ensured that P was the principal element limiting plant growth. Water content was maintained at 70% of field water holding capacity throughout the trial period by weighing the pots daily and adding water to reach the corresponding weight.

Plants were harvested on four occasions when the height of most plants reached 15 cm. For this, the aboveground biomass was cut down to 2–3 cm above the soil surface, then dried at 75°C to constant weight and weighed to determine the aboveground DM. Subsamples were ground using a ball mill and analysed for P concentration in shoots on a Technicon Auto–Analyser after Kjeldahl digestion (McKenzie and Wallace 1954).

After 32 wk, a final harvest was carried out and the root study containers were destructively separated. The *rhizosphere* soil (directly under the mesh) was sliced using a piston microtome starting at a 0.5 mm thickness to sample pure tephra from the 3 mm

tephra layer for AMF hyphae length measurement and P analysis to test the success of using tephra as a P diffusion barrier. Another set of six slices of the *hyphal zone* soil were taken each at 1 mm thickness. All slices were kept separately and stored in a chilled room (< 4^{o}C) for further analysis. The *root zone* soil was carefully removed from the upper compartment and sliced into eight wedges; four of those were randomly selected, then crushed and passed thought a 2–mm sieve. Big roots remaining in the sieves were separated and the soil was air–dried for further analysis.

6.2.5 Measurement of hyphal length

Hyphae present in the *hyphal zone* soil (a 1 mm thick soil right below the tephra) were extracted, stained and measured using a photomicrography - image processing using the ImageJ software (1.47 bundled with 64-bit Java, http://imagej.nih.gov/ij/) following the method described and tested by Shen *et al.* (2016).

6.2.6 Statistical analysis

Unless otherwise stated, results are expressed as means of four replicates with their standard errors. One–way ANOVA with a Tukey post–hoc test was used to evaluate statistical differences (P = 0.05) in plant dry matter (DM) and P uptake between treatments by SPSS software (IBM SPSS Statistics 20). Linear regression models were used to test for correlation among plant yield and soil pH responses.

6.3 Results

6.3.1 Biochar characteristics

The chemical characterization of the investigated biochars showed that, under the conditions studied, the types of feedstock had a greater effect on their properties than pyrolysis temperature (Table 6–2). The ash content of the willow woodchip–derived biochar (BW550) was more than six times as high as that of the two pine–derived biochars (> 10 vs < 2%). This, along with its composition, played an important role in several properties of biochar. The BW550 biochar had values of pH, EC and liming equivalence of 9.4, 1165 μS cm^{-1} and 18.2% $CaCO_3$–eq, respectively. The corresponding pH and EC values for the BP450 and BP550 biochars were < 9 and < 300 μS cm^{-1}, respectively, with no detectable $CaCO_3$–eq in either of them. Total P and available P in BW550 biochar was > 8 and > 17 times higher than the corresponding values in BP450 and BP550 biochar. The available K, Mg and S in BW550 biochar were > 3, > 8 and > 38 times higher than the corresponding values in the biochar derived from pine woodchips.

6.3.2 P status and biochar effects in the root zone

The inferior growth of plants in the LP soil compared with the HP soil (3.4 vs 9.5 g pot^{-1} of shoot DM, respectively, Figure 6–2A) along with correspondingly lower P uptake by plant shoots (2.0 vs 9.0 g pot^{-1}, respectively, Figure 6–2B) and lower P concentration in shoots (0.06% vs 0.1%, data not shown), confirmed the P limitation of

the LP soil and its poor ability to provide *root zone*–derived P. The addition of the BW550 biochar to the LP soil (treatment $\frac{\mathrm{LB}}{\mathrm{LO}}$) partly alleviated this deficiency with a significant ($P < 0.01$) increase of 2.0 g pot^{-1} (by 58%) in plant growth compared with the *root zone* of LP soil treatments without biochar amendments (Figure 6–2A), but plant growth could still be increased by a further 4.1 g pot^{-1} when the HP soil was present in the *root zone* ($\frac{\mathrm{HO}}{\mathrm{LO}}$).

The increment in DM yield of plants grown in the *root zone* of the LP soil amended with BW550 biochar ($\frac{\mathrm{LB}}{\mathrm{LO}}$) compared with its corresponding control amendment ($\frac{\mathrm{LO}}{\mathrm{LO}}$) resulted from a significant ($P < 0.05$) increase (72.6%) in P uptake (Figure 6–2B). The addition of the same biochar to the *root zone* of the HP soil ($\frac{\mathrm{HB}}{\mathrm{LO}}$) had no significant ($P > 0.05$) effect on either plant growth or P uptake (Figure 6–2). When pine–derived biochars (BP450 and BP550) were added to the *root zone* of either the LP soil or the HP soil, neither of them had a significant effect on either plant yield or P uptake (Figure 6–2).

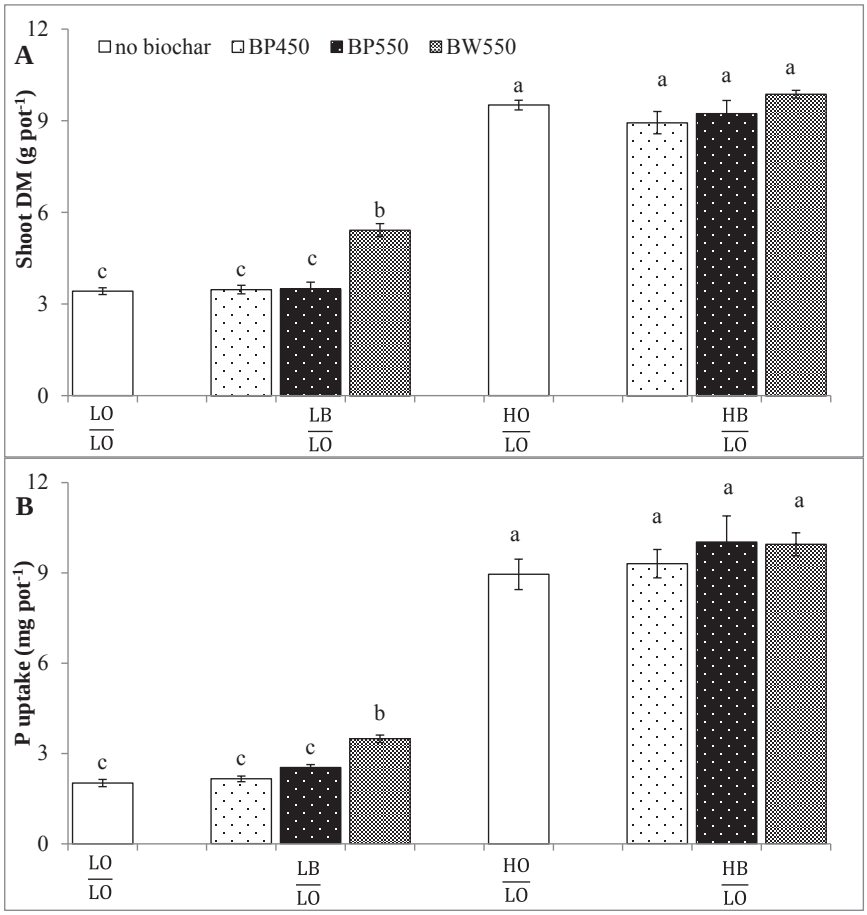

Figure 6–2 Effect of the P status in the root zone soil and biochar on plant growth (shoot DM) (A) and P uptake (B). The data present was the sum of four harvests. The error bars denote 1 SE. Different letters indicate significant differences ($P < 0.05$, $n = 4$) as determined by one–way ANOVA

6.3.3 P status and biochar effects in the hyphal zone

Phosphorus (total P and P fractionation) measurements in pure tephra slices showed that P could not have diffused from the HP soil in the *hyphal zone* to the *root zone* (see Chapter 5). Given that the root also cannot penetrate to the *hyphal zone* to take up P, P uptake by plant from the *hyphal zone* was only possible through direct uptake by

AMF hyphae. The growth analysis confirmed that plants grew significantly ($P < 0.05$) faster when their hyphae could access P from the HP soil in their *hyphal zone*. Plants P uptake was increased by 94% and resulted in a 56% increase in above–ground DM when plants were growing in the $\frac{\text{LO}}{\text{HO}}$ treatment compared with in the $\frac{\text{LO}}{\text{LO}}$ treatment (Figure 6–3).

The addition of biochar BW550 to the *root zone* of the $\frac{\text{LO}}{\text{HO}}$ combination (resulting in $\frac{\text{LB}}{\text{HO}}$ treatment) caused an increase in plant shoot DM, but this effect was not significant ($P > 0.05$) (Figure 6–3). When the biochar was also added to the *hyphal zone* soil (treatment $\frac{\text{LB}}{\text{HB}}$), the pots amended with BP450 had a significant ($P < 0.05$) increase in shoot DM yield and P uptake (by 40 and 76%, respectively) compared with the treatment with biochar only added to the *root zone* of LP soil (treatment $\frac{\text{LB}}{\text{HO}}$). Growth and P uptake was also increased in pots with the *hyphal zones* amended with other biochars, although effects were not significant ($P > 0.05$).

In general, P uptake by plants was more sensitive to the types and the placements (to either *root zone* or *hyphal zone* soil) of biochar than biomass growth. P uptake differed almost five–fold between plants grown with low–P and high–P soils in their *root zones*, whereas growth differed less than three–fold. P uptake and plant growth could be increased by about 50% when BW550 was added to the *root zone*, presumably as an alternative means of supplying the required P directly to roots. Alternatively, a similar enhancement of P uptake and growth was possible through hyphal P uptake when hyphae could grow in the *hyphal zone* of a high–P, and that benefit could be even further enhanced when biochar was added to high–P soils within the *hyphal zone*, with similar benefits for the three different biochar types. In contrast,

there was little effect when any of the biochars was added to high–P *root zones* (Figure 6–4)

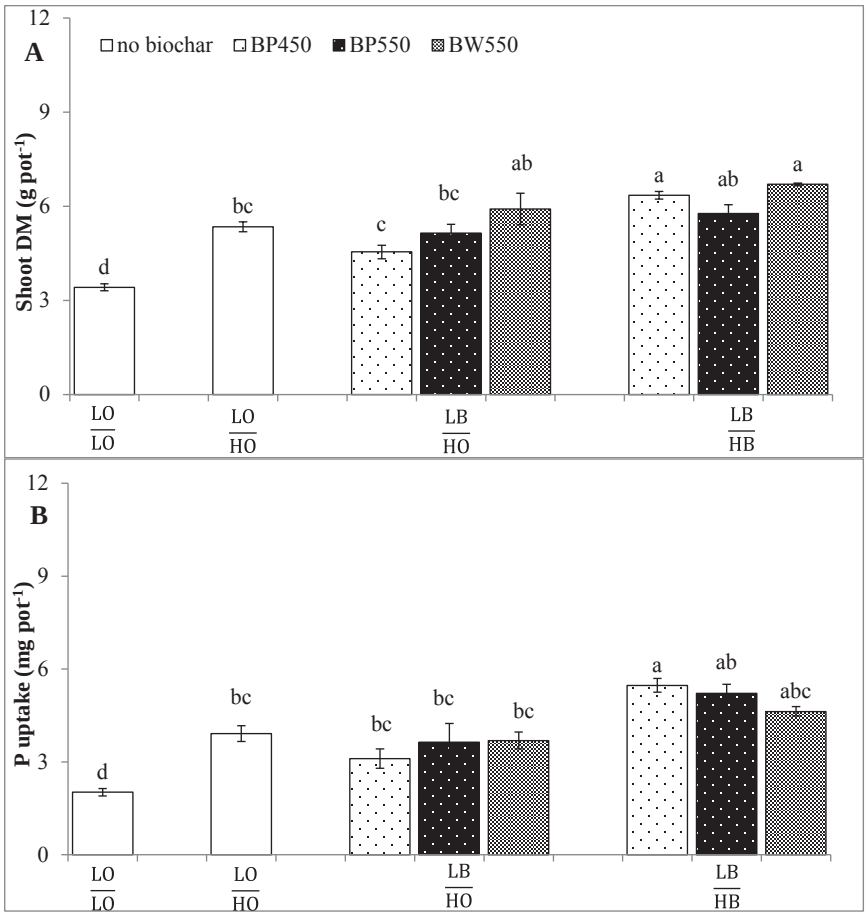

Figure 6–3 Effect of the presence of the HP soil (to which only hyphae had access) below the root zone of LP soil − with and without biochar − on plant growth (shoot DM) (A) and P uptake (B). The data present was the sum of four harvests. The error bars denote 1 SE. Different letters indicate significant differences ($P < 0.05$, n = 4) as determined by one–way ANOVA

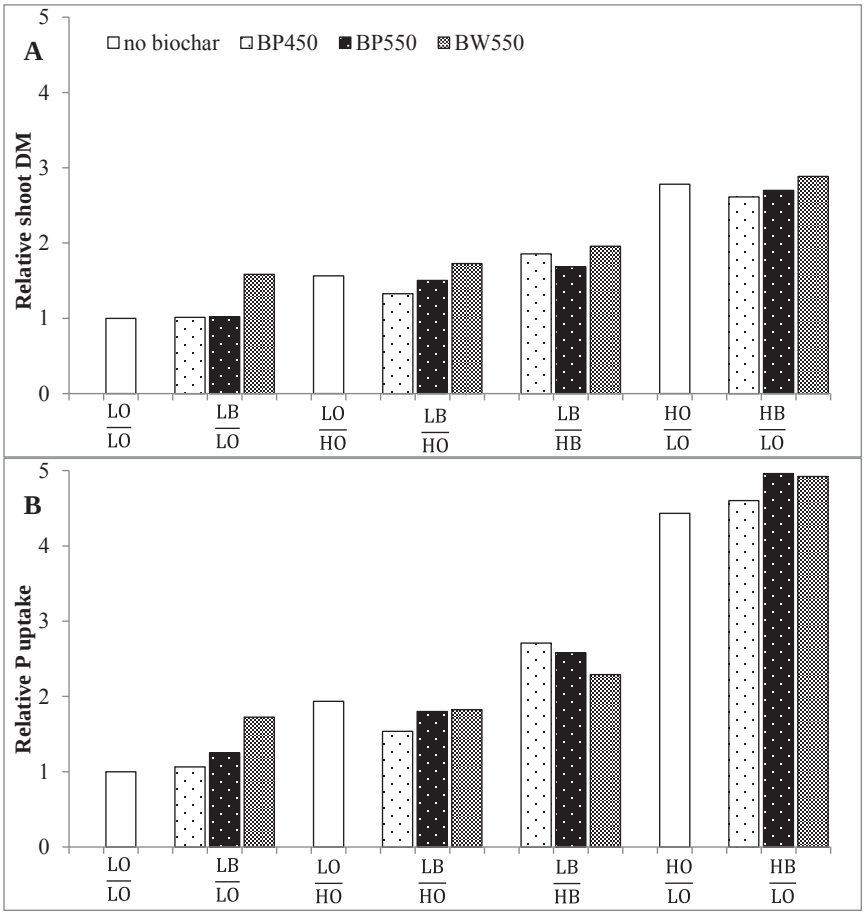

Figure 6–4 The relative plant shoot DM (A) and P uptake (B) were expressed relative to the shoot DM and P uptake of plants grown in the treatment $\frac{\text{LO}}{\text{LO}}$ without any amendments.

6.3.4 Effects of biochar on P bioavailability and pH of the root zone soil

The presence of BW550 biochar significantly ($P < 0.01$) increased the Resin–P in both the HP and the LP soils at time 0 (after 2 wk pre–incubation but before sowing) (Figure 6–5A). BW550 biochar had a higher available P than the BP450 and BP550

biochars (Table 6–2), and thus made a greater contribution to available P in both the HP and the LP soil (Figure 6–5A). Conversely, neither BP450 nor BP550 had discernible effects on plant available P fraction in the LP soil, as expected, but resulted in a significant ($P < 0.05$) reduction when applied to the HP soil. It is likely that this was simply due to the dilution of available phosphorus when pine biochars with very low P concentrations (59 and 69 vs 164 mg kg^{-1}).

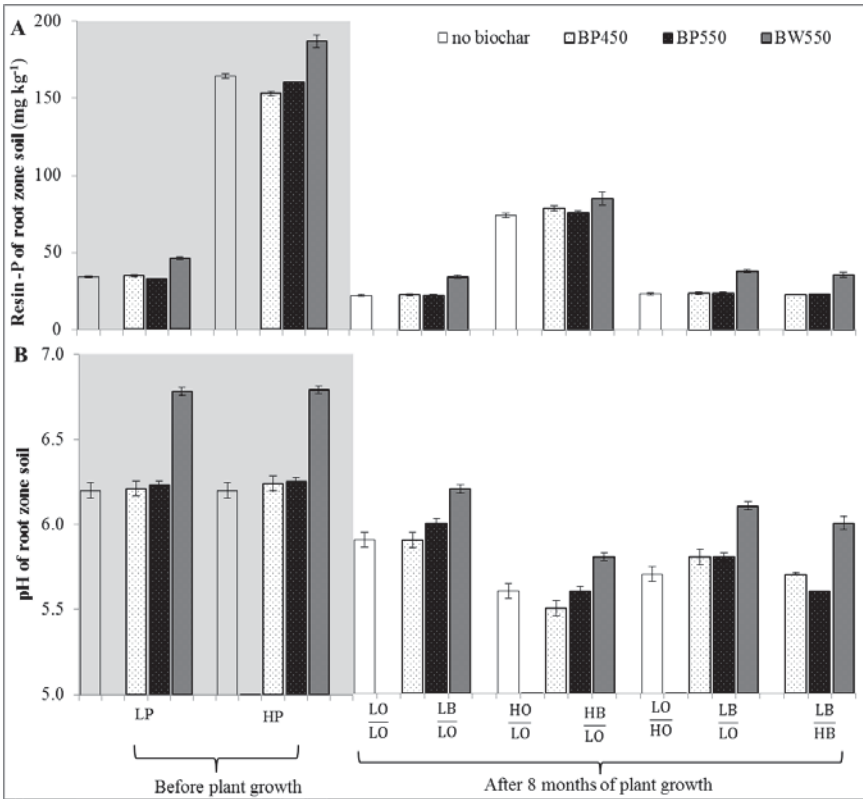

Figure 6–5 Effect of biochar on Resin – P (A) and pH (B) of root zone soil after plant growth

After 8 months of plant growth, the Resin–P in the *root zone* (Figure 6–5A) decreased significantly ($P < 0.05$) in all treatments over the period of plant growth, except for the LP soil amended with BW550. Generally, this decrease was greater in

the HP soil than in LP soil (> 80 vs > 10 mg kg^{-1}, respectively) due to greater plant P uptake in the former. However, the Resin–P in soils amended with BW550 biochar was still significantly ($P < 0.05$) higher (in general ca 10 mg kg^{-1}) than those of the non–amended and pine biochar–amended counterparts (Figure 6–5A).

Over the course of the experiment, soil pH in the *root zone* of non–amended pots also decreased by 0.3 – 0.5 units in the LP soil and 0.6 units in HP soil, respectively (Figure 6–5B). A same pH changed pattern was obtained when pine wood biochars were added to these soils, but the soil amended with BW550 biochar when compared with the soil without any amendments showed a less pH decrease. However, when compared with the soil amended with BW550 at time 0, the decrease pH was actually more pronounced (0.6 – 0.8). Overall, the decrease of soil pH in the *root zone* was correlated ($R^2 = 0.68$) with the above–ground biomass growth (Figure 6–6).

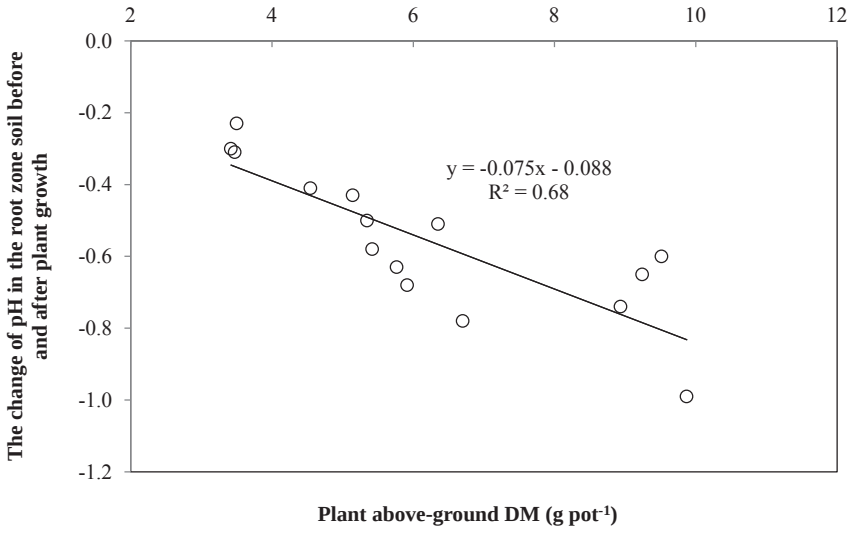

Figure 6–6 The correlation between the plant growth and the decrease of soil pH

6.3.5 Effects of soil type and biochar type on AMF abundance in the hyphal zone

In the non–biochar treatments, hyphal length in the *hyphal zone* significantly ($P < 0.05$) increased with decreasing available P in the soil and plant shoot DM, confirmed with the order that treatment $\frac{\text{LO}}{\text{LO}}$ (4.4 m g^{-1} soil g^{-1} DM) > treatment $\frac{\text{LO}}{\text{HO}}$ (1.9 m g^{-1} soil g^{-1} DM) > treatment $\frac{\text{HO}}{\text{LO}}$ (0.7 m g^{-1} soil g^{-1} DM) (Table 6–3). Compared with a hyphal length of 1.9 m g^{-1} soil g^{-1} DM in treatment $\frac{\text{LO}}{\text{HO}}$, the application of BP450 biochar significantly ($P < 0.05$) increased AMF hyphae length in the *hyphal zone* soil below the tephra with a hyphae length of > 2.6 m g^{-1} soil g^{-1} DM. The incorporation of BP550 biochar also increased hyphal length (2.3–2.4 m g^{-1} soil g^{-1} DM) but not significantly ($P > 0.05$). Conversely, a marginal decrease in hyphal length in the *hyphal zone* was detected when BW550 was added with respect to the non–amended counterpart (1.5–1.6 vs 1.9 m g^{-1} soil g^{-1} DM)

Table 6-3 AMF hyphal lengths in hyphal zone soil below the tephra layer (a 1 mm thick soil right below the tephra) in response to biochar addition (m hyphae g^{-1} soil g^{-1} DM)

LO / LO	HO / LO	LO / HO	LB / HO			LB / HB		
			BP450	BP550	BW550	BP450	BP550	BW550
4.4a	0.7d	1.9c	2.6b	2.3bc	1.5c	2.7b	2.4bc	1.6c

*Different letters within each row indicate significant differences ($P < 0.05$, n = 4) as determined by one–way ANOVA

6.4 Discussion

6.4.1 Biochar classification

According to the biochar classification system of Camps–Arbestain *et al*. (2015) the BP450, BP550 and BW550 biochars were classified as follows: (i) fertiliser values based on an 'average' corn grain crop with a yield of 13 t DM ha^{-1} y^{-1} (classes 0; 0; 3, K_{5t} S_{6t} Mg_{7t}, respectively), and (ii) liming equivalence value (classes 0; 0; 2, respectively). The results thus indicate BW550 biochar would provide an adequate supply of K, S and Mg to an 'average' corn crop at application rates of 5, 6 and 7 t ha^{-1}, respectively. The support of an 'average' lotus crop yield of 11.5 t DM ha^{-1} y^{-1} (Suckling, 1960) would require a biochar application of 7 t ha^{-1} to supply sufficient S and Mg and 20 t ha^{-1} to meet the requirements of P and K. Moreover, the relatively high liming equivalence of the BW550 biochar (18.2% $CaCO_3$–eq) means that this biochar would also reduce soil acidity and/or increase the acid buffering capacity of the amended soil.

6.4.2 P status of soil and biochar in the root zone affects plant growth and P uptake

The plants grown in the LP *root zone* soil (without biochar amendment) suffered from P deficiency as inferred from the inferior growth and lower P uptake by plant shoots compared with those grown in the HP *root zone* soil. Shoot P concentrations of

plants grown in the LP (0.06%) and HP soils (0.10%) were below those commonly reported for lotus (0.15 - 0.25%) (Trolove *et al.* 1996). However, this comparison is misled by the fact that plant growth under glasshouse conditions (9.5 g pot^{-1} in a growth period of 8 months would be equivalent to 27 t DM ha^{-1} y^{-1}) was more than 2.5-fold that under field conditions (11.5 t DM ha^{-1} y^{-1}; Suckling 1960), which caused a dilution effect in shoot P concentration.

The incorporation of BW550 biochar into the LP *root zone* soil caused a considerable increase in P uptake and a concomitant increase in plant yield compared with the non–amended soil. A similar growth enhancement was not observed in the corresponding treatments amended with the pine–based biochars. This difference in response to biochar types was attributed to the additional nutrients provided by the BW550 that riched in ash and, particularly, its input of available P to this P–deficient soil. The addition of BW550 biochar to the LP soil increase resin–P by 12 mg kg^{-1} (Figure 6–5A). Assuming that the difference in P taken up by plants with and without BW550 biochar came from the P in biochar, we estimated that ca 20% of the additional available P introduced by BW550 biochar was taken up by plants. Resin–P has been considered as a good measure of the readily–available P for plant uptake (Hedley et al. 1994) and proposed as a potentially useful test for characterizing P bioavailability in soils amended with P–rich biochars (Wang et al., 2013b).

BW550 biochar also increased the pH–buffering capacity of these soils and helped mitigate the decrease in pH experienced over time which may have also favoured P uptake. The decrease in pH was always greater in the HP soil than in the LP soil, and this could be attributed to their greater root growth and DM accumulation, although there may have also been differences in soil pH–buffering capacities between

the two soils. Plant–P availability is affected by several pH–dependent reactions such as P speciation, precipitation–dissolution and adsorption–desorption, with a pH increase in the acid range generally favouring P mobilization. In addition, the increase in soil pH could also stimulate the mineralisation of organic P (Haynes 1982).

In contrast, biochar addition (regardless of the type used) to the *root zone* of HP soils did not enhance either plant yield or P uptake, and this was attributed to the adequate P supply for plant growth of this soil, as indicated by an Olsen P value of 33.3 mg kg^{-1} and a relatively high yield (27 t DM ha^{-1} yr^{-1}). Usually, an Olsen P value > 32 mg kg^{-1} for a soil with high P retention is considered adequate for most pasture swards to growth (Cornforth, 1998). Other studies have also shown that applying biochar to either a soil with a high P status or along with P fertilizer had no additive or synergistic agronomic effects (Solaiman et al., 2010b; Biederman and Harpole, 2013).

6.4.3 P status and biochar in the hyphal zone affects plant growth and P uptake

The proliferation of AMF hyphae is particularly vital for plant P acquisition as phosphate ions have low mobility in the soil and are often poorly accessible to plant roots (Smith and Read, 2010). The external mycelium is the active part of AMF where nutrients are captured, transported and delivered to the host plant roots (Neumann and George, 2010). The manifested P deficiency in lotus growing in the LP root zone soil ($\frac{\text{LO}}{\text{LO}}$ treatment) was, to a limited extent, mitigated when AMF hyphae had access to HP soil ($\frac{\text{LO}}{\text{HO}}$ treatment), as shown by 56% and 94% increases in plant yield and P uptake,

respectively. Despite these benefits of hyphal P uptake, it could not raise plant growth to the levels possible when plant roots were grown directly in HP soils (cf. $\frac{\mathrm{HO}}{\mathrm{LO}}$ $vs.$ $\frac{\mathrm{LO}}{\mathrm{HO}}$ treatments), which is in agreement with previous studies (Hedley et al., 2005).

There was no effect when biochar (regardless of type) was added to the *root zone* of LP soils that had HP soils in their *hyphal zone* ($\frac{\mathrm{LB}}{\mathrm{HO}}$) compared with the untreated pots ($\frac{\mathrm{LO}}{\mathrm{HO}}$). Conversely, biochar added to the *hyphal zone* HP soil ($\frac{\mathrm{LB}}{\mathrm{HB}}$) did enhance P bioavailability and plant growth compared with the corresponding treatment ($\frac{\mathrm{LB}}{\mathrm{HO}}$). Particular, there was a profounded increase when BP450 biochar was used. Considering the absence of nutrients (such as P) and the lack of liming capability of this biochar, along with the inability of (i) roots to take up P from the HP soil (as a mesh impeded their penetration) and (ii) P to diffuse across the tephra layer (both of which were accomplished in the root study container) (see Chapter 5), this positive response could only be attributed to the stimulation of hyphal development by BP450 biochar in the *hyphal zone* of the HP soil. This was supported by the considerable increase in the length of the AM fungal mycelium of the BP450 treated HP soil in the *hyphal zone* ($\frac{\mathrm{LB}}{\mathrm{HB}}$) when compared with the non–amended treatment ($\frac{\mathrm{LO}}{\mathrm{HO}}$) and only the LP *root zone* soil amended with the BP450 (treatment$\frac{\mathrm{LB}}{\mathrm{HO}}$).

6.5 Conclusion

Plant growth in our experiment was primarily determined by P bioavailability in the soil of the *root zone*. When insufficient P was available for direct root uptake, this could be partly compensated through hyphal P uptake from the *hyphal zone* if that contained high P, but plant growth could not reach the levels possible when there was direct root P uptake.

Amongst the tested biochars, biochar produced from willow woodchips achieved the best results in terms of plant growth and P uptake in a P deficient soil. This was attributed to its high liming equivalence and provision of additional P which made it a useful soil amendment in Andosols with low P fertility by improving P bioavailability and thus plant productivity. Biochars derived from pine woodchips conferred no advantages through nutrient addition but stimulated AMF abundance and hyphal function and thereby increased P accessibility and uptake from high–P soils rendering an enhanced plant growth. We concluded that biochar addition had little effect when plants were growing in a soil with sufficient P supply, but biochar derived from pine woodchips facilitated mycorrhizal P uptake when plants were dependent on mycorrhizae to meet their P requirements.

6.6 Acknowledgements

The authors acknowledge financial support for Qinhua Shen from the New Zealand Biochar Research Centre. The authors are also deeply grateful to Dr James

Hanly for providing the tephra and for help with the OVERSEER® nutrient budget analysis and Dr C Matthew for personal communication on *Lotus* yield and nutrient managements. We are also grateful for the technical support from Mr Ian Furkert, Mr Bob Toes, and Ms Glenys Wallace, and would like to thank Drs Tao Wang and Roberto Calvelo Pereira for inspiring discussions of the experimental results.

Chapter 7

CAN BIOCHAR AMELIORATE ALUMINUM PHYTOTOXICITY?

The biochar made from willow wood chips at temperature 550 °C has been characterized with a level 2 of liming equivalence value (18.2 % $CaCO_3$–eq) and been proved to be able to facilitate Andosols to counterpart the acidification resulting from legume biomass accumulation in Chapter 6. This chapter is to further compare the effectiveness of using this biochar to increase soil pH and ameliorate Al toxicity in two acidic soils of distinct pH buffering capacity and compared with that of the other biochar (e.g., BP550) and the chemical liming agent (e.g., $Ca(OH)_2$ and NaOH).

A paper from this study will be submitted for publication: **Qinhua Shen**, Marta Camps–Arbestain, Mike J. Hedley, Miko U.F. Kirschbaum, Peter Bishop. Can Biochar Ameliorate Aluminium Phytotoxicity? (2015). Geoderma (*To be submitted*)

Abstract

Aims To investigate the mechanisms involved in the amelioration of acid soils by application of biochars of contrasting liming potential.

Methods The amelioration of acid soils with biochars made from either pine or willow woodchips pyrolysed at 550°C (referred to as BP550 and BW550, respectively) was compared with that of NaOH and $Ca(OH)_2$. The responses of alfalfa (*Medicago sativa* L.) to these ameliorants were examined using a seedling radicle elongation bioassay.

Results The amount of BP550 needed to achieve a targeted pH value (5.4, 5.6, 5.8 and 6.4) was 2.5– to 4.8–fold that of BW550. For a given pH, the decrease in soil exchangeable aluminium (Al) resulting from the amendments followed the order: BW550 > $Ca(OH)_2$ ~ BP550 > NaOH. The addition of $Ca(OH)_2$ and BW550 caused a decrease in both inorganic monomeric Al (mainly in AlF^{2+} and Al^{3+}) and colloidal Al, and an increase in aqueous Ca^{2+} compared with the control soil; whereas the addition of NaOH and BP550 caused an increase in Na^{+} and aqueous colloidal Al, and a decrease in soluble Ca^{2+}. The addition of BW550 (at application rates < 9.1 %) and $Ca(OH)_2$ stimulated alfalfa seedling growth, whereas addition of BP550 (at application rates > 2.4 %) and NaOH caused inhibition.

Conclusions BW550 effectively alleviated Al phytotoxicity in acid soils through the reduction of monomeric Al (e.g., AlF^{2+} and Al^{3+}) and the addition of Ca^{2+}, although detrimental effects were detected at very high application rates (i.e. > 5 %; which would correspond to ~ 50 t ha^{-1}); and (ii) the deleterious effect of BP550 regardless of

application rates was ascribed to an unbalanced cation ratio (e.g., caused by an excess of Na) and the associated solubilisation of polymeric Al organic compounds.

Key words

Acidic soil, Al toxicity, Biochar, Liming effect, pH–buffering capacity, Radicle elongation bioassay

7.1 Introduction

Acid soils cover ca 30 % of the total ice–free land area and ca 50 % of the potential arable land of the world (Kochian et al., 2004). In general, these soils are common in well–drained areas where precipitation exceeds evapotranspiration (Uchida and Hue, 2000). Soil acidity can also be caused by soil management activities, mostly through the increase of N and S (sulphur) cycling rates in farming systems (Bolan and Hedley 2003). Rates of acidification vary from 0.7 kmol H^+ ha^{-1} $year^{-1}$ in pristine systems to 40 kmol H^+ ha^{-1} $year^{-1}$ in agricultural systems receiving high rates of ammonium–N fertilizers (Sumner and Noble, 2003). Managing acid soils is challenging given that several plant growth–limiting factors (e.g., Al toxicity and Ca deficiency) act simultaneously (Adams and Hathcock, 1984).

Inorganic liming materials [e.g., $Ca(OH)_2$ and $CaCO_3$] are generally used to alleviate soil acidity and Al toxicity (Pavan et al., 1982; Haynes, 1984; Carvalho and van Raij, 1997; Fageria and Baligar, 2008). For instance, a regular lime application of 1.5 t ha^{-1} $year^{-1}$ is recommended to be added to most manage acid soils in New Zealand

(Cregan et al., 1989). Organic residues (e.g., cattle manure) have also been proposed as alternative liming agents (Haynes and Naidu, 1998; Whalen et al., 2000; Haynes and Mokolobate, 2001; Mokolobate and Haynes, 2002; Naramabuye and Haynes, 2006; Xu et al., 2006), although their net alkalinity should be verified prior to its use, as specific amendments (e.g., anaerobic sewage sludge) may be a net source of acidity due to the subsequent nitrification (Egiarte et al., 2005). Carbonization of organic materials, however, may avoid this problem as during this process (i) there is a preferential removal of acidity (especially when carbonized at temperature > 400°C), which leads to the formation of an alkaline–enriched material (Novak et al., 2009; Gaskin et al., 2010; Domene et al., 2015), and (ii) most of the N becomes incorporated into recalcitrant heterocyclic structures (Novak et al., 2009; Wang et al., 2012a). As for other liming agents, particle size of the amendment and soil properties will also determine the magnitude of the amelioration effect of biochar on the acid soil (Anderson et al., 2011; Yuan et al., 2011a; Yuan et al., 2011b; Yuan and Xu, 2011; Xu et al., 2012).

Alkaline compounds [e.g., CaO, Na_2O, $CaCO_3$, Na_2CO_3 or $CaMg(CO_3)_2$] in biochar (Vassilev et al., 2013a; Wang et al., 2014) may dissolve over time and cause a raise in soil pH that may prompt the hydrolysation and polymerization of Al − with the subsequent formation of less toxic species [e.g., $Al(OH)^{2+}$ and $Al(OH)_4^-$] (Zhao et al., 2009) −, and subsequent precipitation of Al hydroxides (Qian and Chen, 2013; Qian et al., 2013). Furthermore, adsorption of Al species with hydroxyl and carboxyl functional groups at the surface of biochar (Qian and Chen, 2013; Masud et al., 2014) could also contribute to the alleviation of Al toxicity. Besides, any changes in the concentration of certain ions, chelating agents, and/or ionic strength will influence Al toxicity on plants (Perrott et al., 1976; Hue et al., 1986; Ma et al., 2001; Yamada and Takahashi, 2010).

Some base divalent cations (Ca^{2+}, to a lesser extent Mg^{2+}) reduce Al toxicity via improving Ca status of plant roots and blocking Al uptake by roots (Alva et al., 1986; Rengel, 1992; Brady et al., 1993; Silva et al., 2001; Hossain et al., 2014). Excessive Na^{+} may cause cation imbalances and lead to plant toxicity, as well as a weakening soil structure (Bernstein, 1975; Luan et al., 2009; Domene et al., 2015).

In this study the liming potential of woody biochars with contrasting alkalinity and nutrient content, as well as their effects on Al toxicity in acid soils were investigated and compared with those of NaOH and $Ca(OH)_2$. Special attention was paid to changes happening in soil solution ionic composition (especially cations, Al fractionation and speciation), soil pH and exchangeable Al. Moreover, the germination and radicle elongation of alfalfa (*Medicago sativa* L.) grown in soils to which these amendments were added were considered.

7.2 Materials and Methods

7.2.1 Soils

Two soils with contrasting pH–buffering capacities were used: (1) Hautere Silty Clay Loam [Typic Acid Brown Soils (New Zealand Soil Classification; Hewitt and Dymond, 2013); Haplic Cambisol (IUSS Working Group, 2006)] and (2) Ramiha Silt Loam [Acidic Allophanic Brown Soil (New Zealand Soil Classification; Hewitt and Dymond 2013); Andic Umbrisol (IUSS Working Group, 2006)]. They were collected

from Otaki (40°48'36.26"S, 175°9'28.24"E) and Turitea (40°24'7.68"S, 175°42'48.08"E), New Zealand, respectively.

Soil $pH_{1:2.5}$ was determined using a glass electrode in a 1: 2.5 soil: deionized water suspension (w/v). Soil CEC was determined using 1 M ammonium acetate (pH = 7) (Rayment and Lyons, 2011). Phosphorous retention capacity was measured by shaking 5 g of air–dried soil with 25 mL of 1000 mg L^{-1} P solution with respect of KH_2PO_4 for 16 h (Saunders, 1965). The P in the solutions after centrifugation (13700 *rcf.*) and filtration (through Whatman No. 42) were then determined according to the vanadomolybdate (yellow) method (Kitson and Mellon, 1944). Aluminium, Fe and Si in short–range order materials were extracted using acid ammonium oxalate (pH = 3) (Al_{ox}, Fe_{ox} and Si_{ox}); Al and Fe in organic complexes were extracted using sodium pyrophosphate (Al_{py} and Fe_{py}), although this extractant may also solubilize small amounts of inorganic amorphous Al; exchangeable Al was extracted using 1 M KCl solution (Al_{ex}) (García–Rodeja et al., 2004; García–Rodeja et al., 2007). The concentrations of Al, Fe and Si in the extractions were then determined by Atomic Absorption Spectroscopy (AAS, GBC 904 Avanta Ver 1.33, Australia).

The soil alkaline–pH buffering capacity (shortened as alkaline–pH–BC) was measured following the methods described by Hartikainen (1992). For this, titration curves were established by adding a series incremental amount (0.00, 0.01, 0.02, 0.04, 0.08 and 0.16 mmol) of OH^{-1} to a 1:5 soil: deionized water suspensions (w/v) in triplicates. Ionic strength was adjusted to 0.006 M using $CaCl_2$. The suspensions were shaken for 24 h, equilibrated for the following 6 d at 25°C, re–shaken for 2 min on the 7^{th} day and pH subsequently measured. The soil alkaline–pH–BC was calculated from

the slope of the linear portion of the acid–base titration curve (OH^{-1} added vs pH) (Aitken and Moody, 1994).

7.2.2 Biochars

Two types of feedstock were used for biochar production: (a) chipped pine (*Pinus radiata* D. Don) branches and (b) chipped weeping willow (*Salix matsudana* L.) branches. Both of which were pyrolysed at 550°C in a 27–L gas–fired rotating drum kiln with an average heating rate of 10°C min^{-1}. The resultant solid pyrolytic products were referred to as BP550 and BW550, respectively. Biochars were ground to pass through a 2–mm sieve prior to mixing with soil for the radicle elongation trial. Subsamples were further ground to a particle size < 0.3 mm using a ring mill for characterization.

The pH and EC were measured following a modification of the method of Rajkovich et al. (2012) in a suspension of biochar in deionized water (ratio of 1:20; w/w) (IBI 2012). Calcium carbonate equivalence (liming equivalence, % $CaCO_3$–eq) was determined according to IBI standards modified from the method proposed by Rayment and Lyons (1992). For this, 0.5 g of biochar to which 10 mL 1 M HCl solution were added and stood for overnight involving shaking for 2 h, and then the excess HCl was titrated against standardized 1 M NaOH solution under vigorous stirring using an auto titrator (TIM 865 Titration Manager, Radiometer Analytical). In addition, carbonate–C was determined using a titrimetric method (Wang et al., 2014). The acid-pH-buffering capacity (shortened as acid–pH–BC) of the biochars was determined following the

above-described method for measuring alkaline pH-buffering capacity of the soils, but instead of OH^{-1}, H^{+} was added.

Total C and N contents were determined using a TruSpec CHNS analyser (LECO Corp. St. Joseph, MI). The ash contents were determined by thermal analysis using a TG analyser (SDT Q600, TA Instruments, Melbourne, Australia). Total P was determined using a Technicon Auto–Analyser after Kjeldahl digestion (McKenzie and Wallace 1954). Available P (2% formic acid extractable P) was measured according to the method of Wang *et al*. (2012b), available N (6 M HCl hydrolysable N) was measured following the protocol described in Chapter 3 section 3.2.3, respectively. Total Ca, Mg and K were determined using Atomic Absorption Spectroscopy (AAS, GBC 904 Avanta Ver 1.33, Australia) after digestion following modified dry ashing (Enders and Lehmann 2012).

7.2.3 The use of soil amendments to reach specific pH values

Subsamples of the Hautere and Ramiha soils were separately amended with BW550 biochar, BP550 biochar, NaOH, and $Ca(OH)_2$ at different application rates to obtain a series of desired pH values (5.4, 5.6, 5.8 and 6.4). The amount added to achieve a specific pH value was estimated based on the alkaline–pH–BC of the soils and the acid–pH–BC of biochar using the equation [7–1] (Kissel et al., 2012) where ΔpH is the change of pH that results from either the addition or removal of H^{+} (ΔH^{+}, mmol H^{+} kg^{-1}). Additional information is provided in the supplementary information.

$$\Delta pH = \frac{\Delta H^{+}}{pH-BC} \qquad [7–1]$$

The soils were then thoroughly mixed with the amendments at specific application rates in triplicates and wetted with deionized water to 70 % of field capacity. All treatments were incubated in a chamber at 20 ^{o}C for 10 d. Thereafter, the pH was measured and adjusted where needed. Subsamples of the soil mixtures were taken for measuring exchangeable Al and exchangeable acidity following the method described above.

7.2.4 Germination and radicle elongation bioassay

A radicle elongation bioassay technique (Sheppard and Floate, 1984) was modified (Figure 7–1) to assess the responses of alfalfa (*Medicago sativa* L.) to the Hautere and Ramiha soils in the presence or absence of BW550 biochar, BP550 biochar, NaOH and $Ca(OH)_2$. Once the targeted soil pH was achieved, the soil mixtures were packed into Petri dishes (D = 89 mm) to their corresponding soil bulk densities and then wetted with deionized water to 70 % of field capacity, and covered with Whatman No. 42 filter papers. Twenty alfalfa seeds were placed at the surface of the filter paper. All Petri dishes were covered with lids, and placed overnight upside–down so that the seeds became completely immersed with soil solution, facing them up thereafter in an incubator at 20 ^{o}C for 4 d. The number of protrusions inferring germination was recorded every 8 h and the radicle length was measured using a ruler on the 4th day. For each treatment, the relative root length (RRL) was expressed relative to the longest radicle grown in the $Ca(OH)_2$ amended soil at pH 5.8 and used to assess the responses of alfalfa to the amendments.

A 10-days incubation to adjust pH to 5.4, 5.6, 5.8 and 6.4

Amended soils were packed into Patri dishes and covered with Whatman No. 40 filter paper (Water potential = -0.01 bar)

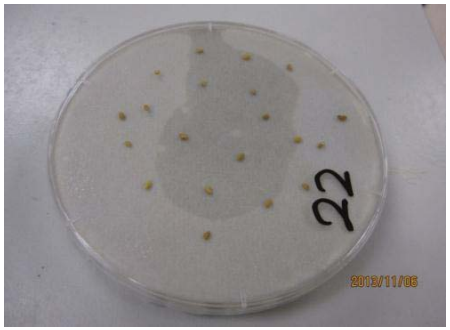

20 *alfalfa* seeds were sown on the surface of the filter paper

Patri dishes sets sat on the bench in an incubator of 20 oC for 4 days

The protrusions and radicle length was recorded.

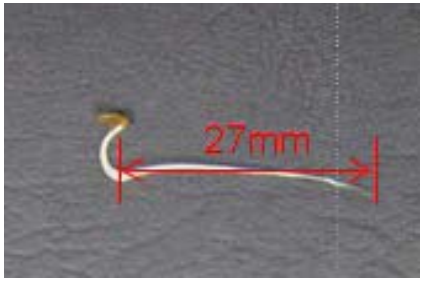

The radicle length was measured.

Figure 7–1 Illustration of a short term incubation for increase acidic soils pH to various desired levels and a germination and radicle elongation bioassay to test the response of *Alfalfa* (*Medicago sativa* L.) to acidic soil amended with various ameliorants [BP55, BW550, NaOH and $Ca(OH)_2$].)

7.2.5 Post-harvest soil solution analysis

Once the radicle elongation test was finalized, the ionic composition of 1:10 soil: deionized water extracts (w/v) was determined (Hartikainen, 1992). Briefly, 15 g of soil mixture was agitated with 150 mL of deionized water for 30 min and equilibrated at 24 ^{o}C for 3 d (agitated for 5 min once a day). Thereafter, the suspensions were filtered through a 0.45–µm filter paper after centrifugation (13700 *rcf.*) for further analysis. The HCO_3^- was measured by titrating 10 mL subsample of supernatant against a standardized 0.01 M H_2SO_4 to pH 4.5 under vigorous stirring using an auto–titrator (TIM 865 Titration Manager, Radiometer Analytical); the pH of the solution prior to titration was also recorded. Dissolved organic carbon (DOC) was determined following method of Walkley (1947); the concentration of Na^+, K^+, Ca^{2+} and Mg^{2+} were measured by Flame Atomic Absorption Spectrometer (AAS, GBC 904AA, Australia); and the concentration of Cl^-, F^-, Br^-, PO_4^{3-} and SO_4^{2-} by ion chromatography (IC5000, LACHAT, USA).

The steps followed to conduct aqueous reactive Al fractionation and monomeric Al speciation are summarized in Figure 7–2. Briefly, aqueous Al fractionation was carried out following the procedure proposed by Driscoll (Driscoll, 1984), which separates Al into 5 pools: total reactive Al (Al_r), acid soluble Al (Al_{as}), total monomeric Al (Al_{Tm}), labile monomeric Al (Al_{Lm}) and non–labile monomeric Al (Al_{NLm}). The speciation of monomeric inorganic Al (Al_{Lm}) – e.g., Al^{3+}, Al–OH and Al–F complexes − were estimated by inputting values of pH and concentrations of Al_{Lm}, basic cations (K^+, Ca^{2+}, Na^+, and Mg^{2+}), and inorganic anions (Cl^-, F^-, Br^-, PO_4^{3-} and SO_4^{2-}) into a chemical equilibrium model (Visual MINTEQ ver. 3.1).

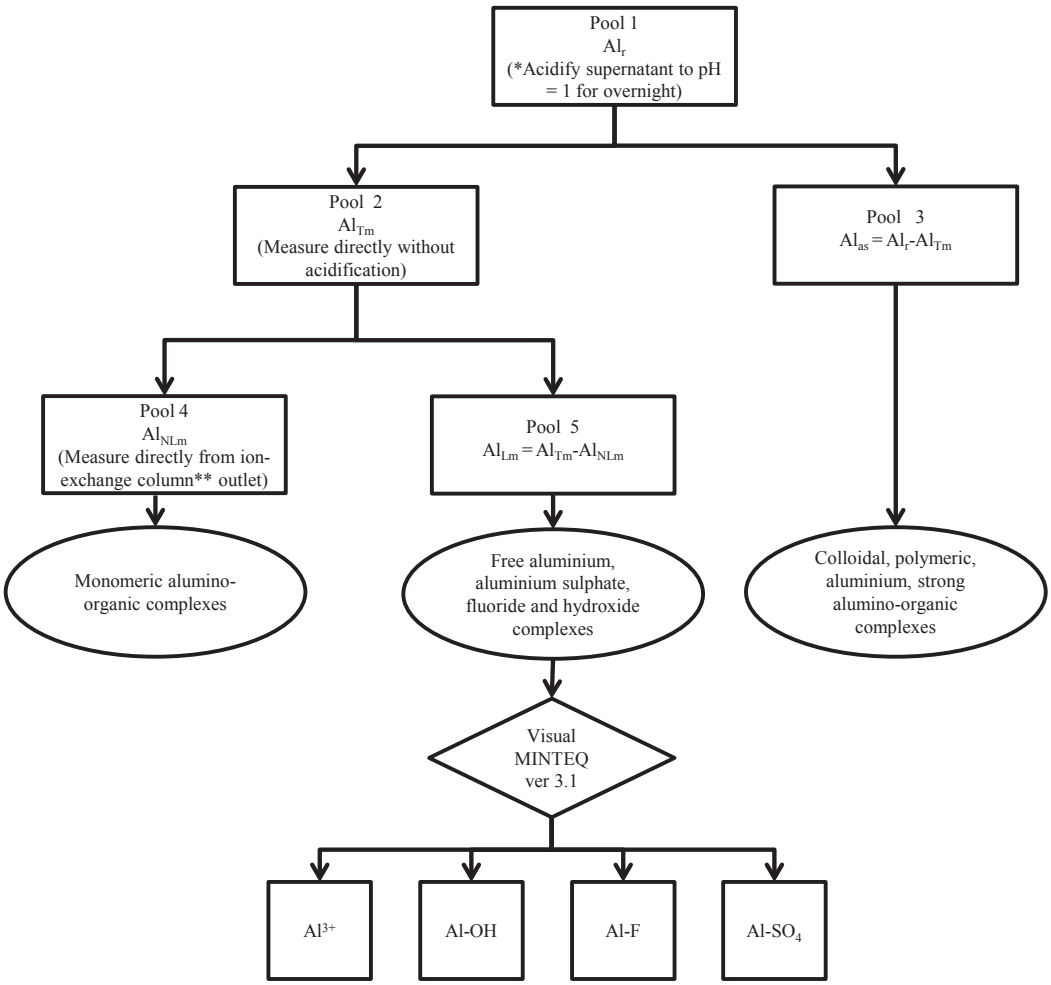

Figure 7–2 A diagram representation of aqueous reactive Al fractionation and monomeric Al speciation procedure and composition

* The Al concentration in each step was measured using the pyrocatecol violet (PCV) method (Dougan and Wilson 1974) after adjusting solution pH to ca 6.0 with 0.1 N HCl. All determinations were carried out in triplicates.

** Ion–exchange column containing both H^+ and Na^+ resin (Amberlite 120)

7.2.6 Statistical analysis

Unless otherwise stated, results were expressed as the mean of three replicates with its standard deviation. One–way ANOVA with a Tukey post–hoc test was used to evaluate statistical differences ($p < 0.05$) in soil Al indices and activities between different treatments using SPSS software (IBM SPSS Statistics 20). A correlation matrix analysis was performed among the RRL and soil solution composition (including Al_{Lm} species).

7.3 Results

7.3.1 Selected properties of soils and biochars

Although both soils had similar initial pH values (5.2 – 5.3) (Table 7–1), the Ramiha soil was characterized by having a higher pH–BC [50.8 vs 28.1 mmol H^+ kg^{-1} $(pH\ unit)^{-1}$] and Al_{ox} and Al_{py} content (2.43 vs 0.56 % and 1.36 vs 0.35 %, respectively) than the Hautere soil. In both soils the reactive Al pools were likely to be associated with organo–Al complexes ($Al_{py}/Al_{ox} > 0.5$). Exchangeable acidity was greater in the Hautere soil than in the Ramiha (3.4 vs 2.7 cmol kg^{-1}), but differences in exchangeable Al were smaller (2.3 vs 2.6 cmol kg^{-1}) − these values being above the threshold (2 cmol kg^{-1}) over which Al toxicity to sensitive plant roots tends to occur (Saigusa et al., 1980). The CEC of the Ramiha soil was 13.8 cmol (+) kg^{-1} and that of the Hautere soil 8.8 cmol (+) kg^{-1}.

Table 7-1 Selected properties of the studied acidic soils [a]

Properties	Units	Hautere soil	Ramiha soil
$pH_{1:2.5}$		5.2	5.3
CEC[b]	cmol(+) kg^{-1}	8.8	13.8
P retention capacity	%	41	88
Alkaline–pH–BC [c]	mmol H^+ kg^{-1} $(pH\ unit)^{-1}$	28.1	50.8
Total C	g kg^{-1}	34	73
Al_{py} [d]	%	0.35	1.36
Al_{ox} [e]	%	0.56	2.43
$Al_{ox}+1/2Fe_{ox}$ [f]	%	1.09	3.14
Al_{py}/Al_{ox}		0.62	0.56
Exchangeable acidity	cmol kg^{-1}	3.4	2.7
Exchangeable Al	cmol kg^{-1}	2.6	2.3

[a] All concentrations are expressed on an oven dry weight basis

[b] Cation exchangeable capacity

[c] Alkaline pH buffering capacity

[d] Sodium pyrophosphate extractable Al

[e] Ammonium oxalate extractable Al

[f] Ammonium oxalate extractable Fe

The two biochars had contrasting properties (Table 7–2). The ash content of the BW550 biochar was more than 6–fold that of the BP550 biochar (10.8 vs 1.6 %). BW550 biochar had a pH, EC, carbonate–C and liming equivalence ($CaCO_3$–eq) of 9.4, 1165 μ*S* cm^{-1}, 8.83 g kg^{-1} and 18.2 % $CaCO_3$–eq, respectively; whereas the pH and EC of BP550 biochars was 8.9 and 283 μ*S* cm^{-1}, with negligible carbonate–C content (0.07 g kg^{-1}) and no detectable $CaCO_3$–eq. According to the biochar classification system proposed by Camps–Arbestain et al (2015), the BP550 and BW550 biochars were classified as having liming classes 0 and 2, respectively. The pH–BC of BW550 biochar was 3–fold that of BP550 biochar [170.5 vs 54.7 mmol H^+ kg^{-1} (pH unit)$^{-1}$]. The higher liming value of BW550 biochar was associated with a higher content of alkaline earth metallic elements (Ca^{2+}, Mg^{2+}, and K^+) than the BP550 (42.9 vs 6.0 g kg^{-1}, 4.4 vs 1.1 g kg^{-1}, and 10.7 vs 2.9 g kg^{-1}, respectively), while Na^+ shown opposite trend with 0.8 vs 1.1 g kg^{-1}.

Table 7-2 Selected properties of the studied biochars [a]

Biochar	Units	BP550	BW550
pH $_{1:20}$		8.9	9.4
EC [b]	μS cm^{-1}	283	1165
Ash	%	1.6	10.8
Liming equivalence	% $CaCO_3$–eq	–	18.2
Carbonate–C	g kg^{-1}	0.07	8.83
Acid–pH–BC [c]	mmol H^+ kg $^{-1}$ (pH unit)$^{-1}$	54.7	170.5
Total C	g kg^{-1}	872	738
Total N	g kg^{-1}	4.8	17.8
Available N	mg kg^{-1}	41.3	383.5
Total P	mg kg^{-1}	490	4234
Available P	mg kg^{-1}	97	1588
Total K	g kg^{-1}	2.9	10.7
Total Mg	g kg^{-1}	1.1	4.4
Total Na	g kg^{-1}	1.1	0.8
Total Ca	g kg^{-1}	6.0	42.9

[a] All concentrations are expressed on an oven dry weight basis

[b] Electrical conductivity

[c] Acid–pH buffering capacity

7.3.2 Contrasting liming effects of BW550 and BP550 biochars on acid soils

For a specific pH value to be obtained, the amount of either BP550 or BW550 biochar added to the Ramiha soil was 1.5– to 2–fold that added to the Hautere soil (Tables embedded in Figures 7–3a and b). Likewise, to achieve a specific pH value in either soil, the amount of BP550 added was 2.5– to 4.8–fold that of BW550 (Figure 7–2). For example, an application rate of BW550 biochar at 4.76 % (w/w) was needed to increase the pH of the Hautere soil from 5.3 to 6.4, whereas the application rate of BP550 biochar needed to achieve the same pH was up to 21.70 % (Table embedded in Figure 7–3a). Likewise, for the Ramiha soil to attain a pH of 6.4, 9.09 % of BW550 and 28.70 % of BP550 were needed, respectively (Table embedded in Figure 7–3b).

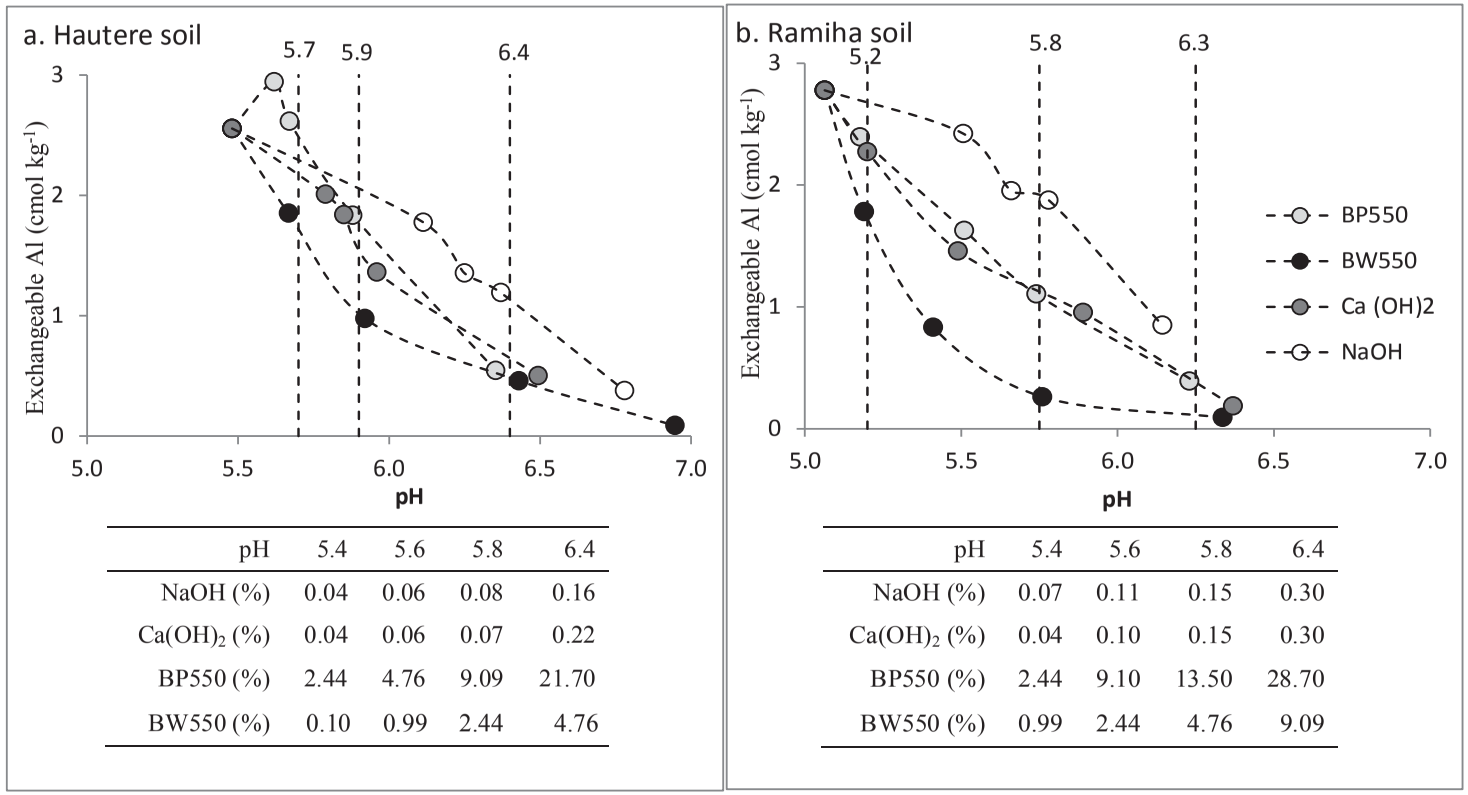

pH	5.4	5.6	5.8	6.4
NaOH (%)	0.04	0.06	0.08	0.16
$Ca(OH)_2$ (%)	0.04	0.06	0.07	0.22
BP550 (%)	2.44	4.76	9.09	21.70
BW550 (%)	0.10	0.99	2.44	4.76

pH	5.4	5.6	5.8	6.4
NaOH (%)	0.07	0.11	0.15	0.30
$Ca(OH)_2$ (%)	0.04	0.10	0.15	0.30
BP550 (%)	2.44	9.10	13.50	28.70
BW550 (%)	0.99	2.44	4.76	9.09

Figure 7–3 Changes in pH and exchangeable Al in (a) Hautere soil and (b) Ramiha soil after amended with NaOH, $Ca(OH)_2$, BP550 and BW550 at different application rates (in tables embedded) to target pH levels

Exchangeable Al was the main contributor to exchangeable acidity, as exchangeable H^+ made < 10% of the contribution (data not shown). The amendments (BW550 biochar, BP550 biochar, NaOH and $Ca(OH)_2$) always reduced Al_{ex} in both soils, except for the BP550 biochar when added to the Hautere soil at an application rate of 2.44 % (Figure 3). In both soils and for a given pH value, the greatest reduction in Al_{ex} was observed with the application of BW550 followed by BP550 and $Ca(OH)_2$, both having similar patterns, and then NaOH. The decrease of Al_{ex} with the amendments was more evident in the Ramiha soil. The addition of 4.76 % BW550 biochar to the Hautere soil caused a decrease in Al_{ex} from 2.6 cmol kg^{-1} to 0.1 cmol kg^{-1} whereas the Al_{ex} level remained at 2.3 cmol kg^{-1} when adding the BP550 biochar at that application rate; in Ramiha soil, values fell from 2.8 to 0.1 cmol kg^{-1} and to 1.9 cmol kg^{-1}, respectively.

7.3.3 Changes in aqueous soil solution composition amended with various amendments

The pH value of the aqueous extracts (1:10 solid: deionized water) from the control and amended soils ranged between 4.9 and 6.5 (Table 7–3). Compared with the unamended Hautere soil, the addition of $Ca(OH)_2$ and BW550 biochar increased soil EC whereas that of NaOH and BP550 biochar tended to decrease it. This contrasted with the changes in EC undergone in the Ramiha soil, as it significantly ($P < 0.05$) increased with all amendments, this increase being specially accentuated at high application rates. The addition of NaOH caused a significant increase ($P < 0.05$) in DOC concentration, this being more noticeable at high application rates; whereas the other amendments only

Table 7-3 Aqueous solution (1:10 solid: deionised water) composition as affected by different amendments

Amendments	Application Rate %	pH	*IS*[a] ($\times 10^{-3}$)	EC[b] $\mu S\ cm^{-1}$	DOC[c] $mg\ kg^{-1}$
Hautere soil					
Nil	0.00	4.9	8.9	685	33
NaOH	0.04	5.0	6.7	515	151
	0.06	5.0	8.0	617	160
	0.08	5.1	7.2	552	185
	0.16	5.4	11.0	843	359
$Ca(OH)_2$	0.04	4.9	12.1	931	30
	0.06	5.0	14.1	1084	30
	0.07	4.9	17.7	1365	82
	0.22	5.0	15.6	1201	40
BP550	2.44	4.9	12.0	925	30
	4.76	5.0	8.4	645	52
	9.09	5.1	6.7	516	41
	21.70	5.4	7.9	609	78
BW550	0.99	5.0	12.7	977	20
	2.44	5.1	13.7	1050	34
	4.76	5.6	14.5	1119	71
	9.09	6.5	19.2	1479	116
Ramiha soil					
Nil	0.00	5.0	6.8	523	53
NaOH	0.07	5.1	9.6	742	104
	0.11	5.2	9.6	739	114
	0.15	5.3	8.6	664	154
	0.30	5.9	15.1	1161	241
$Ca(OH)_2$	0.04	4.9	10.4	801	47
	0.10	5.0	8.2	631	50
	0.15	5.1	7.7	594	70
	0.30	5.5	10.6	815	98
BP550	2.44	4.9	9.7	748	47
	9.10	5.0	10.9	835	57
	13.50	5.1	11.2	862	85
	28.70	5.6	12.0	923	120
BW550	0.99	5.0	9.4	722	58
	2.44	5.3	10.0	772	74
	4.76	5.5	12.5	960	99
	9.09	5.7	20.1	1546	148

[a] Ionic strength

[b] Electronic conductivity

[c] Dissolve organic matter

caused a significant increase ($P < 0.05$) at the highest application rates, with the increase being less prominent (Table 7–3).

As expected, applying $Ca(OH)_2$ and to a lesser extent BW550, significantly ($P < 0.05$) increased Ca^{2+} concentration in both soil solutions, whereas the addition of NaOH and BP550 at high rates (> 9.09 %) caused a significant ($P < 0.05$) reduction in Ca^{2+} (Figures 7–3 and –4). Biochar treatment (either BW550 or to a lesser extent BP550) showed significantly ($P < 0.05$) higher concentrations of K^+ than the control soils. In both soils, Na^+ concentration increased with the addition of NaOH and high application rates of BP550 biochar (> 9.09 %), but showed no change when $Ca(OH)_2$ and BW550 biochar were added. The addition of BW550 biochar at increasing application rates resulted in a steady increase in the soil solution ionic strength, as reflected by the increase of ionic species in solution (Table 7–3 and Figures 7–4 and –5).

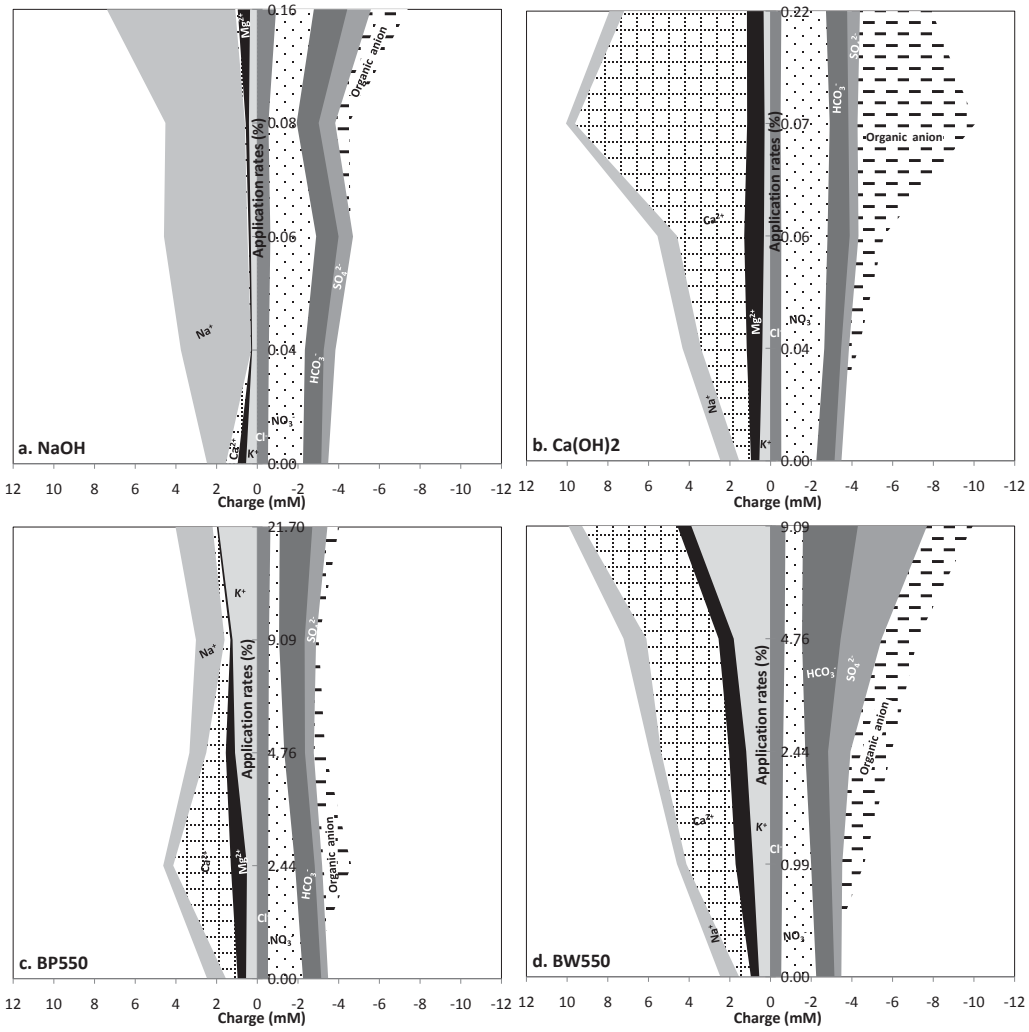

Figure 7–4 Charge balance diagram in aqueous phase (1:10 solid: deionised water) of Hautere soil amended with NaOH (a), $Ca(OH)_2$ (b), BP550 (c) and BW550 (d)

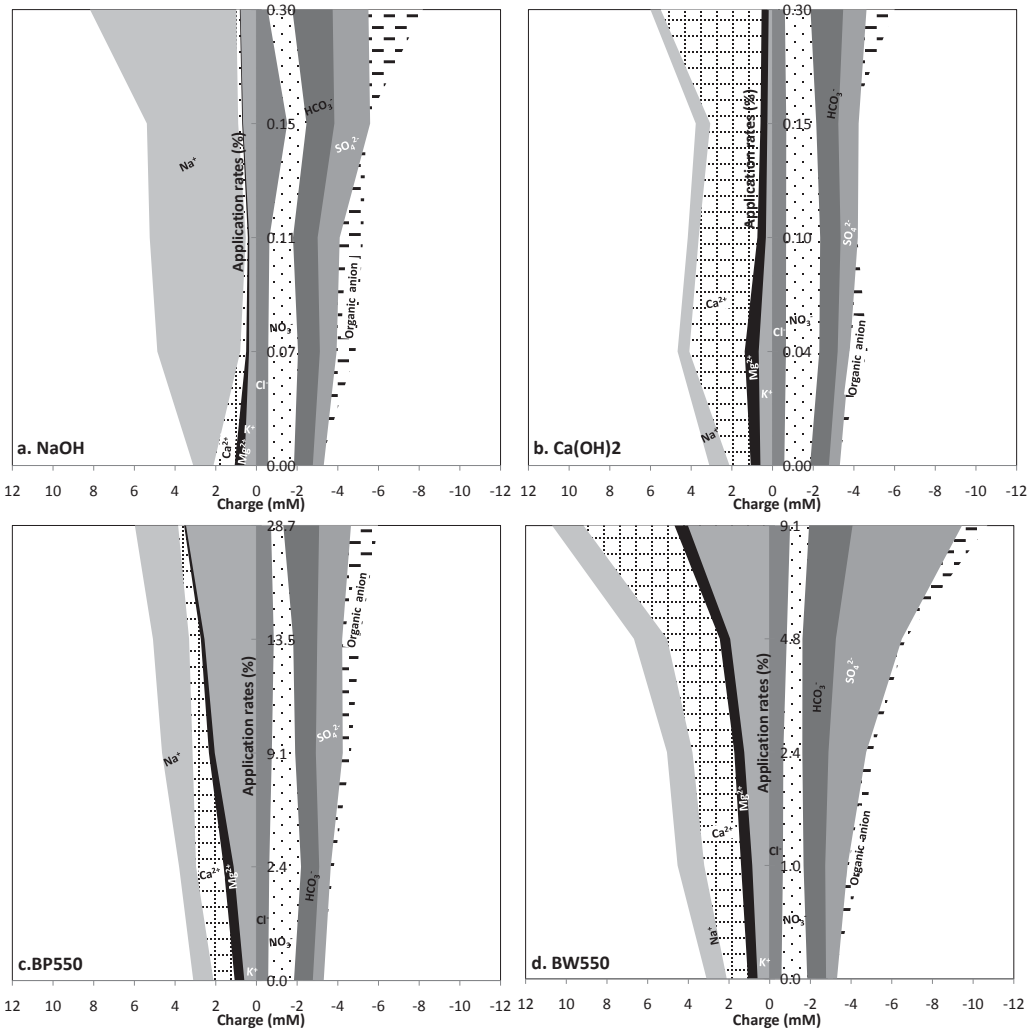

Figure 7–5 Charge balance diagram in aqueous phase (1:10 solid: deionised water) of Ramiha soil amended with NaOH (a), $Ca(OH)_2$ (b), BP550 (c) and BW550 (d)

7.3.4 Behaviour of reactive Al in aqueous soil solution as a result of the amendments

Total reactive Al (Al_r) in the non–amended Hautere and Ramiha soil solution was 2.1 and 2.7 mg L^{-1}, respectively, and was dominated by labile monomeric Al (Al_{Lm})

(61.5 and 62.2 %, respectively), followed by acid soluble Al (Al_{as}) (30.3 and 32.5 %, respectively), and then the non–labile monomeric Al (Al_{NLm}) (Figure 7–6). In both soils, the addition of $Ca(OH)_2$ caused a decrease of Al_r in solution (mainly as Al_{Lm} and to a lesser extent Al_{as}) with an increase in Al_{NLm}. The addition of BW550 biochar followed a similar pattern to that observed with $Ca(OH)_2$ addition, except that the Al_{NLm} remained relatively constant.

In the Hautere soil, both NaOH and BP550 biochar applications caused an initial decrease in Al_r at low application rates followed by an increase at high application rates, mainly in the form of Al_{as}, although total Al_r always remained below that of the control soil (Figure 7–6a). In the Ramiha soil, the NaOH caused an initial decrease in Al_r at low application rates but then this rose to values above those of the control soil (more than 2–fold at the highest application rate) (Figure 7–6b). In this soil, the BP550 biochar only caused a decrease in Al_r values at intermediate application rates.

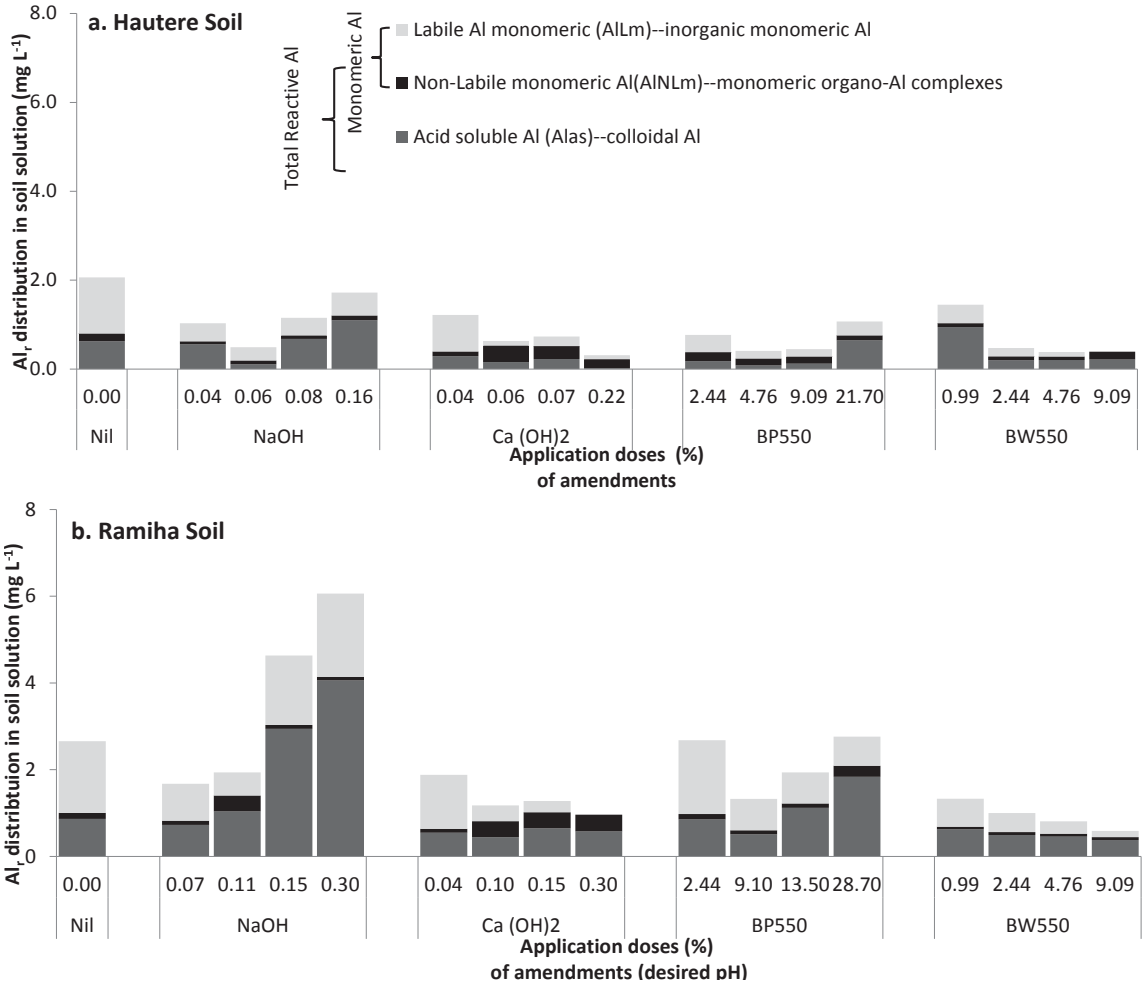

Figure 7–6 Reactive Al (Al_r) fractionation in aqueous phase (1:10 solid: deionised water) of Hautere soil (a) and Ramiha soil (b) amended with NaOH, $Ca(OH)_2$, BP550 and BW550 at different application rates to various pH levels

7.3.5 Behaviour of labile monomeric Al in aqueous soil solution as a result of the amendments

Both soils had a similar Al species distribution, with a dominance of AlF^{2+}, followed by Al^{3+}, $Al(OH)^{2+}$ and AlF_2^+, and then $Al(OH)_2^+$ least dominant (Figure 7–7).

In the Hautere soil, the decrease in Al_{Lm} caused by the amendments studied was associated with reductions in AlF^{2+} and Al^{3+} and to a lesser extent, $Al(OH)^{2+}$ and AlF_2^+ (Figure 7–7a).

In the Ramiha soil, trends in changes in Al speciation with biochar addition were similar to those observed in the Hautere soil (e.g., a predominant reduction in AlF^{2+} and Al^{3+}), except that higher biochar application rates were needed to attain similar decreases (Figure 7–7b). In fact, the addition of BW550 to this soil markedly reduced Al^{3+} to undetectable levels at application rates of 4.76 and 9.09%. The addition of NaOH at high application rates caused a change in Al speciation with an increase in Al–OH [e.g., $Al(OH)_2^+$ and $AlOH^{2+}$] and AlF^{2+}.

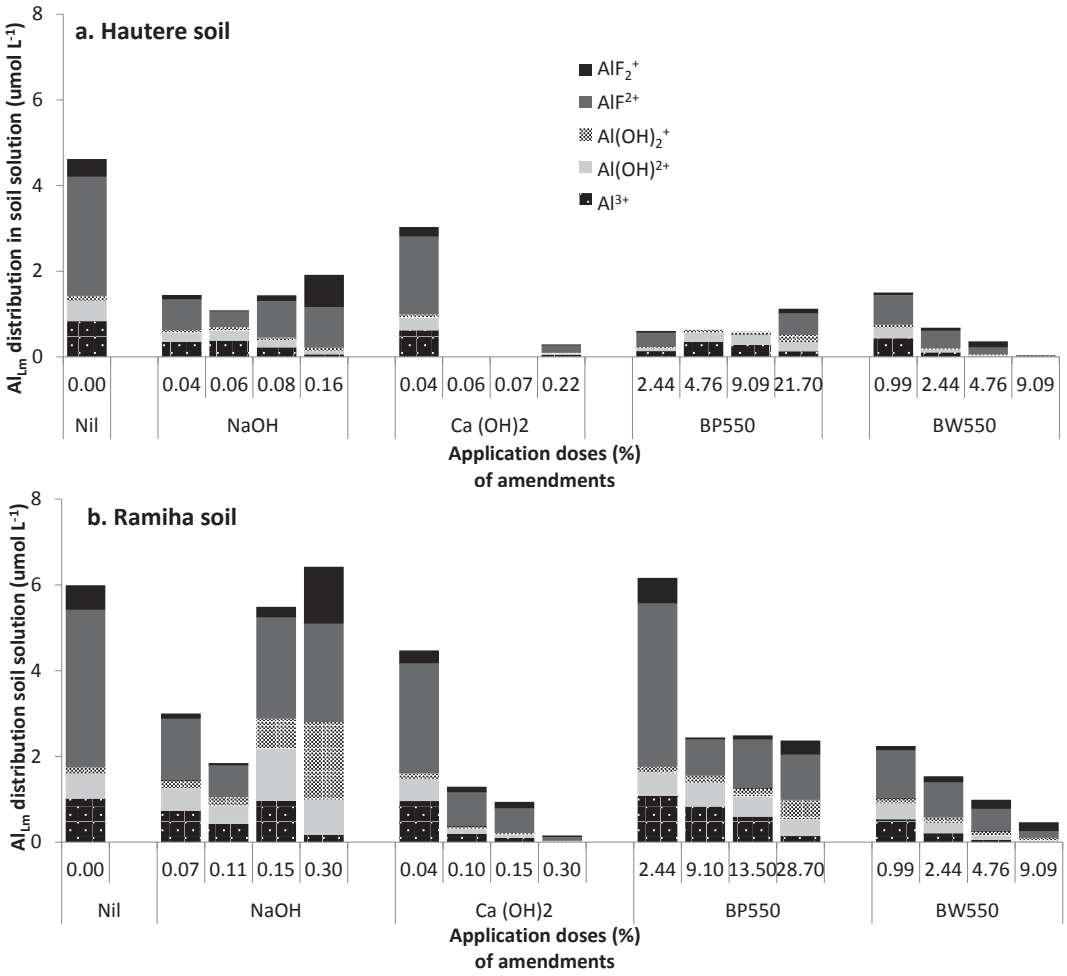

Figure 7–7 Labile monomeric Al (Al_{Lm}) species distribution in aqueous phase (1:10 solid: deionised water) of Hautere soil (a) and Ramiha (b) soils amended with NaOH, $Ca(OH)_2$, BP550 and BW550 at different application rates to various pH levels

7.3.6 Responses of alfalfa seedling to various amendments

Seedling root growth was more sensitive to the amendments than seed germination. The sown seeds mostly germinated on the 2nd day with germination rates > 92% and without any significant (P > 0.05) differences between amendments (data not shown). Regardless of the soil studied, alfalfa root growth was enhanced by the incorporation of either BW550 (< 9.09%) or $Ca(OH)_2$ compared with the unamended treatment (Figure 7–8).

Conversely, root growth was negatively influenced by the addition of BP550 and NaOH to the soils studied (Figure 7–8). This became more severe as application rates increased, with the largest inhibition (40 % reduction in the root length) at BP550 application rates > 20 %. The negative effect of BP550 on RRL was more intense than that of NaOH when added to the Hautere soil, whereas the trend was opposite in the Ramiha soil.

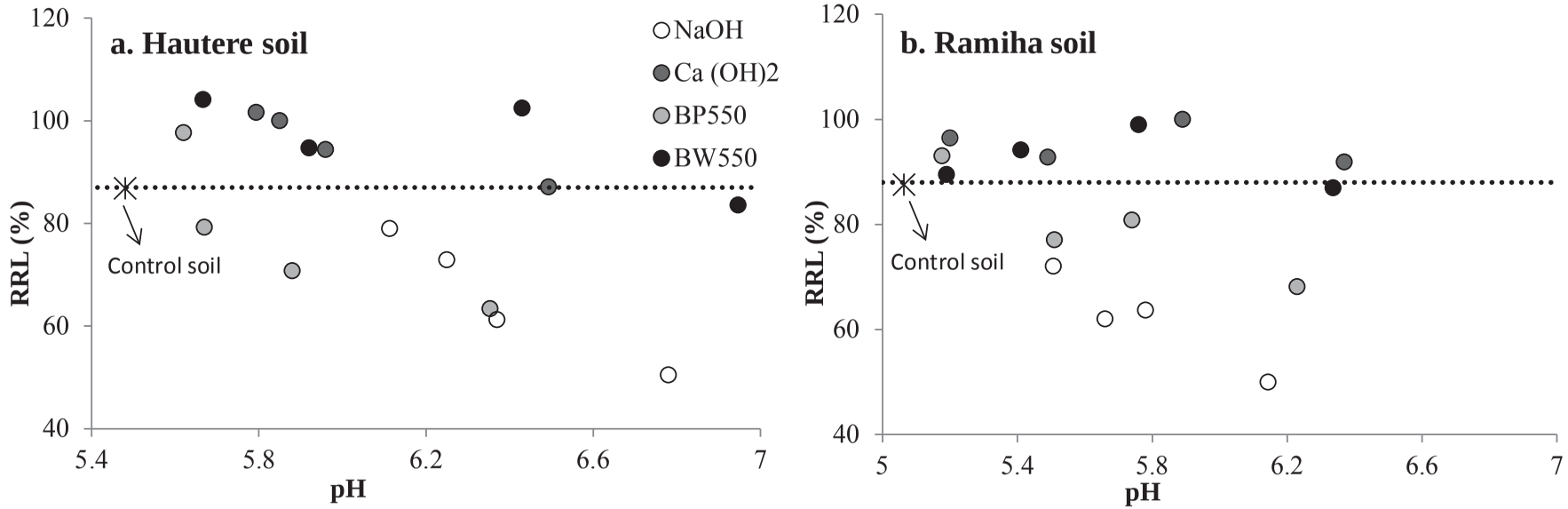

Figure 7–8 Response of alfalfa seedling root growth [relative root length (RRL)] to Hautere soil (a) and Ramiha soil (b) amended with NaOH, $Ca(OH)_2$, BP550 and BW550 at different application rates to target pH levels

7.4 Discussion

The andic properties of the Ramiha soil – associated with the abundance of short–range ordered Al oxy–hydroxides and organo–Al complexes − explains the 1.8–fold greater alkaline–pH–BC compared with the Hautere soil (Climo and Richardson, 1984). The presence of variable charge (e.g., short–range ordered Al oxy–hydroxides) strongly contributes to the pH–BC of these soils. Moreover, when adding a liming material to a soil rich in organo–Al complexes, accompanying exchangeable cations will displace a fraction of the Al complexed with organic matter (Takahashi et al., 1995), which will then react with OH^- (generated by the liming material) forming $Al(OH)_3$ precipitates and thus contributing to the pH–BC of the soil (Takahashi et al., 2006). Indeed, the amount of either BP550 or BW550 biochar added to the Ramiha soil to obtain a specific pH value was 1.5– to 2–fold of that added to the Hautere soil.

The two biochars under study differed in their liming effect. In fact, for either soil to achieve a specific pH value, the amount of BP550 added was 2.5– to 4.8–fold that of BW550. This was ascribed to the fact that willow wood is more enriched in organic salts of alkaline earth elements (e.g., Ca, Mg, and K) than that of pine woodchip (Vassilev et al., 2010). During pyrolysis process acidic organic functional groups are removed and the ash content increases (Ueno et al., 2008; Fuertes et al., 2010; Singh et al., 2010a). This ash is enriched in alkaline salts that differ in their water solubility, and includes (i) readily soluble salts, (ii) carbonates (as alkali traps evolving CO_2 during pyrolysis), (iii) sparingly soluble metal oxides and hydroxides (that will become enriched at temperature > 600 ^oC, at which carbonates thermally decompose), and (iv)

silicates, the latter especially when feedstocks contain soil particles (Glaser et al., 2002; Okuno et al., 2005; Vassilev et al., 2013b, a; Wang et al., 2014). Most of these salts have a considerable liming value (Vassilev et al., 2013b; Smider and Singh, 2014). In addition, the organic functional groups at the surface of biochar particles (e.g., organic anions of carboxyl, lactone and phenolic groups) (Yuan and Xu, 2012) are amphoteric and can thus contribute to either acidity or alkalinity (Boehm, 2002).

The ability of a specific liming material to alleviate soil acidity is routinely assessed by measuring its liming equivalence ($CaCO_3$–eq) by means of a rapid titration (Rayment and Lyons 1992). This methodology has however some drawbacks, e.g., it may underestimate the liming equivalence in the presence of sparingly soluble salts (e.g., whewellite, calcite, and dolomite) which react slowly with acid (Materechera and Mkhabela, 2002). Singh et al. (2010) also highlighted the importance of kinetics when measuring the $CaCO_3$–eq of different biochars. For instance, the $CaCO_3$ equivalence values determined by slow titration to pH = 7 were approximately half of the values obtained by the rapid titration method and this was ascribed to incomplete dissolution of calcite in the latter method. Differences in kinetics of salt solubilisation may also explain the fact that, in the present study, the $CaCO_3$–eq of BP550 biochar was nil whereas the corresponding acid–pH–BC was 57 mmol H^+ kg^{-1} $(pH\ unit)^{-1}$.

The two liming agents that were rich in soluble Ca (BW550 and $Ca(OH)_2$) − as evidenced by the changes in ionic concentration (Figure 7–4 and –5) – caused a decrease in reactive Al in solution (Figure 7–6). This was attributed to the hydrolysis of Al (either originally existent in solution or displaced by Ca^{2+} from exchange sites) and polymerization reactions with subsequent precipitation of Al hydroxides. The other two liming agents were less effective in reducing reactive Al and, in some instances − i.e.,

when NaOH was applied to the Ramiha soil − an increase in reactive Al was observed (Figure 7–6). In the Ramiha soil, both BP550 biochar and NaOH tended to increase the fraction of acid soluble Al, especially when applied at high application rates, and this being especially evident when NaOH was used as amendment. This increase in colloidal, polymeric Al is attributed to the combined effects of (i) a pH increase and (ii) high Na^+ concentration on the dispersion of organic matter – as evidenced by the increase in DOC (Table 7–3). The greater organic matter content of the Ramiha soil compared with the Hautere soil (73 vs 34 g kg^{-1}) and the considerable Al associated with organic matter in the former soil (Al_p was 1.36 % in the Ramiha soil and 0.35 % in the Hautere soil) would explain the differences in the magnitude of colloidal polymeric Al solubilized between the two soils.

The changes in the speciation of labile monomeric Al (Al_{Lm}) caused by the liming agents differed between the two groups of amendments (BW550 and $Ca(OH)_2$ vs BP550 and NaOH). Based on the chemical equilibrium model Visual MINTEQ 3.1, the addition of $Ca(OH)_2$ and BW550 biochar into soils led to a reduction in Al_{Lm} (mainly that of Al^{3+} and AlF^{2+}) in the aqueous phase, but this was not observed when either BP550 biochar or NaOH was added to the Ramiha soil. The reduction in Al_{Lm} was attributed to the above mentioned Al hydrolysis, polymerization and precipitation reactions. Aluminium complexation reactions with biochar organic functional groups followed by precipitation in some instances and/or Al sorption on silicate particles present in biochars should not be dismissed (Qian and Chen, 2013). Finally, it should be noted that differences in the effect of the different biochars on the ionic strength of the soil solution, as reflected by their different EC values (Table 7–2) and subsequent

effects in soil solution (Table 7–3), may have further influenced their pH–BC, given the well–known effect that ionic strength has on pH–BC (Aitken and Moody, 1994).

The radicle elongation (RRL) was improved with the presence of either BW550 or $Ca(OH)_2$ as these amendments alleviated the toxicity of Al species (e.g., Al^{3+} and AlF^{2+}) and added Ca^{2+} important for root elongation. The significant negative correlations between RRL and AlF_2^+ ($r = -0.401$, $P < 0.05$), $AlOH^{2+}$ ($r = -0.422$, $P < 0.01$), $Al(OH)_2^+$ ($r = -0.530$, $P < 0.01$) further support the cause–effect relationship between a decrease of these toxic Al species and root elongation (Kinraide and Parker, 1990; Hede et al., 2001; Rout et al., 2001). Moreover, a significant positive correlation between RRL and Ca^{2+} ($r = 0.613$, $P < 0.01$) was detected (Table 7–4). On the other hand, an unbalanced cation ratio (e.g., caused by an excess of Na) and/or the solubilisation of polymeric Al organic compounds in the presence of NaOH and BP550 biochar led to inhibition on radicle elongation. There was in fact a significant negative correlation between RRL and Na^+ ($r = -0.840$, $P < 0.01$). Other authors have reported negative effects on plant performance when adding Na–enriched biochars to soil (Domene et al., 2015). Nonetheless, it should be noted that the addition of either BW550 or BP550 biochars had no effects on alfalfa seed germination, in agreement with study of Free et al (2010) and that of Rogovska et al (2012). Therefore, seed germination may not be a suitable method for testing potential negative effects of specific biochars on plant growth.

Table 7-4 Correlation matrix of the compositions of soil solution and relative radicle length (RRL)

	Ca^{2+}	Na^{+}	DOC[a]	Al_r	Al_{as}	Al^{3+}	$AlOH^{2+}$	$Al(OH)_2^{+}$	AlF_2^{+}
RRL	0.613**	–0.840**	–0.735**	–0.477**	–0.571**	–0.044	–0.422*	–0.530**	–0.401*
pH	0.099	0.252	0.451**	0.146	0.325	–0.459**	–0.10	0.360*	0.239

[a] Dissolve organic matter

** Correlation is significant at the 0.01 level (2–tailed).

* Correlation is significant at the 0.05 level (2–tailed).

7.5 Conclusion

Biochar generated from willow woodchips at 550°C (BW550) has ash content and a higher liming potential than that of biochar produced from pine woodchips at the same temperature (BP550). Thus, BW550 resulted to be a more effective liming agent compared with BP550. BW550 reduced exchangeable Al concentration to a greater extent. The alfalfa seedling radicle elongation bioassay in conjunction with the Al fractionation and speciation were suitable techniques for demonstrating alleviation of Al phytotoxicity by amending soil with biochar made from willow woodchips.

7.6 Acknowledgements

The authors acknowledge financial support for Qinhua Shen from New Zealand Biochar Research Centre. The authors are also deeply grateful to Ms Ruth Morrison for providing the alfalfa seed; we are grateful for the technical support from Mr Ian Furkert, Mr Bob Toes, and Ms Glenys Wallace; and thank Dr Peter Bishop and Dr Roberto Calvelo Pereira for inspiring discussions the experimental results.

Chapter 8

OVERALL SUMMARY AND RECOMMENDATIONS FOR FUTURE RESEARCH

This chapter provides (i) a general summary of the main achievements of this study; (ii) the highlights of this research; and (iii) some recommendations for future research.

8.1 Overall summary

Given the ever–increasing interest in the use of biochar as soil amendment to improve soil functions this thesis posed the question "can biochar be specifically used to increase the bioavailability of residual P in high P–affinity soils (e.g., Andosols) and/or alleviate Al phytotoxicity in acid soils?" After reviewing the literature (Chapter 2), the mechanisms through which biochar might influence the above–mentioned limitations (i.e., P and Ca deficiency, and Al phytotoxicity) were identified: (i) an increase in soil pH associated with the liming properties of biochar may cause an increase in P availability and a decrease in soluble Al; (ii) the addition of nutrients originally present in the biochar (e.g., P and Ca) may contribute to alleviate their deficiency in plants; and (iii) the stimulation of AMF hyphae development may contribute to increase P uptake by plants.

8.1.1 Analytical methods for biochar characterization

Initially, the suitability of some analytical methodologies to characterize biochars (specifically the pH–buffering capacity – pH–BC – and available N) was tested. For this, 19 biochars produced from a variety of feedstocks and under different processes conditions (e.g., different highest heating temperatures) were used (Chapter 3). Different pH–buffering capacity (pH–BC) methodologies (single vs multiple acid additions, short vs long equilibration times) originally developed for soils were tested along with the method proposed to measure the liming equivalence of biochars (IBI, 2012). The methodologies were thereafter validated by incubating two acid soils – to which separate amendments of the 19 biochars were made at the rates estimated using

both methodologies – for 10 d to target a final pH of 6.5. The results indicated that the relationship established between the pH–BC of the 19 biochars under study after 30–min equilibration ($pH–BC_{30min}$) with a single acid addition and that obtained after a 5–d equilibration ($pH–BC_{5d}$) (predicted $pH–BC_{5d} = 2.2 \times pH–BC_{30min} + 20.4$) made it possible to estimate adequately the liming potential of biochars. The liming equivalence was found to be more accurate (narrow range of final pH values) but less precise (average not as close to the targeted value as when using the predicted $pH–BC_{5d}$ methodology). Both protocols were considered suitable to make the recommendation of the biochar application rate.

Acid (6 M HCl) hydrolysis at 105°C for 24 h followed by oxidizing the hydrolysate with potassium peroxodisulfate, originally developed by Wang et al (2012a) using biochars rich in N, proved un suitable for biochars with low N concentrations. The same procedure but with a smaller dilution factor (242), was found to be sufficiently adequate to overcome the chloride interferences while avoiding over diluting the sample when measuring the biochar (e.g., woody biochar) with lower content of available N. This procedure was therefore recommended in this study.

Three different biochars – two biochars were produced from chipped pine (*Pinus radiata* D. Don) branches at 450°C and 550°C (referred to as BP450 and BP550, respectively) and a third one from chipped weeping willow (*Salix matsudana* L.) branches at 550°C (referred to as BW550) – were prepared to investigate the possibility of using biochar to increase the bioavailability of residual P in a high P–affinity soils (e.g., Andosols) and/or alleviate Al phytotoxicity in acid soils. These biochars (BP450, BP550 and BW550) were then classified based on the Camps Arbestain et al. (2015) classification system as follows: (i) organic C storage value: classes 4; 4; 5,

respectively; (ii) fertilizer value: classes 0; 0; 3; P_{30t} K_{4t} S_{7t} Mg_{7t}, respectively; and (iii) liming equivalence values: classes 0; 0; 2, respectively.

8.1.2 Mobilization of P immobilized in high P affinity Andosols using biochar

The soils investigated in this part of study were two sil–andic Andosols of contrasting P status (Olsen P of 4.3 vs 33.3 mg kg^{-1}, referred to as LP and HP soil, respectively). This section comprised three chapters (Chapter 4–6). The first two chapters focused on the development of methodologies to accurately (i) estimate external hyphal length in soil (Chapter 4), and (ii) evaluate the P transferred by AMF hyphae to plants (Chapter 5). Both have been key to the study of the feasibility of using biochar to increase P bioavailability in high–P affinity soils via its stimulation on AMF growth (Chapter 6).

The traditional visual gridline intersection (VGI) method commonly used to measure the length of AMF hyphae distribution in soil was modified with (i) that using a digital photomicrography technique (DGI) method, and (ii) the processing of the images using ImageJ software (PIP) method. Before measuring the hyphal length in the LP and HP soils where *Lotus pedunculatus cv* barsille was grown for 32 wk, these methods were first tested with known lengths of possum fur. The study confirmed that both DGI and PIP methods are suitable and easy methods to study the density and distribution of AMF hyphae in the soil, but the PIP method provides less uncertainty. A manuscript on this study (Chapter 4) – Qinhua Shen, Miko U.F. Kirschbaum, Mike J.

Hedley, Marta Camps–Arbestain. Testing an alternative method for estimating the length of fungal hyphae using photomicrography and image processing (2016) – has been accepted to be published on the journal of *PLoS ONE*.

Another challenge confronted when working on the effect of biochar on AMF hyphae growth using a root study container was the need to discriminate the P uptake associated with AMF from that of P diffusion caused by spatial patchiness of available P (i.e., when adding a biochar rich in P to soil or a biochar with liming properties). The plant growth medium was divided into two sections – (i) a *root zo*ne to which root and hyphal have full access and (ii) an *hyphal zone* to which only AMF hyphae has access – by a polyester mesh (30–µm opening) (Hedley et al., 1994). This was further modified by placing a "P diffusion break" (made of a 3–mm thick of tephra) under the polyester mesh. This layer of tephra proved to be sufficient to halt P diffusion from the HP soil to the LP soil for a plant growth period of 32 wk (Chapter 5). Given the inability of (i) root to penetrate into the *hyphal zone* of HP soil to take up P and (ii) P in the *hyphal zone* of HP soil to diffuse to the *root zone* of LP soil, the increase in P uptake by plant growth in a combination of a *root zone* of LP soil and a *hyphal zone* of HP soil (compared with that in which both *root* and *hyphal zones* were filled with LP soil) was only ascribed to the transfer of P from HP soil to LP soil by AMF hyphae. This novel root study container allows the biochar to be added to either the *root zone* or the *hyphal zone* and evaluate the effect of biochar on AMF hyphae development and P uptake. Therefore, this device can help discern whether biochar can influence AMF development and enhance P bioavailability. A manuscript entitled "A novel technique for evaluating the phosphorus transferred by arbuscular mycorrhizal fungi hyphae" is currently being prepared for submission to *Soil Research*.

Lotus pedunculatus cv barsille was grown in LP and HP soils separately amended with BP450, BP550 and BW550 biochars at an application rate of 10 t ha^{-1} using the root study container for 32 wk without any further P and N fertilization (Chapter 6). The results showed that (i) none of the tested biochars conferred any specific advantages to the soil with high P content (i.e., HP soil); (ii) the BW550 biochar with high P content and liming potential increased plant growth by 59 % and P uptake by 73 %, whereas the pine–based biochar (e.g., BP450 and BP550) did not provided extra nutrients uptake neither contributed to plant growth in the P–deficient soil (e.g., LP soil); and (iii) biochar produced from BP450 biochar caused a 70% P uptake increase (and 40% plant growth increase) by stimulating AMF growth (by 0.8 m hyphae g^{-1} soil g^{-1} DM) and accessing a high–P area (HP soil) to which plant root had no access. The positive effects of BW550 and BP450 biochars were ascribed to (i) the provision of supplemental nutrients (especially P) from the BW550 biochar, along with its liming effect and related increase in P availability, and (ii) the stimulation of AMF growth and access to P by the BP450 biochar. However, the current research was unable to unravel the underlying mechanisms through which BP450 stimulated AMF hyphae development. A manuscript based on this study (Chapter 6) has been recently accepted to be published on the *Journal of Soil Science and Plant Nutrition*: Qinhua Shen, Mike J. Hedley, Marta Camps–Arbestain, Miko U.F. Kirschbaum. Can biochar increase the bioavailability of phosphorus? (2016).

8.1.3 Amelioration effect of biochar on acid soil

The liming effect of BW550 and BP550 biochars on two acidic soils was compared with that resulting from adding either $Ca(OH)_2$ or NaOH to the same soils, and the mechanisms involved in the amelioration of soil acidity and Al toxicity to plant growth were investigated (Chapter 7). A seedling radicle elongation bioassay using Alfalfa (*Medicago sativa* L.) was carried out. Results showed that the BW550 biochar was a more effective liming agent compared with the BP550 biochar: (i) less amount of BW550 needed to achieve a targeted pH value (5.4, 5.6, 5.8 and 6.4) than that BP550; (ii) for a given pH, the decrease in exchangeable Al resulting from the amendments was greater when adding the BW550 biochar compared with the addition of the BP550 biochar. The addition of BW550 biochar (at application rates < 9.1 %) stimulated alfalfa seedling growth, whereas addition of BP550 (at application rates > 2.4 %) caused inhibition. These different responses were explained by the fact that the former caused a decrease in both inorganic monomeric Al (mainly in AlF^{2+} and Al^{3+}) and colloidal Al, and an increase in aqueous Ca^2, while the latter caused an unbalanced cation ratio (e.g., caused by an excess of Na) and the subsequent solubilisation of polymeric Al organic compounds. A manuscript entitled "Can Biochar Ameliorate Aluminium Phytotoxicity?" has been prepared and will be submitted to *Geoderma Journal*.

We concluded that willow wood chip can be used as a suitable feedstock to produce a biochar with liming and fertilizer values (e.g., P, Ca and K), and is therefore able to alleviate Al toxicity in acid soil and increase P bioavailability in a P infertile soil, in addition to contributing to C storage. While the biochar produced from the pine

woodchips has no nutrients and liming values, it has the potential to stimulate AMF mycelium development and enhance plant P uptake via hyphal P acquisition from a soil patch rich in P.

8.2 Highlights of the thesis

- A methodology was developed to determine the pH–buffering capacity of biochar consisting of a 30–min incubation of biochar after a single acid addition and a correction factor to account for the lack of the equivalence (Predicted pH–BC_{5d} = 2.2 × pH–BC_{30min} + 20.4) (Chapter 3).
- The methodology of available N in biochar was modified to account for this fraction in biochars low in N (e.g., woody biochar). The modification consisted in avoiding over diluting the digestate while minimising interferences with chloride (Chapter 3).
- A less subjective and rapid method (photomicrography–image analysis) was obtained to measure the length of AMF hyphae in soil compared with the visual gridline intersection method (Chapter 4).
- The root study container commonly used to study the role of hyphae on nutrient plant uptake was modified with a novel "P diffusion break" made of a layer of 3–mm tephra to avoid the interference of P diffusion caused by spatial patchiness of available P (Chapter 5).
- Biochar produced from willow woodchips at 550°C (BW550) was shown to be suitable soil amendment if it is intended to enhance the P fertility of sil–andic Andosols with low P status (Chapter 6).

- Biochar produced from pine woodchips at 450°C (BP450) was shown to be a suitable soil amendment if it is intended to stimulate AMF development and increase P uptake by plants grown in sil–andic Andosols (Chapter 6).
- Biochar produced from willow woodchips at 550 °C (BW550) was shown to be a suitable soil amendment if it is intended to alleviate Al toxicity and enhance root elongation in acid soils (Chapter 7).
- Biochar produced from pine woodchips at 550°C (BP550) was shown to inhibit root elongation but the underlying mechanism was not identified (Chapter 7).

8.3 Future research recommendations

8.3.1 Applying the techniques of photomicrography and image processing to determine the AMF root colonization

The major challenge when studying the influence of AMF on environmental and agricultural functions is the measurement of AMF colonization and external hyphal growth in soil. This is generally carried out using the gridline intersection method, which is time–demanding and fatigue–inducing. The alternative method proposed here using photomicrography and image processing has been proved to be efficient and less prone to error (e.g., associated not only to user bias but also to bias caused by the distribution of hyphae on the grid). This method also possesses a potential advantage for

determining AMF root colonization by the same principle but this needs to be tested before being applied.

8.3.2 The underlying mechanisms through which biochar stimulates AMF hyphal abundance and functionality

The application of biochar BP450 was found to stimulate AMF hyphae development and subsequently favour plant P uptake, although the underpinned mechanisms remained unclear. The presence of biochar may not only modify the soil chemical properties, but also soil physical properties (Herath et al., 2013) and this may result in a more favourable environment for AMF growth; biochar may also (ii) interfere the signalling path between the host plant and fungus (as suggested by Warnock et al., (2007)); and (iii) provide AM fungi with a C source (Quilliam et al. 2013). More research is needed to provide a mechanistic explanation.

8.3.3 The potential of biochar to reduce cadmium bioavailability in soils (with special interest in soils to which long term phosphate fertilization has been carried out)

Applications of phosphate fertilizers that were estimated to contain in the range of 20 – 50 mg cadmium (Cd) kg^{-1} led to significant increases in the Cd concentration of

the topsoils (Loganathan et al., 2003). Indeed, 1.3 mg Cd kg^{-1} was found in the HP soil sampled in an area of grazed ryegrass/clover pasture with a long–term P fertilization history (data not shown). Given the potential toxicity of Cd to humans and other living organisms, concerns have been raised about the effects of its gradual long–term accumulation in New Zealand soils. The application of biochar may decrease the availability of cationic heavy metals as a result of their ability to contribute to soil cation exchange capacity (CEC) and to increase soil pH (if a biochar with liming properties) (Uchimiya et al., 2010).

References

Abbott, L.K., Robson, A.D., De Boer, G., 1984. The effect of phophorus on the formation of hyphae in soil by the vesicular–arbuscular mycorrhizal fungus, Glomus Fasciculatum. New Phytologist 97, 437–446.

Abràmoff, M.D., Magalhães, P.J., Ram, S.J., 2004. Image processing with ImageJ. Biophotonics international 11, 36–43.

Adams, F., 1981. Nutritional imbalances and constraints to plant growth on acid soils. Journal of Plant Nutrition 4, 81–87.

Adams, F., Hathcock, P.J., 1984. Aluminum toxicity and calcium deficiency in acid subsoil horizons of two coastal plains soil series. Soil Science Society of America Journal 48, 1305–1309.

Aitken, R., 1992. Relationships between extractable Al, selected soil properties, pH buffer capacity and lime requirement in some acidic Queensland soils. Soil Research 30, 119–130.

Aitken, R., Moody, P., 1994. The effect of valence and Ionic–strength on the measurement of pH buffer capacity. Soil Research 32, 975–984.

Aitken, R., Moody, P., Mckinley, P., 1990. Lime requirement of acidic Queensland soils.II. Comparison of laboratory methods for predicting lime requirement. Soil Research 28, 703–715.

Alleoni, L.R., Cambri, M.A., Caires, E.F., Garbuio, F.J., 2010. Acidity and aluminum speciation as affected by surface liming in tropical no–till soils. Soil Science Society of America Journal 74, 1010–1017.

Almendros, G., Knicker, H., González–Vila, F.J., 2003. Rearrangement of carbon and nitrogen forms in peat after progressive thermal oxidation as determined by solid–state 13C– and 15N–NMR spectroscopy. Organic Geochemistry 34, 1559–1568.

Alva, A., Asher, C., Edwards, D., 1986. The role of calcium in alleviating aluminum toxicity. Crop and Pasture Science 37, 375–382.

Anderson, C.R., Condron, L.M., Clough, T.J., Fiers, M., Stewart, A., Hill, R.A., Sherlock, R.R., 2011. Biochar induced soil microbial community change: Implications for biogeochemical cycling of carbon, nitrogen and phosphorus. Pedobiologia 54, 309–320.

Barceló, J., Poschenrieder, C., Vázquez, M.D., Gunsé, B., 1995. Aluminum phytotoxicity. Fertilizer Research 43, 217–223.

Bardgett, R.D., 1991. Proceedings of the International Workshop on Modern Techniques in Soil Ecology Relevant to Organic Matter Breakdown, Nutrient Cycling and Soil Biological Processes The use of the membrane filter technique for comparative measurements of hyphal lengths in different grassland sites. Agriculture, Ecosystems & Environment 34, 115–119.

Barreto, P.L.M., Pires, A.T.N., Soldi, V., 2003. Thermal degradation of edible films based on milk proteins and gelatin in inert atmosphere. Polymer Degradation and Stability 79, 147–152.

Baisden, W.T., Parfitt, R., Ross, C., Schipper, L., Canessa, S., 2013. Evaluating 50 years of time–series soil radiocarbon data: towards routine calculation of robust C residence times. Biogeochemistry 112, 129–137.

Beck, M.A., Robarge, W.P., Buol, S.W., 1999. Phosphorus retention and release of anions and organic carbon by two Andisols. European Journal of Soil Science 50, 157–164.

Beesley, L., Moreno–Jiménez, E., Gomez–Eyles, J.L., Harris, E., Robinson, B., Sizmur, T., 2011. A review of biochars' potential role in the remediation, revegetation and restoration of contaminated soils. Environmental Pollution 159, 3269–3282.

Berek, A., Radjagukguk, B., Maas, A., 1995. The effect of different organic materials on the alleviation of Al toxicity in soybean on a red–yellow podzolic soil, In: Date, R.A., Grundon, N.J., Rayment, G.E., Probert, M.E. (Eds.), Plant–Soil Interactions at Low pH: Principles and Management. Springer Netherlands 579–584.

Bernstein, L., 1975. Effects of Salinity and Sodicity on Plant Growth. Annual Review of Phytopathology 13, 295–312.

Biederman, L.A., Harpole, W.S., 2013. Biochar and its effects on plant productivity and nutrient cycling: a meta–analysis. GCB Bioenergy 5, 202–214.

Blackwell, P., Krull, E., Butler, G., Herbert, A., Solaiman, Z., 2010. Effect of banded biochar on dryland wheat production and fertiliser use in south–western Australia: an agronomic and economic perspective. Soil Research 48, 531–545.

Bloom, P., 2000. Soil pH and pH buffering. CRC Press, Boca Raton, FL., B333–B352.

Boddington, C.L., Bassett, E.E., Jakobsen, I., Dodd, J.C., 1999. Comparison of techniques for the extraction and quantification of extra–radical mycelium of arbuscular mycorrhizal fungi in soils. Soil Biology and Biochemistry 31, 479–482.

Boehm, H.P., 2002. Surface oxides on carbon and their analysis: a critical assessment. Carbon 40, 145–149.

Bolan, N., 1991. A critical review on the role of mycorrhizal fungi in the uptake of phosphorus by plants. Plant and Soil 134, 189–207.

Bolan, N.S., Adriano, D.C., Curtin, D., 2003. Soil acidification and liming interactions with nutrientand heavy metal transformationand bioavailability. Advances in Agronomy 78, 215–272.

Bolan, N.S., Hedley, M.J., 2003. Role of carbon, nitrogen, and sulfur cycles in soil acidification, 29–56.

Bolan, N.S., Hedley, M.J., White, R.E., 1991. Processes of soil acidification during nitrogen cycling with emphasis on legume based pastures. Plant and Soil 134, 53–63.

Bolan, N.S., Naidu, R., Syers, J.K., Tillman, R., 1999. Surface charge and solute interactions in soils. Advances in Agronomy 67, 87–140.

Bose, J., Babourina, O., Rengel, Z., 2011. Role of magnesium in alleviation of aluminium toxicity in plants. Journal of Experimental Botany 62, 2251–2264.

Bourke, J., Manley–Harris, M., Fushimi, C., Dowaki, K., Nunoura, T., Antal, M.J., 2007. Do All Carbonized Charcoals Have the Same Chemical Structure? 2. A Model of the Chemical Structure of Carbonized Charcoal†. Industrial & engineering chemistry research 46, 5954–5967.

Brady, D.J., Edwards, D.G., Asher, C.J., Blamey, F.P.C., 1993. Calcium amelioration of aluminium toxicity effects on root hair development in soybean [Glycine max (L.) Merr.]. New Phytologist 123, 531–538.

Brundrett, M., 1994. Chapter 2 Extracting, staining and measuring hyphae from soil. In: Brundrett, M., Melville, L., Peterson, L. (Eds.). Practical methods in mycorrhiza research. Department of Biology, University of Waterloo.

Butterly, C.R., Baldock, J.A., Tang, C., 2013. The contribution of crop residues to changes in soil pH under field conditions. Plant and Soil 366, 185–198.

Buurman, P., Peterse, F., Almendros Martin, G., 2007. Soil organic matter chemistry in allophanic soils: a pyrolysis - GC/MS study of a Costa Rican Andosol catena. European Journal of Soil Science 58, 1330 - 1347.

Buurman, P., van Lagen, B., Piccolo, A., 2002. Increase in stability against thermal oxidation of soil humic substances as a result of self association. Organic Geochemistry 33, 367–381.

Calvelo–Pereira, R., Arbestain, M.C., Sueiro, M.V., Maciá–Agulló, J.A., 2015. Assessment of the surface chemistry of wood–derived biochars using wet chemistry, FTIR, and X–ray photoelectron spectroscopy. Soil Research 53(7) 753-762

Calvelo Pereira, R., Camps–Arbestain, M., Kaal, J., Vazquez Sueiro, M., Sevilla, M., Hindmarsh, J., 2014. Detailed carbon chemistry in charcoals from pre–European Māori gardens of New Zealand as a tool for understanding biochar stability in soils. European Journal of Soil Science 65, 83–95.

Camenzind, T., Rillig, M.C., 2013. Extraradical arbuscular mycorrhizal fungal hyphae in an organic tropical montane forest soil. Soil Biology and Biochemistry 64, 96–102.

Camps–Arbestain, M., Amonette, J. E., Singh, B., Wang, T., Schmidt, H. P. (2015). A biochar classification system and associated test methods. In Lehmann J. and

Joseph S., eds. Biochar for Environmental Management: Science, Technology and Implementation, 165–194.

Camps–Arbestain, M., Barreal, M., Mourenza, C., Álvarez, E., Kidd, P., Macías, F., 2003. Rhizosphere chemistry in acid forest soils that differ in their degree of Al–saturation of organic matter. Soil Science 168, 267–279.

Camps–Arbestain, M., Saggar, S., Leifeld, J., 2014. Environmental benefits and risks of biochar application to soil. Agriculture, Ecosystems & Environment 191, 1–4.

Cao, X., Harris, W., 2010. Properties of dairy–manure–derived biochar pertinent to its potential use in remediation. Bioresource Technology 101, 5222–5228.

Carvalho, M.C.S., van Raij, B., 1997. Calcium sulphate, phosphogypsum and calcium carbonate in the amelioration of acid subsoils for root growth. Plant and Soil 192, 37–48.

Cayuela, M.L., Sánchez–Monedero, M.A., Roig, A., Hanley, K., Enders, A., Lehmann, J., 2013. Biochar and denitrification in soils: when, how much and why does biochar reduce N_2O emissions? Scientific Reports 3, 1732.

Cayuela, M.L., van Zwieten, L., Singh, B.P., Jeffery, S., Roig, A., Sánchez–Monedero, M.A., 2014. Biochar's role in mitigating soil nitrous oxide emissions: A review and meta–analysis. Agriculture, Ecosystems & Environment 191, 5–16.

Chan, K.Y., Van Zwieten, L., Meszaros, I., Downie, A., Joseph, S., 2007. Agronomic values of greenwaste biochar as a soil amendment. Australian Journal of Soil Research 45, 629–634.

Chan, K.Y., Van Zwieten, L., Meszaros, I., Downie, A., Joseph, S., 2008. Using poultry litter biochars as soil amendments. Australian Journal of Soil Research 46, 437–444.

Chan, K.Y., Xu, Z., 2009. Biochar: Nutrient properties and their enhancement, In: Lehmann, J., Joseph, S.M. (Eds.), Biochar for environmental management: Science and technology. Earthscan, London UK. 67–84.

Chen, J., Liu, X., Zheng, J., Zhang, B., Lu, H., Chi, Z., Pan, G., Li, L., Zheng, J., Zhang, X., Wang, J., Yu, X., 2013. Biochar soil amendment increased bacterial but decreased fungal gene abundance with shifts in community structure in a slightly acid rice paddy from Southwest China. Applied Soil Ecology 71, 33–44.

Cheng, C.–H., Lehmann, J., Engelhard, M.H., 2008. Natural oxidation of black carbon in soils: Changes in molecular form and surface charge along a climosequence. Geochimica et Cosmochimica Acta 72, 1598–1610.

Cheng, C.–H., Lehmann, J., Thies, J.E., Burton, S.D., Engelhard, M.H., 2006. Oxidation of black carbon by biotic and abiotic processes. Organic Geochemistry 37, 1477–1488.

Chintala, R., Mollinedo, J., Schumacher, T.E., Malo, D.D., Julson, J.L., 2013. Effect of biochar on chemical properties of acidic soil. Archives of Agronomy and Soil Science, 1–12.

Choi, D., Makoto, K., Quoreshi, A., Qu, L., 2009. Seed germination and seedling physiology of Larix kaempferi and Pinus densiflora in seedbeds with charcoal and elevated CO2. Landscape and Ecological Engineering 5, 107–113.

Clark, H., Kelliher, F., Pinares–Patino, C., 2011. Reducing CH4 emissions from grazing ruminants in New Zealand: challenges and opportunities. Asian–Australian Journal of Animal Science 24, 295–302.

Climo, W.J., Richardson, M.A., 1984. Factors affecting the susceptibility of 3 soils in the Manawatu to stock treading. New Zealand Journal of Agricultural Research 27, 247–253.

Cornforth, I.S., 2013. The fate of phosphate fertilizer in soil. http://nzic.org.nz/ChemProcesses/soils/2D.pdf

Collins, T.J., 2007. ImageJ for microscopy. Biotechniques 43, 25–30.

Cordell, D., Drangert, J.–O., White, S., 2009. The story of phosphorus: Global food security and food for thought. Global Environmental Change 19, 292–305.

Cornforth, I., 1998. Practical Soil Management. Lincoln University Press with Whitireia Publishing and Daphne Brasell Associates Ltd.

Cregan, P., Hirth, J., Conyers, M., Robson, A., 1989. Amelioration of soil acidity by liming and other amendments. Soil acidity and plant growth, 205–264.

Curtin, D., Syers, J.K., 2001. Lime–Induced Changes in Indices of Soil Phosphate Availability. Soil Science Society of America Journal 65, 147–152.

Dahlgren, R.A., Saigusa, M., Ugolini, F.C., 2004. The Nature, Properties and Management of Volcanic Soils, Advances in Agronomy. Academic Press. 113–182.

Dane, J., Hopmans, J., 2002. Water retention and storage. Methods of soil analysis. Part 4, 671–717.

Dodd, J., 1994. Approaches to the study of the extraradical mycelium of arbuscular mycorrhizal fungi, Impact of arbuscular mycorrhizas on sustainable agriculture and natural ecosystems. Springer, pp. 147–166.

Domene, X., Enders, A., Hanley, K., Lehmann, J., 2015. Ecotoxicological characterization of biochars: Role of feedstock and pyrolysis temperature. Science of the Total Environment 512–513, 552–561.

Douda, J., Basiuk, V.A., 2000. Pyrolysis of amino acids: recovery of starting materials and yields of condensation products. Journal of Analytical and Applied Pyrolysis 56, 113–121.

Driscoll, C.T., 1984. A procedure for the fractionation of aqueous aluminum in dilute acidic waters. International Journal of Environmental Analytical Chemistry 16, 267–283.

Edmeades, D., Pringle, R., Mansell, G., Shannon, P., 1984. Effects of lime on pasture production on soils in the North Island of New Zealand: 1. Introduction and description of data base. New Zealand Journal of Agricultural Research 27, 349–356.

Edmeades, D.C., Ridley, A.M., 2003. Using lime to ameliorate topsoil and subsoil acidity. Handbook of soil acidity. Marcel Dekker, New York, 297–336.

Egiarte, G., Camps–Arbestain, M., Alonso, A., Ruíz–Romera, E., Pinto, M., 2005. Effect of repeated applications of sewage sludge on the fate of N in soils under Monterey pine stands. Forest Ecology and Management 216, 257–269.

Elmholt, S., Kjøller, A., 1987. Measurement of the length of fungal hyphae by the membrane filter technique as a method for comparing fungal occurrence in cultivated field soils. Soil Biology and Biochemistry 19, 679–682.

Fageria, N.K., Baligar, V.C., 2008. Chapter 7 Ameliorating Soil Acidity of Tropical Oxisols by Liming For Sustainable Crop Production, In: Donald, L.S. (Ed.), Advances in Agronomy. Academic Press. 345–399.

Fang, Y., Singh, B.P., Singh, B., 2014. Temperature sensitivity of biochar and native carbon mineralisation in biochar–amended soils. Agriculture, Ecosystems & Environment 191, 158–167.

Fardeau, J.C., Zapata, F., 2002. Phosphorus fertility recapitalization of nutrient–depleted tropical acid soils with reactive phosphate rock: an assessment using the isotopic exchange technique. Nutrient Cycling in Agroecosystems 63, 69–79.

Farrell, M., Macdonald, L.M., Butler, G., Chirino–Valle, I., Condron, L.M., 2013. Biochar and fertiliser applications influence phosphorus fractionation and wheat yield. Biology and Fertility of Soils, 1–10.

Fieldes, M., Perrott, K.W., 1966. The nature of allophane in soils Part 3– Rapid field and laboratory test for allophane. New Zealand Journal Science 9, 623–629.

Foy, C.D., 1988. Plant adaptation to acid, aluminum–toxic soils. Communications in Soil Science & Plant Analysis 19, 959 – 987.

Free, H.F., McGill, C.R., Rowarth, J.S., Hedley, M.J., 2010. The effect of biochars on maize (Zea mays) germination. New Zealand Journal of Agricultural Research 53, 1–4.

Fuertes, A.B., Arbestain, M.C., Sevilla, M., Maciá–Agulló, J.A., Fiol, S., López, R., Smernik, R.J., Aitkenhead, W.P., Arce, F., Macias, F., 2010. Chemical and structural properties of carbonaceous products obtained by pyrolysis and hydrothermal carbonisation of corn stover. Soil Research 48, 618–626.

García–Rodeja, E., Nóvoa, J.C., Pontevedra, X., Martínez–Cortizas, A., Buurman, P., 2007. Aluminium and iron fractionation of European volcanic soils by selective dissolution techniques, In: Arnalds, Ó., Óskarsson, H., Bartoli, F.,

Buurman, P., Stoops, G., García–Rodeja, E. (Eds.), Soils of Volcanic Regions in Europe. Springer Berlin Heidelberg. 325–351.

García–Rodeja, E., Nóvoa, J.C., Pontevedra, X., Martínez–Cortizas, A., Buurman, P., 2004. Aluminium fractionation of European volcanic soils by selective dissolution techniques. Catena 56, 155–183.

Garcia–Rodeja, E., Silva, B.M., MacÍAs, F., 1987. Andosols developed from non–volcanic materials in Galicia, NW Spain. Journal of Soil Science 38, 573–591.

Gaskin, J.W., Speir, R.A., Harris, K., Das, K.C., Lee, R.D., Morris, L.A., Fisher, D.S., 2010. Effect of Peanut Hull and Pine Chip Biochar on Soil Nutrients, Corn Nutrient Status, and Yield. Agronomy Journal 102, 623–633.

Giovannetti, M., Mosse, B., 1980. An evaluation of techniques for measuring vesicular arbuscular mycorrhizal infection in roots. New Phytologist 84, 489–500.

Glaser, B., Lehmann, J., Zech, W., 2002. Ameliorating physical and chemical properties of highly weathered soils in the tropics with charcoal – a review. Biology and Fertility of Soils 35, 219–230.

Goldberg, S., Sposito, G., 1985. On the mechanism of specific phosphate adsorption by hydroxylated mineral surfaces: A review. Communications in Soil Science and Plant Analysis 16, 801–821.

Gomez, J.D., Denef, K., Stewart, C.E., Zheng, J., Cotrufo, M.F., 2013. Biochar addition rate influences soil microbial abundance and activity in temperate soils. European Journal of Soil Science,65 (1): 28–39.

Government of Western Australia, 2015. Causes of soil acidity. Available at: https://www.agric.wa.gov.au/soil-acidity/causes-soil-acidity

Grain S.A., 2013. Soil acidity and its management in crop production 2. Available at: http://www.grainsa.co.za/soil-acidity-and-its-management-in-crop-production-2

Green, D.C., Newsam, R., Jeffries, P., Dodd, J.C., Vilariño, A., 1994. Quantification of mycelial development of arbuscular mycorrhizal fungi using image analysis. Mycorrhiza 5, 105–113.

Gregory, S., Anderson, C., Camps–Arbestain, M., McManus, M., 2014. Response of plant and soil microbes to biochar amendment of an arsenic–contaminated soil. Agriculture, Ecosystems & Environment 191, 133–141.

Grinsted, M., Hedley, M., White, R., Nye, P., 1982. Plant ‐ induced changes in the rhizosphere of rape (Brassica napus var. Emerald) seedlings. New Phytologist 91, 19 ‐ 29.

Grossman, J., O'Neill, B., Tsai, S., Liang, B., Neves, E., Lehmann, J., Thies, J., 2010. Amazonian Anthrosols Support Similar Microbial Communities that Differ Distinctly from Those Extant in Adjacent, Unmodified Soils of the Same Mineralogy. Microbial Ecology 60, 192–205.

Gul, S., Whalen, J.K., Thomas, B.W., Sachdeva, V., Deng, H., 2015. Physico–chemical properties and microbial responses in biochar–amended soils: Mechanisms and future directions. Agriculture, Ecosystems and Environment 206, 46–59.

Habte, M., Antal, M., 2010. Reaction of mycorrhizal and nonmycorrhizal Leucaena leucocephala to charcoal amendment of mansand and soil. Communications in Soil Science and Plant Analysis 41, 540–552.

Hammer, E.C., Balogh–Brunstad, Z., Jakobsen, I., Olsson, P.A., Stipp, S.L.S., Rillig, M.C., 2014. A mycorrhizal fungus grows on biochar and captures phosphorus from its surfaces. Soil Biology and Biochemistry 77, 252–260.

Hanly, J.A., Hedley, M.J., Horne, D.J., 2008. Evaluation of tephra for removing phosphorus from dairy farm drainage waters. Soil Research 46, 542–551.

Hartikainen, H., 1992. Soil response to acid input in a titration experiment. Agricultural Science in Finland 1, 577–585.

Hass, A., Gonzalez, J.M., Lima, I.M., Godwin, H.W., Halvorson, J.J., Boyer, D.G., 2012. Chicken Manure Biochar as Liming and Nutrient Source for Acid Appalachian Soil. Journal of Environment Quality 41, 1096–1106.

Haynes, R., 1982. Effects of liming on phosphate availability in acid soils. Plant and Soil 68, 289–308.

Haynes, R., 1983. Soil acidification induced by leguminous crops. Grass and Forage Science 38, 1–11.

Haynes, R., 1984. Lime and phosphate in the soil–plant system. Advances in Agronomy 37, 249–315.

Haynes, R., Mokolobate, M., 2001. Amelioration of Al toxicity and P deficiency in acid soils by additions of organic residues: a critical review of the phenomenon and the mechanisms involved. Nutrient Cycling in Agroecosystems 59, 47–63.

Haynes, R., Naidu, R., 1998. Influence of lime, fertilizer and manure applications on soil organic matter content and soil physical conditions: a review. Nutrient Cycling in Agroecosystems 51, 123–137.

Hede, A.R., Skovmand, B., Lopez–Cesati, J., 2001. Chapter 15, Acid Soils and Aluminum Toxicity, In: M.P. Reynolds, J.I.O.–M., and A. McNab, E. (Eds.), Application of physiology in wheat breeding. 172–182.

Hedges, J.I., Keil, R.G., 1995. Sedimentary organic matter preservation: an assessment and speculative synthesis. Marine Chemistry 49, 81–115.

Hedley, M., Kirk, G., Santos, M., 1994. Phosphorus efficiency and the forms of soil phosphorus utilized by upland rice cultivars. Plant and Soil 158, 53–62.

Hedley, M., McLaughlin, M., Sims, J., Sharpley, A., 2005. Reactions of phosphate fertilizers and by–products in soils. Phosphorus: agriculture and the environment, 181–252.

Hedley, M.J., Stewart, J.W.B., Chauhan, B.S., 1982a. Changes in inorganic and organic soil phosphorus fractions induced by cultivation practices and by laboratory incubations. Soil Science Society of America Journal 46, 970–976.

Hedley, M.J., White, R.E., Nye, P.H., 1982b. Plant–induced changes in the rhizosphere of rape (*Brassica Napus var*. Emerald) seedlings. New Phytologist 91, 45–56.

Herath, H.M.S.K., Camps–Arbestain, M., Hedley, M., 2013. Effect of biochar on soil physical properties in two contrasting soils: An Alfisol and an Andisol. Geoderma 209–210, 188–197.

Herrera–Estrella, L., 1999. Transgenic plants for tropical regions: some considerations about their development and their transfer to the small farmer. Proceedings of the National Academy of Sciences 96, 5978–5981.

Hewitt, A., Dymond, J., 2013. Survey of New Zealand soil orders. Ecosystem services in New Zealand: conditions and trends, 121–131.

Hina, K., Bishop, P., Arbestain, M.C., Calvelo–Pereira, R., Maciá–Agulló, J.A., Hindmarsh, J., Hanly, J.A., Macías, F., Hedley, M.J., 2010. Producing biochars with enhanced surface activity through alkaline pretreatment of feedstocks. Soil Research 48, 606–617.

Hossain, M.A., Ashrafuzzaman, M., Hossain, A., Ismail, M.R., Koyama, H., 2014. Role of Accumulated Calcium in Alleviating Aluminum Injury in Wheat Plants. The Scientific World Journal 2014. http://dx.doi.org/10.1155/2014/457187

Hossain, M.K., Strezov, V., Yin Chan, K., Nelson, P.F., 2010. Agronomic properties of wastewater sludge biochar and bioavailability of metals in production of cherry tomato (Lycopersicon esculentum). Chemosphere 78, 1167–1171.

Hue, N.V., Craddock, G.R., Adams, F., 1986. Effect of Organic Acids on Aluminum Toxicity in Subsoils. Soil Science Society of America Journal 50, 28–34.

Hue, N.V., Ikawa, H., Silva, J.A., 1994. Increasing plant–available phosphorus in an Ultisol with a yard–waste compost. Communications in Soil Science & Plant Analysis 25, 3291 – 3303.

Hynes, M.M., Zasoski, R.J., Bledsoe, C.S., 2008. Evaluation of two techniques for quantification of hyphal biomass, 2008. Proceedings of the 6th California oak Symposium: Today's Challenges, Tomorrow's Opportunities. General Technical ReportsPSW–GTR–217. Department of Agriculture, Forest Service, Pacific Southwest Research Station, Albany,. 139–148.

IBI, 2012. Standardized product definition and product testing guidelines for biochar that is used in soil. International Biochar Initiative. Available at: http://www.biochar-international.org/

Imai, H., Goulding, K.W.T., Talibudeen, O., 1981. Phosphate adsorption in allophanic soils. Journal of Soil Science 32, 555–570.

Ishii, T., Kadoya, K., 1994. Effects of charcoal as a soil conditioner on citrus growth and vesicular–arbuscular mycorrhizal development. Journal of the Japanese Society for Horticultural Science 63 (3): 529–535.

IUSS Working Group, W., 2006. World reference base for soil resources. World Soil Resour. Rep 103.

Iyamuremye, F., Dick, R., 1996. Organic amendments and phosphorus sorption by soils. Advances in Agronomy 56, 139–185.

Jackman, R., 1964a. Accumulation of organic matter in some New Zealand soils under permanent pasture: I. Patterns of change of organic carbon, nitrogen, sulphur, and phosphorus. New Zealand Journal of Agricultural Research 7, 445–471.

Jackman, R., 1964b. Accumulation of organic matter in some New Zealand soils under permanent pasture: II. Rates of mineralisation of organic matter and the supply of available nutrients. New Zealand Journal of Agricultural Research 7, 472–479.

Jeffery, S., Bezemer, T.M., Cornelissen, G., Kuyper, T.W., Lehmann, J., Mommer, L., Sohi, S.P., van de Voorde, T.F.J., Wardle, D.A., van Groenigen, J.W., 2015. The way forward in biochar research: targeting trade–offs between the potential wins. GCB Bioenergy 7, 1–13.

Jeffery, S., Verheijen, F.G.A., van der Velde, M., Bastos, A.C., 2011. A quantitative review of the effects of biochar application to soils on crop productivity using meta–analysis. Agriculture, Ecosystems & Environment 144, 175–187.

Jiang, J., Peng, Y., Yuan, M., Hong, Z., Wang, D., Xu, R., 2015. Rice Straw–Derived Biochar Properties and Functions as Cu(II) and Cyromazine Sorbents as Influenced by Pyrolysis Temperature. Pedosphere 25, 781–789.

Johnson, B.B., Ivanov, A.V., Antzutkin, O.N., Forsling, W., 2002. 31P Nuclear Magnetic Resonance Study of the Adsorption of Phosphate and Phenyl Phosphates on γ–Al_2O_3. Langmuir 18, 1104–1111.

Kelley, K.R., Stevenson, F.J., 1995. Forms and nature of organic N in soil. Nutrient Cycling in Agroecosystems 42, 1–11.

Kidd, P.S., Proctor, J., 2001. Why plants grow poorly on very acid soils: are ecologists missing the obvious? Journal of Experimental Botany 52, 791–799.

Kim, J.–S., Sparovek, G., Longo, R.M., De Melo, W.J., Crowley, D., 2007. Bacterial diversity of terra preta and pristine forest soil from the Western Amazon. Soil Biology and Biochemistry 39, 684–690.

Kinraide, T.B., 1991. Identity of the rhizotoxic aluminium species, Plant–Soil Interactions at Low pH. Springer, pp. 717–728.

Kinraide, T.B., 1994. Use of a Gouy–Chapman–Stern model for membrane–surface electrical potential to interpret some features of mineral rhizotoxicity. Plant Physiology 106, 1583–1592.

Kinraide, T.B., 1998. Three mechanisms for the calcium alleviation of mineral toxicities. Plant Physiology 118, 513–520.

Kinraide, T.B., Parker, D.R., 1987. Cation amelioration of aluminum toxicity in wheat. Plant Physiology 83, 546–551.

Kinraide, T.B., Parker, D.R., 1990. Apparent phytotoxicity of mononuclear hydroxy - aluminum to four dicotyledonous species. Physiologia Plantarum 79, 283–288.

Kissel, D., Sonon, L., Cabrera, M., 2012. Rapid measurement of soil pH buffering capacity. Soil Science Society of America Journal 76, 694–699.

Kissel, D.E., Isaac, R.A., Hitchcock, R., Sonon, L.S., Vendrell, P.F., 2007. Implementation of soil lime requirement by a single–addition titration method. Communications in Soil Science and Plant Analysis 38, 1341 – 1352.

Kitson, R., Mellon, M., 1944. Colorimetric determination of phosphorus as molybdivanadophosphoric acid. Industrial & Engineering Chemistry Analytical Edition 16, 379–383.

Knicker, H., Hatcher, P.G., 1997. Survival of protein in an organic–rich sediment: Possible protection by encapsulation in organic matter. Naturwissenschaften 84, 231–234.

Knicker, H., Scaroni, A.W., Hatcher, P.G., 1996. ^{13}C and ^{15}N NMR spectroscopic investigation on the formation of fossil algal residues. Organic Geochemistry 24, 661–669.

Kochian, L.V., Hoekenga, O.A., Piñeros, M.A., 2004. How do crop plants tolerate acid soils? Mechanisms of aluminum tolerance and phosphorous efficiency. Annual Review of Plant Biology 55, 459–493.

Kuchenbuch, R., Jungk, A., 1982. A method for determining concentration profiles at the soil–root interface by thin slicing rhizospheric soil. Plant and Soil 68, 391–394.

Laird, D.A., Fleming, P., Davis, D.D., Horton, R., Wang, B., Karlen, D.L., 2010. Impact of biochar amendments on the quality of a typical Midwestern agricultural soil. Geoderma 158, 443–449.

Landcare Research Centre, 2013. Soil Orders from the New Zealand Soil Classification (NZSC). Available at: http://soils.landcareresearch.co.nz/contents/SoilNames_NZSoilClassification_SoilOrders.aspx?currentPage=SoilNames_NZSoilClassification_SoilOrders%26

Larney, F.J., Angers, D.A., 2012. The role of organic amendments in soil reclamation: A review. Canadian Journal of Soil Science 92, 19–38.

Leake, J., Johnson, D., Donnelly, D., Muckle, G., Boddy, L., Read, D., 2004. Networks of power and influence: the role of mycorrhizal mycelium in controlling plant communities and agroecosystem functioning. Canadian Journal of Botany 82, 1016–1045.

Lehmann, J., Gaunt, J., Rondon, M., 2006. Bio–char sequestration in terrestrial ecosystems – A review. Mitig Adapt Strateg Glob Change 11, 395–419.

Lehmann, J., Joseph, S., 2015. Biochar for environmental management: An introduction, In: Lehmann, J., Joseph, S. (Eds.), Biochar for environmental management: Science and technology. Earthscan, London UK. 1–15.

Lehmann, J., Rillig, M.C., Thies, J., Masiello, C.A., Hockaday, W.C., Crowley, D., 2011. Biochar effects on soil biota – A review. Soil Biology and Biochemistry 43, 1812–1836.

Leifheit, E.F., Verbruggen, E., Rillig, M.C., 2015. Arbuscular mycorrhizal fungi reduce decomposition of woody plant litter while increasing soil aggregation. Soil Biology and Biochemistry 81, 323–328.

Li, L., Stanforth, R., 2000. Distinguishing adsorption and surface precipitation of phosphate on goethite (α–FeOOH). Journal of Colloid and Interface Science 230, 12–21.

LIC, S., 2013–14. New Zealand Dairy Statistics. Statistics LIC. Available at: http://www.dairynz.co.nz/media/1327583/nz-dairy-statistics-2013-2014-web.pdf

Liesch, A.M., 2010. Wastewater phosphorus removal by two different types of andesitic volcanic tephra. Journal of Natural Resources & Life Sciences Education 39, 40–44.

Liu, M., Kissel, D.E., Cabrera, M.L., Vendrell, P.F., 2005. Soil lime requirement by direct titration with a single addition of calcium hydroxide. Soil Science Society of America Journal 69, 522–530.

Liu, N., Huo, K., McDowell, M.T., Zhao, J., Cui, Y., 2013. Rice husks as a sustainable source of nanostructured silicon for high performance Li–ion battery anodes. Scientific Reports 3, 1919.

Loganathan, P., Hedley, M.J., Grace, N.D., Lee, J., Cronin, S.J., Bolan, N.S., Zanders, J.M., 2003. Fertiliser contaminants in New Zealand grazed pasture with special reference to cadmium and fluorine: a review. Australian Journal of Soil Research 41, 501–532.

Lowe, D.J., Palmer, D.J., 2005. Andisols of New Zealand and Australia. Journal of Integrated Field Science, 2, 39–65.

Lu, Q., He, Z.L., Stoffella, P.J., 2012. Land Application of Biosolids in the USA: A Review. Applied and Environmental Soil Science 2012, 11.

Luan, S., Lan, W., Chul Lee, S., 2009. Potassium nutrition, sodium toxicity, and calcium signaling: connections through the CBL–CIPK network. Current Opinion in Plant Biology 12, 339–346.

Ma, J.F., Ryan, P.R., Delhaize, E., 2001. Aluminium tolerance in plants and the complexing role of organic acids. Trends in Plant Science 6, 273–278.

Macías, F., Camps–Arbestain, M., 2010. Soil carbon sequestration in a changing global environment. Mitigation and Adaptation Strategies for Global Change 15, 511–529.

Magdoff, F.R., Bartlett, R.J., 1985. Soil pH Buffering Revisited. Soil Science Society of America Journal 49, 145–148.

Maher, W., Krikowa, F., Wruck, D., Louie, H., Nguyen, T., Huang, W.Y., 2002. Determination of total phosphorus and nitrogen in turbid waters by oxidation with alkaline potassium peroxodisulfate and low pressure microwave digestion, autoclave heating or the use of closed vessels in a hot water bath: comparison with Kjeldahl digestion. Analytica Chimica Acta 463, 283–293.

Major, J., Rondon, M., Molina, D., Riha, S., Lehmann, J., 2010. Maize yield and nutrition during 4 years after biochar application to a Colombian savanna oxisol. Plant and Soil 333, 117–128.

Mansell, G., Pringle, R., Edmeades, D., Shannon, P., 1984. Effects of lime on pasture production on soils in the North Island of New Zealand: 3. Interaction of lime with phosphorus. New Zealand Journal of Agricultural Research 27, 363–369.

Marschner, P., Rengel, Z., 2012. Chapter 12. Nutrient Availability in Soil In:Marschner (Ed.), P., Marschner's mineral nutrition of higher plants, 3rd ed. Academic press. 315–330.

Martinsen, V., Alling, V., Nurida, N.L., Mulder, J., Hale, S.E., Ritz, C., Rutherford, D.W., Heikens, A., Breedveld, G.D., Cornelissen, G., 2015. pH effects of the

addition of three biochars to acidic Indonesian mineral soils. Soil Science and Plant Nutrition, 1–14.

Masud, M.M., Li, J.–Y., Xu, R.–K., 2014. Use of alkaline slag and crop residue biochars to promote base saturation and reduce acidity of an acidic Ultisol. Pedosphere 24, 791–798.

Materechera, S.A., Mkhabela, T.S., 2002. The effectiveness of lime, chicken manure and leaf litter ash in ameliorating acidity in a soil previously under black wattle (Acacia mearnsii) plantation. Bioresource Technology 85, 9–16.

Matsubara, Y., Harada, T., Yakuwa, T., 1995. Effect of inoculation density of vesicular–arbuscular mycorrhizal fungal spores and addition of carbonized material to bed soil on growth of welsh onion [Allium fistulosum] seedlings. Journal of the Japanese Society for Horticultural Science 64 (3): 549–554.

Matsubara, Y., Hasegawa, N., Fukui, H., 2002. Incidence of Fusarium root rot in asparagus seedlings infected with arbuscular mycorrhizal fungus as affected by several soil amendments. Jounal japanese socienty for hoticultural science 71, 370–374.

McDowell, R., Sharpley, A., Brookes, P., Poulton, P., 2001. Relationship between soil test phosphorus and phosphorus release to solution. Soil Science 166, 137–149.

McGonigle, T., Miller, M., Evans, D., Fairchild, G., Swan, J., 1990. A new method which gives an objective measure of colonization of roots by vesicular–arbuscular mycorrhizal fungi. New Phytologist 115, 495–501.

McKenzie, H., Wallace, H., 1954. The Kjeldahl determination of nitrogen: A critical study of digestion conditions–temperature, catalyst, and oxidizing agent. Australian Journal of Chemistry 7, 55–70.

Mia, S., van Groenigen, J.W., van de Voorde, T.F.J., Oram, N.J., Bezemer, T.M., Mommer, L., Jeffery, S., 2014. Biochar application rate affects biological nitrogen fixation in red clover conditional on potassium availability. Agriculture, Ecosystems & Environment 191, 83–91.

Middleton, K.R., Toxopeus, M.R.J., 1973. Diagnosis and measurement of multiple soil deficiencies by a subtractive technique. Plant and Soil 38, 219–226.

Miller, R.M., Jastrow, J.D., Reinhardt, D.R., 1995. External hyphal production of vesicular–arbuscular mycorrhizal fungi in pasture and tallgrass prairie communities. Oecologia 103, 17–23.

Mizota, C., Van Reeuwijk, L., 1989. Clay mineralogy and chemistry of soils formed in volcanic material in diverse climatic regions. ISM Monograph.185

Mokolobate, M., Haynes, R., 2002. Comparative liming effect of four organic residues applied to an acid soil. Biology and Fertility of Soils 35, 79–85.

Moreno–Castilla, C., López–Ramón, M.V., Carrasco–Marín, F., 2000. Changes in surface chemistry of activated carbons by wet oxidation. Carbon 38, 1995–2001.

Morgan, P., Cooper, C.J., Battersby, N.S., Lee, S.A., Lewis, S.T., Machin, T.M., Graham, S.C., Watkinson, R.J., 1991. Automated image analyss method to determine fungal biomass in soils and on solid matrices. Soil Biology and Biochemistry 23, 609–616.

Munns, D.N., Fox, R.L., 1976. The Slow Reaction which Continues After Phosphate Adsorption: Kinetics and Equilibrium in Some Tropical Soils1. Soil Science Society of America Journal 40, 46–51.

Murphy, J., Riley, J.P., 1962. A modified single solution method for the determination of phosphate in natural waters. Analytica Chimica Acta 27, 31–36.

Nanzyo, M., 2002. Unique properties of volcanic ash soils. Global Environmental Research 6, 99–112.

Naramabuye, F.X., Haynes, R.J., 2006. Effect of organic amendments on soil pH and Al solubility and use of laboratory indices to predict their liming effect. Soil Science 171, 754–763.

Nelson, P.N., Su, N., 2010. Soil pH buffering capacity: a descriptive function and its application to some acidic tropical soils. Soil Research 48, 201–207.

Neumann, E., George, E., 2010. Nutrient Uptake: The Arbuscular Mycorrhiza Fungal Symbiosis as a Plant Nutrient Acquisition Strategy, In: Koltai, H., Kapulnik, Y. (Eds.), Arbuscular Mycorrhizas: Physiology and Function. Springer Netherlands. 137–167.

Ninjatacoshell, 2015. World Soil pH. Available at: https://en.wikipedia.org/wiki/Soil_pH

Novak, J.M., Busscher, W.J., Laird, D.L., Ahmedna, M., Watts, D.W., Niandou, M.A.S., 2009. Impact of Biochar Amendment on Fertility of a Southeastern Coastal Plain Soil. Soil Science 174, 105–112.

Novak, J.M., Cantrell, K.B., Watts, D.W., 2013. Compositional and Thermal Evaluation of Lignocellulosic and Poultry Litter Chars via High and Low Temperature Pyrolysis. BioEnergy Research 6, 114–130.

Nzanza, B., Marais, D., Soundy, P., 2012. Effect of arbuscular Mycorrhizal fungal inoculation and biochar amendment on growth and yield of tomato. International Journal of Agriculture and Biology 14 (6): 965–969

Odlare, M., Arthurson, V., Pell, M., Svensson, K., Nehrenheim, E., Abubaker, J., 2011. Land application of organic waste – Effects on the soil ecosystem. Applied Energy 88, 2210–2218.

Okuno, T., Sonoyama, N., Hayashi, J.–i., Li, C.–Z., Sathe, C., Chiba, T., 2005. Primary release of alkali and alkaline earth metallic species during the pyrolysis of pulverized biomass. Energy & Fuels 19, 2164–2171.

Olsen, S.R., Cole, C.V., Watanabe, F.S., 1954. Estimation of available phosphorus in soils by extraction with sodium bicarbonate. Circular / United States Department of Agriculture; no. 939. USDA, Washington.

Pacovsky, R.S., Bethlenfalvay, G.J., 1982. Measurement of the extraradical mycelium of a vesicular–arbuscular mycorrhizal fungus in soil by chitin determination. Plant and Soil 68, 143–147.

Pansu, M., Gautheyrou, J., 2006. Chapter 14. Organic forms of nitrogen, mineralizable nitrogen (and carbon), In: Pansu, M., Gautheyrou, J. (Eds.), Handbook of soil analysis: Mineralogical, organic and inorganic methods. Springer Berlin, Heidelberg, New York. 497–547.

Parfitt, R., 1978. Anion adsorption by soils and soil materials. Advances in Agronomy 30, 1–42

Parfitt, R., 1989. Phosphate reactions with natural allophane, ferrihydrite and goethite. Journal of Soil Science 40, 359–369.

Parfitt, R.L., Hume, L.J., Sparling, G.P., 1989. Loss of availability of phosphate in New Zealand soils. Journal of Soil Science 40, 371–382.

Patton, C.J., Kryskalla, J.R., 2003. Methods of analysis by the US Geological Survey National Water Quality Laboratory: Evaluation of alkaline persulfate digestion

as an alternative to kjeldahl digestion for determination of total and dissolved nitrogen and phosphorus in water. Avaialbe at: http://nwql.usgs.gov/WRIR-03-4174.shtml

Pavan, M.A., Bingham, F.T., Pratt, P.F., 1982. Toxicity of Aluminum to Coffee in Ultisols and Oxisols Amended with CaCO3, MgCO3, and CaSO4·2H2O1. Soil Science Society of America Journal 46, 1201–1207.

Perrott, K., Sarathchandra, S., 1987. Nutrient and organic matter levels in a range of New Zealand soils under established pasture. New Zealand Journal of Agricultural Research 30, 249–259.

Perrott, K.W., Maher, F.M., Thorrold, B.S., 1989. Accumulation of phosphorus fractions in yellow–brown pumice soils with development. New Zealand Journal of Agricultural Research 32, 53–62.

Perrott, K.W., Smith, B.F.L., Mitchell, B.D., 1976. Effect of pH on the reaction of sodium fluoride with hydrous oxides of silicon, aluminium, and iron, and with poorly ordered aluminosilicates. Journal of Soil Science 27, 348–356.

Petersen, S.O., Henriksen, K., Mortensen, G.K., Krogh, P.H., Brandt, K.K., Sørensen, J., Madsen, T., Petersen, J., Grøn, C., 2003. Recycling of sewage sludge and household compost to arable land: fate and effects of organic contaminants, and impact on soil fertility. Soil and Tillage Research 72, 139–152.

Phillips, J., Hayman, D., 1970. Improved procedures for clearing roots and staining parasitic and vesicular–arbuscular mycorrhizal fungi for rapid assessment of infection. Transactions of the British Mycological Society 55, 158–161.

Pietikäinen, J., Kiikkilä, O., Fritze, H., 2000. Charcoal as a habitat for microbes and its effect on the microbial community of the underlying humus. Oikos 89, 231–242.

Prakongkep, N., Gilkes, R.J., Wiriyakitnateekul, W., 2015. Forms and solubility of plant nutrient elements in tropical plant waste biochars. Journal of Plant Nutrition and Soil Science 178, 732–740.

Prendergast–Miller, M.T., Duvall, M., Sohi, S.P., 2014. Biochar–root interactions are mediated by biochar nutrient content and impacts on soil nutrient availability. European Journal of Soil Science 65, 173–185.

Qayyum, M.F., Ashraf, I., Abid, M., Steffens, D., 2015. Effect of biochar, lime, and compost application on phosphorus adsorption in a Ferralsol. Journal of Plant Nutrition and Soil Science,178, 576–581.

Qian, L., Chen, B., 2013. Dual role of biochars as adsorbents for aluminum: The effects of oxygen–containing organic components and the scattering of silicate particles. Environmental Science & Technology 47, 8759–8768.

Qian, L., Chen, B., Hu, D., 2013. Effective Alleviation of Aluminum Phytotoxicity by Manure–Derived Biochar. Environmental Science & Technology 47, 2737–2745.

Quilliam, R.S., Glanville, H.C., Wade, S.C., Jones, D.L., 2013. Life in the 'charosphere'–Does biochar in agricultural soil provide a significant habitat for microorganisms? Soil Biology and Biochemistry. 65, 287–293.

Quin, P.R., Cowie, A.L., Flavel, R.J., Keen, B.P., Macdonald, L.M., Morris, S.G., Singh, B.P., Young, I.M., Van Zwieten, L., 2014. Oil mallee biochar improves soil

structural properties – A study with x–ray micro–CT. Agriculture, Ecosystems & Environment 191, 142–149.

Rajkovich, S., Enders, A., Hanley, K., Hyland, C., Zimmerman, A., Lehmann, J., 2012. Corn growth and nitrogen nutrition after additions of biochars with varying properties to a temperate soil. Biology and Fertility of Soils 48, 271–284.

Rayment, G.E., Higginson, F.R., 1992. Australian laboratory handbook of soil and water chemical methods. Reed International Books, Australia/ Inkata Press Port Melbourne.

Rayment, G.E., Lyons, D.J., 2011. Soil chemical methods: Australasia. CSIRO publishing. Collingwood, Victoria, Australia.

Rengel, Z., 1992. Role of calcium in aluminium toxicity. New Phytologist 121, 499–513.

Rezaul Karim, M., 2011. Evaluation of soil fertility level on present crop practice in munshiganj and comilla districts of bangladesh. Journal of Developments in Sustainable Agriculture 6, 189–198.

Rillig, M.C., 2004. Arbuscular mycorrhizae, glomalin, and soil aggregation. Canadian Journal of Soil Science 84, 355–363.

Rillig, M.C., Mummey, D.L., 2006. Mycorrhizas and soil structure. New Phytologist 171, 41–53.

R Core Team (2015). R: A language and environment for statistical computing. R Foundation for Statistical Computing, Vienna, Austria. URL https://www.R–project.org/.

Ritchie, G., 1994. Role of dissolution and precipitation of minerals in controlling soluble aluminum in acidic soils. Advances in Agronomy 53, 47.

Robarge, W.P., 1999. Chapter 5 Precipitation/dissolution reactions in soils. In: Donald L. Sparks (Ed.) Soil physical chemistry 2. New York, Washington D.C.

Rodriguez, L., Salazar, P., Preston, T.R., 2009. Effect of biochar and biodigester effluent on growth of maize in acid soils. Livestock Research for Rural Development 21, 110.

Rout, G., Samantaray, S., Das, P., 2001. Aluminium toxicity in plants: a review. Agronomie 21, 3–21.

Russelle, M.P., McGraw, R.L., Grava, J., Beuselinck, P.R., 1985. Elemental composition of birdsfoot trefoil. Communications in Soil Science and Plant Analysis 16, 987–1013.

Ryden, J., Syers, J., 1975. Use of tephra for the removal of dissolved inorganic phosphate from sewage effluent. New Zealand Journal of Science 18, 3–16.

Saggar S, Hedley MJ, White RE (1990) A simplified resin membrane technique for extracting phosphorus from soils. Nutr Cycl Agroecosyst 24:173–180

Saigusa, M., Shoji, S., Takahashi, T., 1980. Plant Root Growth in Acid Andosols from Northeastern Japan: 2. Exchange Acidity Y1 as A Realistic Measure of Aluminum Toxicity Potential. Soil Science 130, 242–250.

Saunders, W., 1959a. Effect of phosphate topdressing on a soil from Andesitic Volcanic Ash: effect on distribution of phosphorus and on related chemical properties. New Zealand Journal of Agricultural Research 2, 445–462.

Saunders, W., 1959b. Effect of phosphate topdressing on a soil from andesitic volcanic ash: Phosphate retention and pH. New Zealand Journal of Agricultural Research 2, 659–665.

Saunders, W., 1965. Phosphate retention by New Zealand soils and its relationship to free sesquioxides, organic matter, and other soil properties. New Zealand Journal of Agricultural Research 8, 30–57.

Schachtman, D.P., Reid, R.J., Ayling, S., 1998. Phosphorus uptake by plants: from soil to cell. Plant Physiology 116, 447–453.

Schüepp, H., Miller, D.D., Bodmer, M., 1987. A new technique for monitoring hyphal growth of vesicular–arbuscular mycorrhizal fungi through soil. Transactions of the British Mycological Society 89, 429–435.

Shackley, S., Carter, S., Knowles, T., Middelink, E., Haefele, S., Sohi, S., Cross, A., Haszeldine, S., 2012. Sustainable gasification–biochar systems? A case–study of rice–husk gasification in Cambodia, Part I: Context, chemical properties, environmental and health and safety issues. Energy Policy 42, 49–58.

Sheffield, J.B., 2008. An introduction to ImageJ: A useful tool for biological image processing and analysis. Microscopy and Microanalysis 14, 898–899.

Sheppard, L.J., Floate, M.J.S., 1984. The effects of soluble–Al on root growth and radicle elongation. Plant and Soil 80, 301–306.

Shen Q, Kirschbaum M.U.F., Hedley MJ, Camps-Arbestain M. Testing an alternative method for estimating the length of fungal hyphae using photomicrography and image processing (2016). PLoS ONE (accepted)

Silva, I.R., Smyth, T.J., Israel, D.W., Raper, C.D., Rufty, T.W., 2001. Magnesium is more efficient than calcium in alleviating aluminum rhizotoxicity in soybean and its ameliorative effect is not explained by the Gouy–Chapman–Stern Model. Plant and Cell Physiology 42, 538–545.

Singh, B., Singh, B.P., Cowie, A.L., 2010a. Characterisation and evaluation of biochars for their application as a soil amendment. Australian Journal of Soil Research 48, 516–525.

Singh, B.P., Hatton, B.J., Singh, B., Cowie, A.L., Kathuria, A., 2010b. Influence of Biochars on Nitrous Oxide Emission and Nitrogen Leaching from Two Contrasting Soils. Journal of Environment Quality 39, 1224–1235.

Slavich, P.G., Sinclair, K., Morris, S.G., Kimber, S.W.L., Downie, A., Van Zwieten, L., 2013a. Contrasting effects of manure and green waste biochars on the properties of an acidic ferralsol and productivity of a subtropical pasture. Plant and Soil 366, 213–227.

Smider, B., Singh, B., 2014. Agronomic performance of a high ash biochar in two contrasting soils. Agriculture, Ecosystems and Environment 191, 99–107.

Smith, M., Ha, S., Amonette, J.E., Dallmeyer, I., Garcia–Perez, M., 2015. Enhancing cation exchange capacity of chars through ozonation. Biomass and Bioenergy 81, 304–314.

Smith, S.E., Read, D.J., 2010. Mycorrhizal symbiosis. Access Online via Elsevier.

Solaiman, Z., Sarcheshmehpour, M., Abbott, L., Blackwell, P., Gilkes, R., 2010a. Effect of biochar on arbuscular mycorrhizal colonisation, growth, P nutrition and leaf gas exchange of wheat and clover influenced by different water regimes, Proceedings of the 19th World Congress of Soil Science: Soil solutions for a changing world, Brisbane, Australia, 1–6 August 2010. International Union of Soil Sciences (IUSS), c/o Institut für Bodenforschung, Universität für Bodenkultur. 35–37.

Solaiman, Z.M., Blackwell, P., Abbott, L.K., Storer, P., 2010b. Direct and residual effect of biochar application on mycorrhizal root colonisation, growth and nutrition of wheat. Australian Journal of Soil Research 48, 546–554.

Solomon, D., Lehmann, J., Zech, W., 2001. Land use effects on amino sugar signature of chromic Luvisol in the semi–arid part of northern Tanzania. Biology and Fertility of Soils 33, 33–40.

Sparks, D.L., 2003. Environmental soil chemistry. Academic press.

Staddon, P.L., Ramsey, C.B., Ostle, N., Ineson, P., Fitter, A.H., 2003. Rapid Turnover of Hyphae of Mycorrhizal Fungi Determined by AMS Microanalysis of 14C. Science 300, 1138–1140.

Stahl, P.D., Parkin, T.B., Eash, N.S., 1995. Sources of error in direct microscopic methods for estimation of fungal biomass in soil. Soil Biology and Biochemistry 27, 1091–1097.

Stanford, G., DeMent, J.D., 1957. A Method for Measuring Short–Term Nutrient Absorption by Plants: I. Phosphorus1. Soil Science Society of America Journal 21, 612–617.

Stass, A., Wang, Y., Eticha, D., Horst, W., 2006. Aluminium rhizotoxicity in maize grown in solutions with Al^{3+} or $Al(OH)_4^-$ as predominant solution Al species. Journal of Experimental Botany 57, 4033–4042.

Su, Y., Zhang, W., Xu, F., Chen, W., 2015. Natural Volcanic Tephra for Phosphate Removal from Rural Micro–polluted Wastewater. Water, Air, & Soil Pollution 226, 1–11.

Suckling, F.E.T., 1960. Productivity of pasture species on Hill Country. New Zealand Journal of Agricultural Research 3, 579–591.

Sumner, M.E., Noble, A.D., 2003. Soil acidification: the world story. Handbook of Soil Acidity, Marcel Dekker, New York, 1–28.

Sylvia, D.M., 1992. Quantification of External Hyphae of Vesicular–arbuscular Mycorrhizal. Techniques for the Study of Mycorrhiza, 53.

Tabti, Z., Ruiz–Rosas, R., Quijada, C., Cazorla–Amorós, D., Morallón, E., 2014. Tailoring the Surface Chemistry of Activated Carbon Cloth by Electrochemical Methods. ACS Applied Materials & Interfaces 6, 11682–11691.

Takahashi, T., Fukuoka, T., Dahlgren, R.A., 1995. Aluminum solubility and release rates from soil horizons dominated by aluminum–humes complexes. Soil Science and Plant Nutrition 41, 119–131.

Takahashi, T., Ikeda, Y., Fujita, K., Nanzyo, M., 2006. Effect of liming on organically complexed aluminum of nonallophanic Andosols from northeastern Japan. Geoderma 130, 26–34.

Takahashi, T., Nanzyo, M., Hiradate, S., 2007. Aluminum status of synthetic Al–humic substance complexes and their influence on plant root growth. Soil Science and Plant Nutrition 53, 115–124.

Tammeorg, P., Simojoki, A., Mäkelä, P., Stoddard, F.L., Alakukku, L., Helenius, J., 2014. Short–term effects of biochar on soil properties and wheat yield formation with meat bone meal and inorganic fertiliser on a boreal loamy sand. Agriculture, Ecosystems & Environment 191, 108–116.

Teichmann, I., 2014. Technical greenhouse–gas mitigation potentials of biochar soil incorporation in Germany: Data documentation. DIW Berlin, German Institute for Economic Research. Available at:

https://www.diw.de/documents/publikationen/73/diw_01.c.479813.de/dp1406.pdf

Tennant, D., 1975. A test of a modified line intersect method of estimating root length. The Journal of Ecology, 995–1001.

Thipkhunthod, P., Meeyoo, V., Rangsunvigit, P., Rirksomboon, T., 2007. Describing sewage sludge pyrolysis kinetics by a combination of biomass fractions decomposition. Journal of Analytical and Applied Pyrolysis 79, 78–85.

Thomas, G.W., Hargrove, W.L., 1984. The Chemistry of Soil Acidity. Agronomy Monograph no. 12 (2nd Edition)

Thompson, J., Kissel, D., Cabrera, M., Sonon, L., 2010. Equilibration reaction from single addition of base to determine soil lime requirement. Soil Science Society of America Journal 74, 663–669.

Toor, G.S., Hunger, S., Peak, J.D., Sims, J.T., Sparks, D.L., 2006. Advances in the characterization of phosphorus in organic wastes: Environmental and agronomic applications. Advances in Agronomy 89, 1–72.

Trolove, S., Hedley, M., Caradus, J., Mackay, A., 1996. Uptake of phosphorus from different sources by *Lotus Pedunculatus* and three genotypes of *Trifolium Repens* .1. Plant yield and phosphate efficiency. Soil Research 34, 1015–1026.

Trolove, S.N., Hedley, M.J., Kirk, G.J.D., Bolan, N.S., Loganathan, P., 2003. Progress in selected areas of rhizosphere research on P acquisition. Australian Journal of Soil Research 41, 471–499.

Uchida, R., Hue, N., 2000. Soil acidity and liming. Plant nutrient management in Hawaii's soils. Coll. Tropical Agric. Human Res., Univ. Hawaii. Honolulu, HI, 101–111.

Uchimiya, M., Hiradate, S., 2014. Pyrolysis temperature–dependent changes in dissolved phosphorus speciation of plant and manure biochars. Journal of Agricultural and Food Chemistry 62, 1802–1809.

Uchimiya, M., Hiradate, S., Antal, M.J., 2015. Dissolved phosphorus speciation of flash carbonization, slow pyrolysis, and fast pyrolysis biochars. ACS Sustainable Chemistry & Engineering. 3, 1642–1649

Uchimiya, M., Lima, I.M., Thomas Klasson, K., Chang, S., Wartelle, L.H., Rodgers, J.E., 2010. Immobilization of heavy metal ions (CuII, CdII, NiII, and PbII) by broiler litter–derived biochars in water and soil. Journal of Agricultural and Food Chemistry 58, 5538–5544.

Uchimiya, M., Wartelle, L.H., Klasson, K.T., Fortier, C.A., Lima, I.M., 2011. Influence of pyrolysis temperature on biochar property and function as a heavy metal sorbent in soil. Journal of Agricultural and Food Chemistry 59, 2501–2510.

Ueno, M., Kawamitsu, Y., Komiya, Y., Liya, S., 2008. Carbonisation and gasification of bagasse for effective utilisation of sugarcane biomass. International Sugar Journal 110, 22–25, 27.

Van Zwieten, L., Kimber, S., Morris, S., Chan, K.Y., Downie, A., Rust, J., Joseph, S., Cowie, A., 2010. Effects of biochar from slow pyrolysis of papermill waste on agronomic performance and soil fertility. Plant and Soil 327, 235–246.

Van Zwieten, L., Singh, B.P., Kimber, S.W.L., Murphy, D.V., Macdonald, L.M., Rust, J., Morris, S., 2014. An incubation study investigating the mechanisms that impact N_2O flux from soil following biochar application. Agriculture, Ecosystems & Environment 191, 53–62.

Vanek, S., Lehmann, J., 2014. Phosphorus availability to beans via interactions between mycorrhizas and biochar. Plant and Soil, 395, 105–123.

Vassilev, S.V., Baxter, D., Andersen, L.K., Vassileva, C.G., 2010. An overview of the chemical composition of biomass. Fuel 89, 913–933.

Vassilev, S.V., Baxter, D., Andersen, L.K., Vassileva, C.G., 2013a. An overview of the composition and application of biomass ash. Part 1. Phase–mineral and chemical composition and classification. Fuel 105, 40–76.

Vassilev, S.V., Baxter, D., Andersen, L.K., Vassileva, C.G., 2013b. An overview of the composition and application of biomass ash.: Part 2. Potential utilisation, technological and ecological advantages and challenges. Fuel 105, 19–39.

Ventura, M., Zhang, C., Baldi, E., Fornasier, F., Sorrenti, G., Panzacchi, P., Tonon, G., 2014. Effect of biochar addition on soil respiration partitioning and root dynamics in an apple orchard. European Journal of Soil Science 65, 186–195.

Vilariño, A., Arines, J., Schüepp, H., 1993. Extraction of Vesicular–Arbuscular mycorrhizal mycelium from sand samples. Soil Biology and Biochemistry 25, 99–100.

Von Uexküll, H., Mutert, E., 1995. Global extent, development and economic impact of acid soils. Plant and Soil 171, 1–15.

Wada, K., 1985. The distinctive properties of Andosols, Advances in soil science. Springer, 173–229.

Walkley, A., 1947. A critical examination of a rapid method for determining organic carbon in soils–effect of variations in digestion conditions and of inorganic soil constituents. Soil Science 63, 251–264.

Wan, Q., Yuan, J.–H., Xu, R.–K., Li, X.–H., 2014. Pyrolysis temperature influences ameliorating effects of biochars on acidic soil. Environmental Science and Pollution Research 21, 2486–2495.

Wang, C., Anderson, C., Suárez–Abelenda, M., Wang, T., Camps–Arbestain, M., Ahmad, R., Herath, H.M.S.K., 2015a. The chemical composition of native organic matter influences the response of bacterial community to input of biochar and fresh plant material. Plant and Soil, 395, 87–104.

Wang, T., Camps–Arbestain, M., Hedley, M., 2013a. The fate of phosphorus of ash–rich biochars in a soil–plant system. Plant and Soil, 375, 61–74.

Wang, T., Camps–Arbestain, M., Hedley, M., 2013b. Predicting C aromaticity of biochars based on their elemental composition. Organic Geochemistry 62, 1–6.

Wang, T., Camps–Arbestain, M., Hedley, M., Singh, B.P., Calvelo–Pereira, R., Wang, C., 2014. Determination of carbonate–C in biochars. Soil Research 52, 495–504.

Wang, T., Camps–Arbestain, M., Hedley, M., Bishop, P., 2012a. Chemical and bioassay characterisation of nitrogen availability in biochar produced from dairy manure and biosolids. Organic Geochemistry 51, 45–54.

Wang, T., Camps–Arbestain, M., Hedley, M., Bishop, P., 2012b. Predicting phosphorus bioavailability from high–ash biochars. Plant and Soil 357, 173–187.

Wang, Y., Lin, Y., Chiu, P.C., Imhoff, P.T., Guo, M., 2015b. Phosphorus release behaviors of poultry litter biochar as a soil amendment. Science of the Total Environment 512–513, 454–463.

Warnock, D.D., Lehmann, J., Kuyper, T.W., Rillig, M.C., 2007. Mycorrhizal responses to biochar in soil – concepts and mechanisms. Plant and Soil 300, 9–20.

Warnock, D.D., Mummey, D.L., McBride, B., Major, J., Lehmann, J., Rillig, M.C., 2010. Influences of non–herbaceous biochar on arbuscular mycorrhizal fungal abundances in roots and soils: Results from growth–chamber and field experiments. Applied Soil Ecology 46, 450–456.

Weber, B., Stadlbauer, E.A., Schlich, E., Eichenauer, S., Kern, J., Steffens, D., 2014. Phosphorus bioavailability of biochars produced by thermo – chemical conversion. Journal of Plant Nutrition and Soil Science 177, 84 ‐ 90.

Whalen, J.K., Chang, C., Clayton, G.W., Carefoot, J.P., 2000. Cattle manure amendments can increase the pH of acid soils T4L 1W1.LRC Contribution No. 387–9953. Soil Science Society of America Journal 64, 962–966.

Wilson, G.W.T., Rice, C.W., Rillig, M.C., Springer, A., Hartnett, D.C., 2009. Soil aggregation and carbon sequestration are tightly correlated with the abundance of arbuscular mycorrhizal fungi: results from long–term field experiments. Ecology Letters 12, 452–461.

Winsley, P. (2007). Biochar and bioenergy production for climate change mitigation. New Zealand Science Review, 64(1), 5–10.

Wright, S.F., Upadhyaya, A., 1998. A survey of soils for aggregate stability and glomalin, a glycoprotein produced by hyphae of arbuscular mycorrhizal fungi. Plant and Soil 198, 97–107.

Xie, T., Reddy, K.R., Wang, C., Yargicoglu, E., Spokas, K., 2014. Characteristics and Applications of Biochar for Environmental Remediation: A Review. Critical Reviews in Environmental Science and Technology 45, 939–969.

Xu, J., Tang, C., Chen, Z.L., 2006. The role of plant residues in pH change of acid soils differing in initial pH. Soil Biology and Biochemistry 38, 709–719.

Xu, R.–k., Zhao, A.–z., Yuan, J.–h., Jiang, J., 2012. pH buffering capacity of acid soils from tropical and subtropical regions of China as influenced by incorporation of crop straw biochars. Journal of Soils and Sediments 12, 494–502.

Yamada, K., Takahashi, T., 2010. Possible toxicity of aluminium–humus complexes in Andosols, Proceedings of the 19th World Congress of Soil Science: Soil solutions for a changing world, Brisbane, Australia, 1–6 August 2010. International Union of Soil Sciences (IUSS), c/o Institut für Bodenforschung, Universität für Bodenkultur, 82–85.

Yang, F., Lee, X.Q., Wang, B., 2015. Characterization of biochars produced from seven biomasses grown in three different climate zones. Chinese Journal of Geochemistry 34 (4): 592–600

Yip, K., Tian, F., Hayashi, J.–I., Wu, H., 2009. Effect of alkali and alkaline earth metallic species on biochar reactivity and syngas compositions during steam gasification. Energy & Fuels 24, 173–181.

Yuan, J.–H., Xu, R.–K., 2012. Effects of biochars generated from crop residues on chemical properties of acid soils from tropical and subtropical China. Soil Research 50, 570–578.

Yuan, J.–H., Xu, R.–K., Qian, W., Wang, R.–H., 2011a. Comparison of the ameliorating effects on an acidic ultisol between four crop straws and their biochars. Journal of Soils and Sediments 11, 741–750.

Yuan, J.–H., Xu, R.–K., Zhang, H., 2011b. The forms of alkalis in the biochar produced from crop residues at different temperatures. Bioresource Technology 102, 3488–3497.

Yuan, J.H., Xu, R.K., 2011. The amelioration effects of low temperature biochar generated from nine crop residues on an acidic Ultisol. Soil Use and Management 27, 110–115.

Zhai, L., CaiJi, Z., Liu, J., Wang, H., Ren, T., Gai, X., Xi, B., Liu, H., 2014. Short–term effects of maize residue biochar on phosphorus availability in two soils with different phosphorus sorption capacities. Biology and Fertility of Soils, 51, 113–122.

Zhao, H., Liu, H., Qu, J., 2009. Effect of pH on the aluminum salts hydrolysis during coagulation process: Formation and decomposition of polymeric aluminum species. Journal of Colloid and Interface Science 330, 105–112.

Zhao, R., Jiang, D., Coles, N., Wu, J., 2015. Effects of biochar on the acidity of a loamy clay soil under different incubation conditions. Journal of Soils and Sediments 15, 1919–1926.

Zhu, Y.–G., Michael Miller, R., 2003. Carbon cycling by arbuscular mycorrhizal fungi in soil–plant systems. Trends in Plant Science 8, 407–409.

Zoysa, A.K.N., Loganathan, P., Hedley, M.J., 1997. A technique for studying rhizosphere processes in tree crops: soil phosphorus depletion around camellia (Camellia japonica L.) roots. Plant and Soil 190, 253–265.

Zoysa, A.K.N., Loganathan, P., Hedley, M.J., 1999. Phosphorus utilisation efficiency and depletion of phosphate fractions in the rhizosphere of three tea (Camellia sinensis L.) clones. Nutrient Cycling in Agroecosystems 53, 189–201.

Zwetsloot, M.J., Lehmann, J., Solomon, D., 2015. Recycling slaughterhouse waste into fertilizer: how do pyrolysis temperature and biomass additions affect

phosphorus availability and chemistry? Journal of the Science of Food and Agriculture 95, 281–288.